CHAPTER 4

RESULTS FROM VIBRATIONAL STUDIES BY FTIR

4.1 Introduction

The IR vibrational bands corresponding to the carbonyl (C=O) and ester (C–O–C_2H_5) groups in PEMA; the CF_2 and CF_3 groups in PVdf–HFP as well as the CF_3 and SO_3 groups of the triflate anion are studied to show the interactions between PEMA and PVdF–HFP as well as to ascertain if complexation has occurred between the polymers and LiTf in the PEMA/PVdF–HFP–LiTf system. The vibrational modes of EC and PC especially corresponding to its carbonyl group (C=O) as well as the IR bands of polar groups of PEMA and PVdF–HFP will be studied to determine whether interaction has occurred between EC or PC with the optimized polymer blend–salt system. As with the BMII and BMITf–added PE systems, the interactions between BMII and BMITf with PEMA, PVdF–HFP and LiTf were investigated by studying the vibrational modes due to the imidazolium cation (BMI^+).

According to Huang and Frech (1992), Li^+ cations interact with the triflate anions, $CF_3SO_3^-$ through the SO_3^- end. The non–degenerate vibrational mode of $\nu_s(SO_3)$ can also be used to distinguish between free ions (*i.e.* $CF_3SO_3^-$) which do not interact directly with Li^+, ion–pairs (*i.e.* LiTf, $Li(CF_3SO_3)_2^-$, $Li(CF_3SO_3)_3^{2-}$) and highly–aggregated ions (*i.e.* $Li_2CF_3SO_3^+$, $Li_3CF_3SO_3^{2+}$) in the region between 1030 and 1034 cm^{-1}, 1040 and 1045 cm^{-1} and 1049 and 1053 cm^{-1}, respectively. Hence, the symmetrical SO_3 stretching [$\nu_s(SO_3)$] mode of LiTf salt in all systems was deconvoluted to determine the amount of free ions, ion pairs and ion aggregates present.

4.2 Solid PEMA/PVdF–HFP–LiTf Polymer Electrolyte System

4.2.1 Interactions between PEMA and PVdF–HFP

The IR spectra of PEMA, PVdF–HFP and the polymer blend (S–0) sample were investigated to show miscibility between the two polymers. Table 4.1 shows the assignment of IR bands belonging to PEMA and PVdF–HFP obtained from literature.

Table 4.1 Assignment of FTIR vibrational bands of PEMA and PVdF–HFP

Assignment of bands	Wavenumber (cm^{-1})	Reference
ν(C–H) of (C)CH_3 and (O)C_2H_5 of PEMA	2982, 2939, 2910	Rajendran et al. (2008)
ν(C=O) of PEMA	1725	Rajendran et al. (2008)
CH_2 rocking of PEMA	1555	Avarindan et al. (2009)
ester group of PEMA	1261 and 1240	Rajendran et al. (2008)
ν(C–O–C) of PEMA	1150–1260	Hummel (1974)
ν(CH) of PVdF–HFP	3100–2990	Angulakshmi et al. (2011)
ω(CH_2) of PVdF–HFP	1403	Li et al. (2004)
δ(CF_2) of PVdF–HFP	1390	Ulaganathan and Rajendran (2010)
ν_s(CF_2) of PVdF–HFP	1276	Aravindan and Vickraman (2009)
ν_a(CF_2) of PVdF–HFP	1188	Li et al. (2004)
γ(CF_3) of PVdF–HFP	1069	Li et al. (2004)
α–phase of PVdF phase	762, 796, 976, 1401	Pandey et al. (2009); Saikia et al. (2011)
β–phase of PVdF phase	842, 880, 1287	Du et al., (2006)
–CF_2 stretching of PVdF–HFP	882	Saikia et al. (2011)
amorphous phase of PVdF–HFP	879, 839	Pandey et al. (2009)
γ–phase of PVdF phase	842	Gregorio and Cestari (1994)

The FTIR spectra of PEMA, PVdF–HFP and S–0 blend film in the regions 3800–2800 cm^{-1} and 1800–800 cm^{-1} are shown in Figure 4.1 (a–i, ii, iii) and Figure 4.1 (b–i, ii, iii) respectively. In this work, the vibrational modes of PEMA due to the carbonyl stretch [ν(C=O)], asymmetric O–C_2H_5 bending [γ(OC_2H_5)] and asymmetric stretch vibration of C–O–C bond [ν_a(COC)] are observed at 1723, 1446 and 1142 cm^{-1}, respectively. The ν(CO) stretch modes of –COO– and –OC_2H_5 group are found at 1265

and 1175 cm^{-1} respectively, while two bands located at 1249 and 1142 cm^{-1} come from the asymmetric C–O–C stretch [ν_{as}(COC)] [Hummel, 1966; Lee et al., 1996].

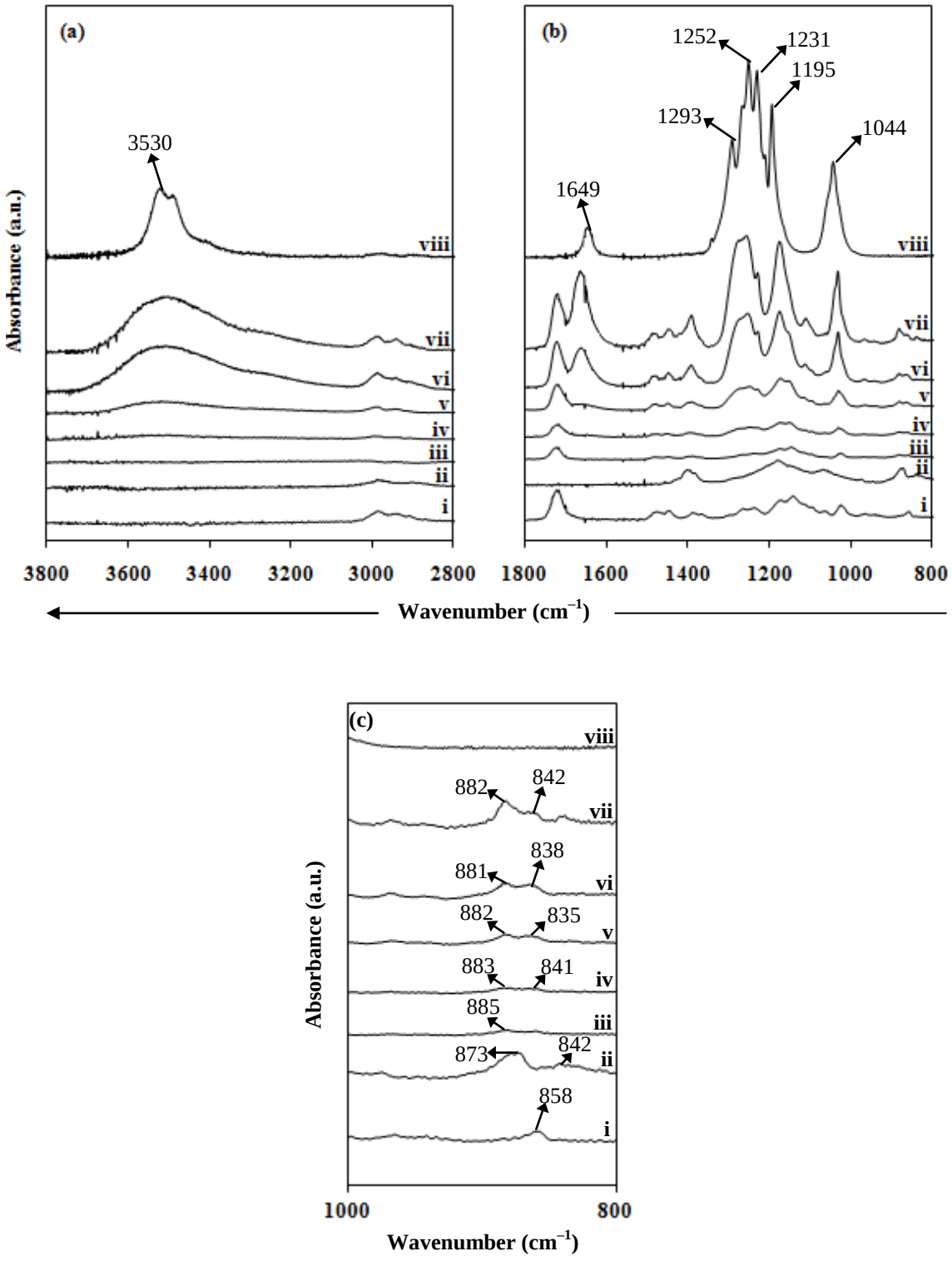

Figure 4.1 FTIR spectra in the region (a) 3800–2800 cm^{-1}, (b) 1800–800 cm^{-1} and (c) 1000–800 cm^{-1} (enlarged) of i. PEMA, ii. PVdF–HFP, iii. S–0, iv. S–10, v. S–20, vi. S–30, vii. S–40 and viii. LiTf

Since the aim of this sub–section is to show miscibility between PEMA and PVdF–HFP, the changes of ν(CH) (~2900 cm^{-1}), ν(CO) (~1140–1160 cm^{-1}), ν(C=O) (~1720 cm^{-1}) vibrations of PEMA, and ν(CH) (~2900 cm^{-1}), $\nu_a(CF_2)$ (~1170 cm^{-1}) and $\gamma(CF_3)$ vibrations (~1060 cm^{-1}) as well as the amorphous region (~880 cm^{-1}) of PVdF–HFP will be checked in the S–0 spectrum. The changes in the IR spectra of PEMA and PVdF–HFP observed in the spectrum of S–0 blend are shown in Figure 4.2.

In S–0, the bands located at 2989, 2946 and 2924 cm^{-1} are formed through the merging and overlapping between C–H bands of both PEMA and PVdF–HFP, Figure 4.2 (a–i, ii and iii).

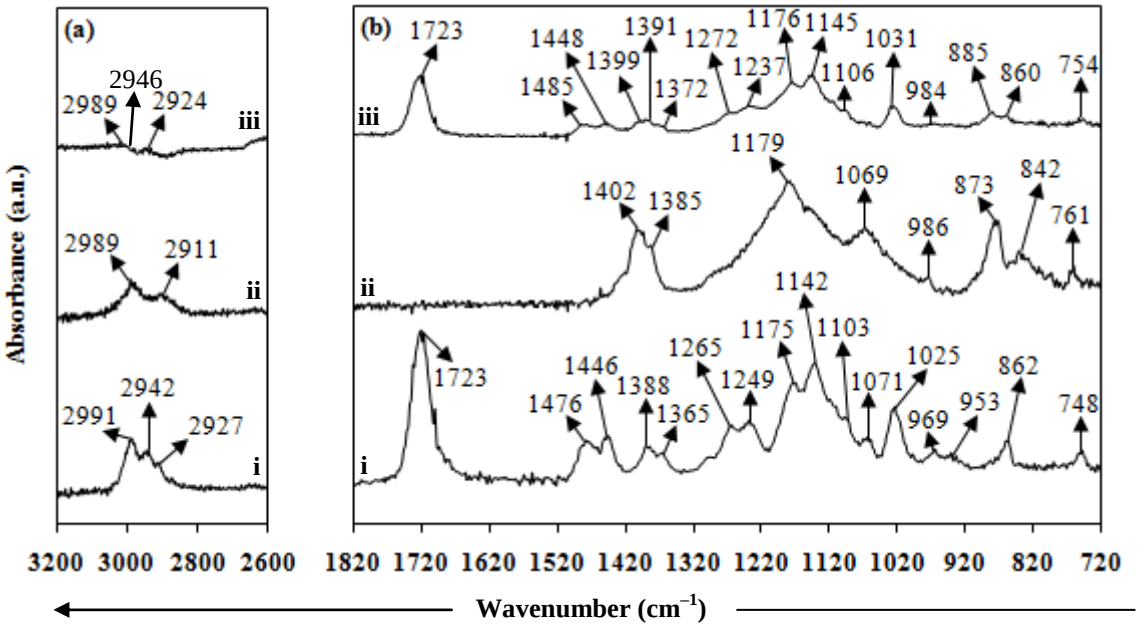

Figure 4.2 FTIR spectra in the region (a) 3200–2600 cm^{-1} and (b) 1820–720 cm^{-1} of i. PEMA, ii. PVdF–HFP and iii. PEMA/PVdF–HFP(70:30) or S–0

The peak due to carbonyl (C=O) group from PEMA remained at 1723 cm^{-1} but appeared with lower intensity (about 2.5 multiples), in proportion to the composition of PEMA (70 wt.%) in the blend. Bands at 1476 and 1446 cm^{-1} assigned to the $\delta(CH_2)$ and $\gamma(O–C_2H_5)$ vibrational modes in PEMA shifted to 1485 and 1448 cm^{-1}, respectively when blended with PVdF–HFP. Figure 4.3 illustrates the deconvoluted IR bands of

PEMA, PVdF–HFP and S–0 samples in the IR regions 1440–1340 cm^{-1}, 1220–1100 cm^{-1} and 1080–980 cm^{-1}. The $\tau(CH_2)$ mode at 1388 cm^{-1} and an unidentified characteristic band of PEMA located at 1365 cm^{-1} merged with the IR bands located at 1402 and 1385 cm^{-1} of PVdF–HFP to form several bands at 1399, 1391, 1385 and 1372 cm^{-1} in the spectrum of the S–0, Figure 4.3 (a–i, ii, iii).

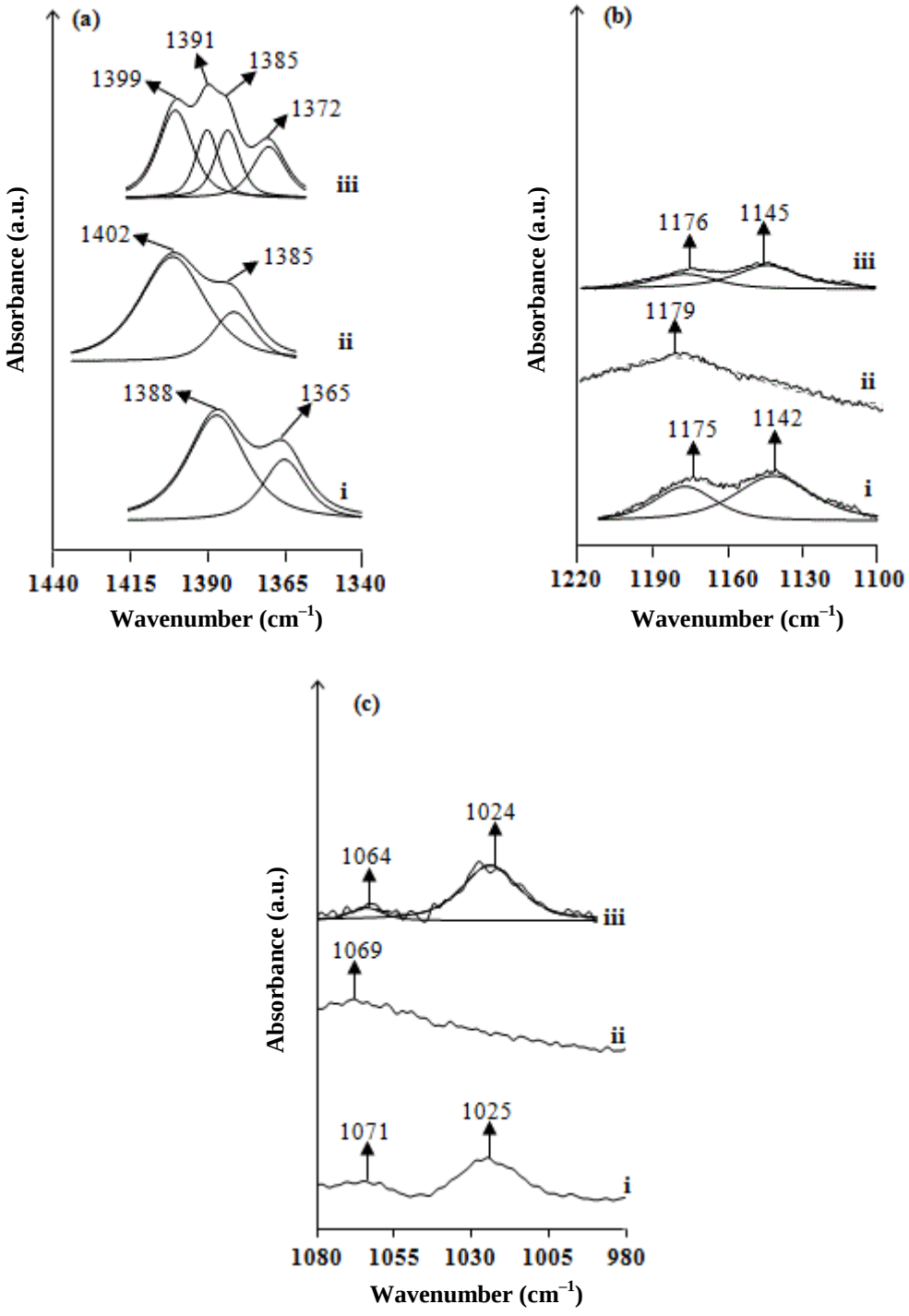

Figure 4.3 Deconvolution and band–fitting components in the region (a) 1440–1340 cm^{-1}, (b) 1220–1100 cm^{-1} and (c) 1080–980 cm^{-1} of i. PEMA, ii. PVdF–HFP and iii. S–0

The 1399 cm^{-1} is 1402 cm^{-1} from PVdF–HFP, 1391 cm^{-1} from 1388 cm^{-1} of PEMA. Likewise 1385 cm^{-1} corresponds to that of PVdF–HFP and 1372 cm^{-1} is the shifted 1365 cm^{-1} from PEMA. The shift of such bands is attributed to the superposition of the vibrations from PEMA polymer and PVdF–HFP co–polymer. Besides that, the different IR vibrational modes of the ester group in PEMA at 1265 cm^{-1} due to ν(CO) of –COO– group and 1249 cm^{-1} of ν_a(COC) shifted to 1272 and 1241 cm^{-1} respectively. As another example, consider the ν(CO) stretch from the $–OC_2H_5$ group in PEMA at 1175 cm^{-1} merged with $\nu_a(CF_2)$ of PVdF–HFP at 1179 cm^{-1} to form a small peak at 1176 cm^{-1}. It is to be noted that PVdF–HFP does not exhibit such a band in its spectrum.

The ν_a(COC) mode of PEMA which is located at 1142 cm^{-1} shifted to 1145 cm^{-1} in the spectrum of S–0, Figure 4.3 (b–i, ii, iii). Figure 4.3 (c–i, ii, iii) show that the characteristic band of PEMA originally located at 1071 cm^{-1} overlapped with a PVdF–HFP band at 1069 cm^{-1} to form a band at 1064 cm^{-1} in S–0. The vibrational band of PVdF–HFP at 842 cm^{-1} due to the β–phase of the polymer as well as the spectral band at 969 and 953 cm^{-1} due to PEMA disappeared in the spectrum of the polymer blend.

Table 4.2 Assignment of FTIR vibrational modes in PEMA, PVdF–HFP and PEMA/PVdF–HFP (70:30) blend films

Assignment of bands	Wavenumber (cm^{-1})		
	PEMA	**PVdF–HFP**	**S–0**
ν(CH)	2991, 2942, 2927	2989, 2911	2989, 2946, 2924
ν(C=O) of PEMA	1723	–	1723
$\delta(CH_2)$ of PEMA	1476	–	1485
$\gamma(OC_2H_5)$ of PEMA	1446	–	1448
$\omega(CH_2)$ of PVdF–HFP	–	1402	1399
$\tau(CH_2)$ of PEMA	1388	–	1391
$\delta(CF_2)$ of PVdF–HFP	–	1385	1385
ν(CO) of –COO– group of PEMA	1265	–	1272
ν_a(COC) of PEMA	1249	–	1241
$\nu_a(CF_2)$ of PVdF–HFP	–	1179	1176
ν(CO) of $–OC_2H_5$ group of PEMA	1175	–	1176
ν_a(COC) of PEMA	1142	–	1145
$\gamma(CF_3)$ of PVdF–HFP	–	1069	–
δ(C–H) of PEMA	1025	–	1024
α–phase of PVdF–HFP	–	986	984
Amorphous region of PVdF–HFP	–	873	885
β–phase of PVdF–HFP	–	842	–

Assignments of IR vibrational modes for PEMA, PVdF–HFP and PEMA/PVdF–HFP (70:30) or S–0 are shown in Table 4.2. Table 4.2 shows wavenumber shifts of vibrational modes which indicate that interactions have occurred between the polar atoms in each polymer with H atoms in another polymer to form a polymer blend: ν(CH), $\delta(CH_2)$, $\tau(CH_2)$, ν_a(COC), ν(CO) of –COO– and ν(CO) of $–OC_2H_5$ group of PEMA; and ν(CH), $\omega(CH_2)$, $\nu_a(CF_2)$, IR bands corresponding to the α–phase and amorphous region of PVdF–HFP. Figure 4.4 shows the schematic diagrams of the polymer chains in pure PEMA, PVdf–HFP and the intermolecular interactions within and between polymers are represented by dotted lines. From the results in this section, PEMA and PVdF–HFP are miscible with each other to form a polymer blend through the interactions between the carbon (C) atom in the C=O group of PEMA with the fluorine (F) atoms in CF_3 group of PVdF–HFP, and between the C atom of CF_3 group of PVdF–HFP with the oxygen (O) atom in –COC– group of PEMA.

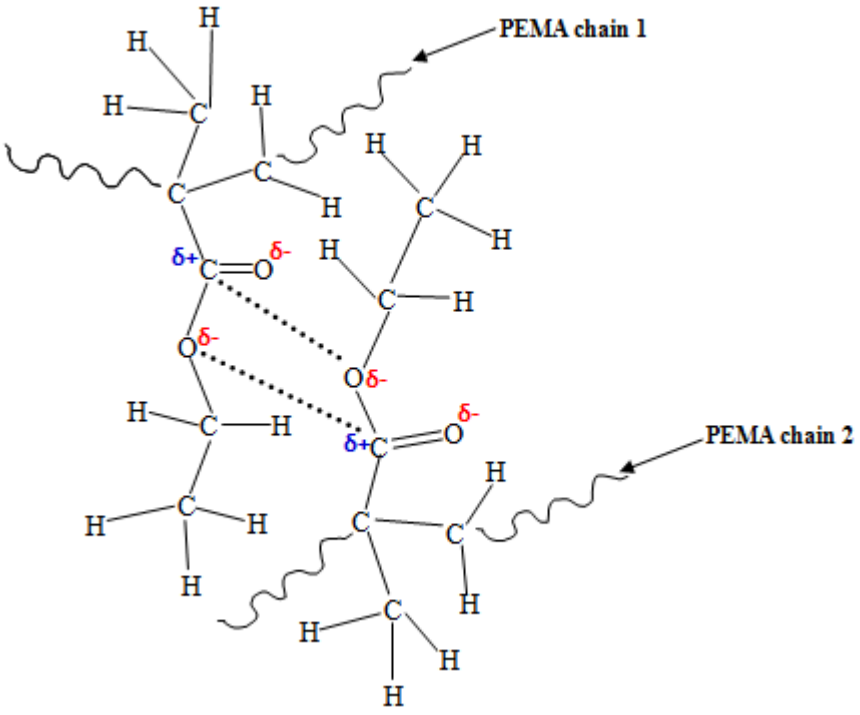

(a)

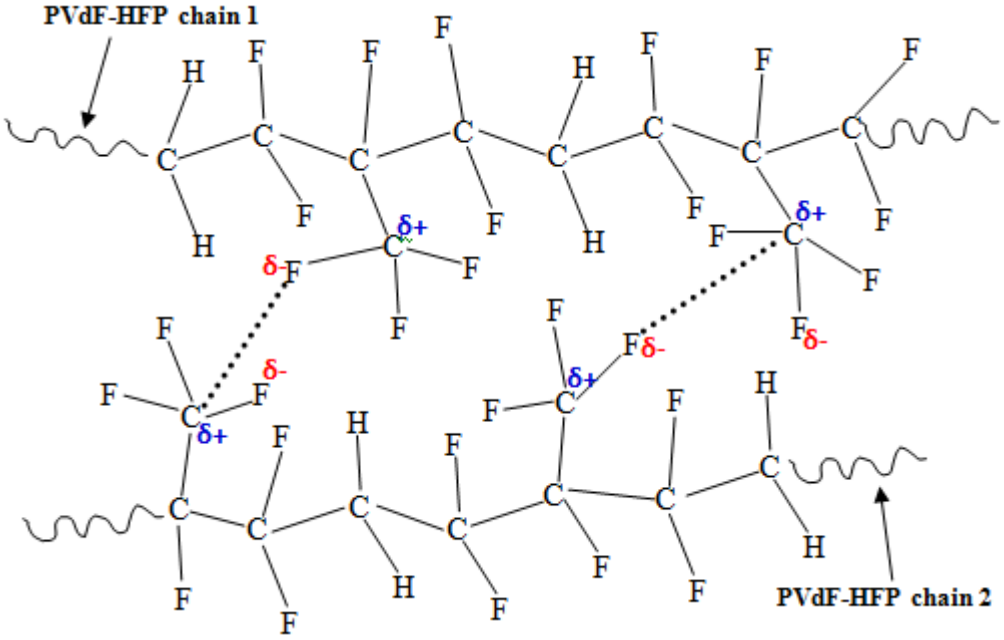

(b)

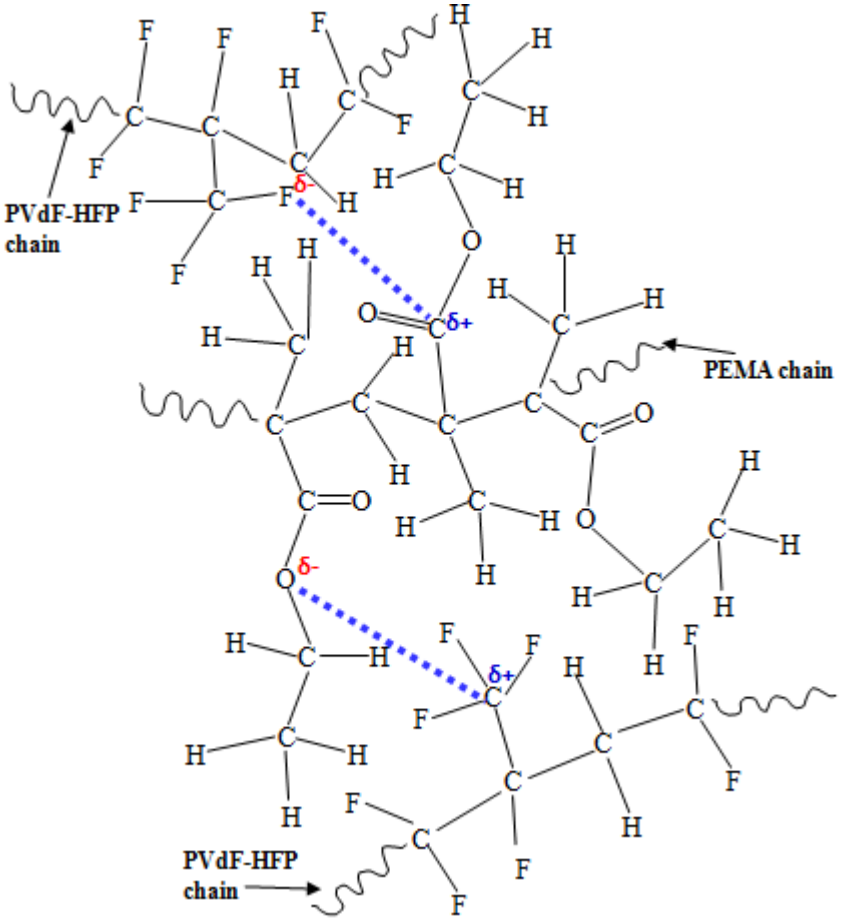

(c)

Figure 4.4 Schematic diagram of possible interactions in (a) PEMA, (b) PVdF–HFP and (c) S–0 (where•••• represents interactions within a polymer and▪▪▪ represents intermolecular interactions between PEMA and PVdF–HFP)

4.2.2 Interactions between PEMA/PVdF–HFP blend and LiTf

Now that the IR results have shown that interactions have occurred between PEMA and PVdF–HFP to form a polymer blend which shows miscibility, it is now of our interest to study the effect of LiTf on PEMA/PVdF–HFP blend system. The IR spectra of 70 wt.% PEMA–30 wt.% LiTf and 70 wt.% PVdF–HFP–30 wt.% LiTf films were used as references and compared with the spectrum of S–30. The triflate (Tf^-) ion is very sensitive to its state of coordination hence changes to its environment can be detected by different IR vibrational bands [MacFarlane et al., 1995]. The IR bands of LiTf from literature are tabulated in Table 4.3.

Table 4.3 Assignment of FTIR vibrational bands of LiTf

Assignment of bands	Wavenumber (cm^{-1})	Reference
$\delta(CF_3)$	756	Pandey and Hashmi (2009)
$\nu_a(SO_3)$	1251	Kumar et al. (2005)
	1263	Subban and Arof (2004)
$\nu_s(CF_3)$	1229	Kumar et al. (2005)
	1228	Subban and Arof (2004)
$\nu_s(SO_3)$	1032	Kumar et al. (2005)
	1033	Subban and Arof (2004)
$\nu_a(CF_3)$	1167	Kumar et al. (2005)
	1181	Subban and Arof (2004)

In our work, it was observed that the Tf^- anion exhibited fundamental vibrational modes at 1252, 1231, 1195 and 1044 cm^{-1} due to asymmetric SO_3 stretch [$\nu_a(SO_3)$], symmetric CF_3 stretch [$\nu_s(CF_3)$], asymmetric CF_3 stretch [($\nu_a(CF_3)$] and symmetric SO_3 stretch [$\nu_s(SO_3)$] vibrational modes, respectively [Kumar et al., 2005; Subban and Arof, 2004], Figure 4.1 (b–viii). Other characteristic bands of LiTf were observed around 3530, 1293 and 1649 cm^{-1}, Figure 4.1 (a–viii and b–viii). Table 4.4 shows the IR vibrational frequencies of PEMA/PVdF–HFP blend PE films incorporated with different amounts of LiTf salt.

The band of $\nu_s(SO_3)$ of pure LiTf was observed at 1044 cm^{-1} and appeared as peaks at 1031–1032 cm^{-1} which increased in intensity with increasing salt contents in the polymer blend–salt complexes. The $\nu_s(CF_3)$ band originally located at 1231 cm^{-1} appeared in S–20, S–30 and S–40 at 1229 cm^{-1}. The band due to in–plane deformation of CF_3 [$\delta_s(CF_3)$] of LiTf was observed to shift from 773 cm^{-1} to lower wavenumbers at 763 cm^{-1} in S–20, and 762 cm^{-1} in both S–30 and S–40 samples with increased intensities at higher salt contents. The appearance of characteristic bands due to Tf^- anion in polymer blend–salt complexes indicates that the incorporation of LiTf into the polymer blend has been achieved. Figure 4.5 (a) to (h) depict the IR spectra of LiTf–based polymer electrolytes and LiTf salt from 1800 to 1600 cm^{-1} of the ν(C=O) of PEMA.

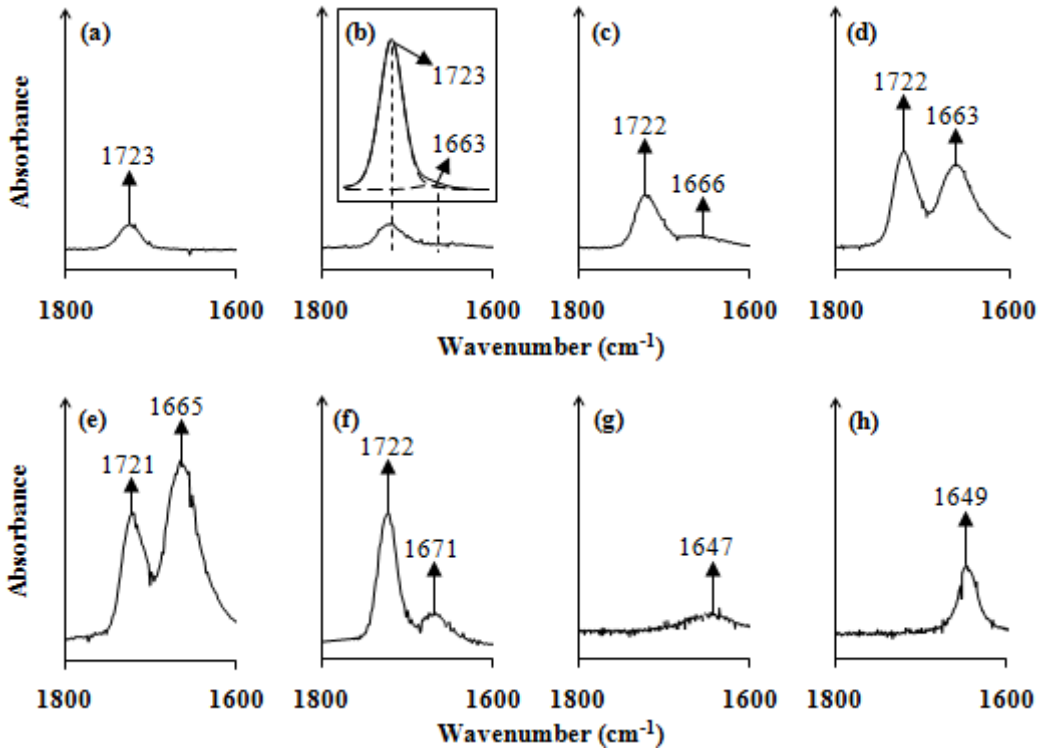

Figure 4.5 FTIR spectra in the region 1800–1600 cm^{-1} for (a) S–0, (b) S–10 (Inset: Enlarged deconvoluted bands of S–10), (c) S–20, (d) S–30, (e) S–40, (f) 70 wt.% PEMA–30 wt.% LiTf, (g) 70 wt.% PVdF–HFP–30 wt.% LiTf and (h) LiTf

The IR band located at 1721–1723 cm^{-1} is attributed to the ν(C=O) band of PEMA. The fact that this peak did not exhibit much change from its original position in pure PEMA and in pure PEMA/PVdF–HFP blend when added with LiTf probably implies that complexation must have mainly occurred at the O atom in the $–OC_2H_5$ ethylene group. However, the increase in intensity of the ν(C=O) band observed in S–20, S–30 and S–40 is also an indication that a greater amount of Li^+ ions have complexed with the oxygen atom in C=O upon increase in salt content.

Figure 4.6 depicts the IR bands of polymer blend–salt complexes situated in the region 1220–1120 cm^{-1} where the ν_a(COC) (band **II**) and ν(CO) of $–OC_2H_5$ group belonging to PEMA and the $\nu_a(CF_2)$ band of PVdF–HFP (band **I**) are located. In S–0, the band due to the ν_a(COC) band from the ester group shifted from 1145 cm^{-1} to 1148 cm^{-1} in S–10, 1153 cm^{-1} in S–20 and became a shoulder at 1155 cm^{-1} in S–30, Figure 4.6 (a) to (d). The ν_a(COC) band gradually diminished to form a shoulder in S–30 could not be observed in S–40, Figure 4.6 (e). This is caused by the tremendous increase in the intensity of the IR band located at 1176 cm^{-1} which is due to the overlapping between $\nu_a(CF_2)$ of PVdF–HFP at 1179 cm^{-1} and the ν(CO) of $–OC_2H_5$ group of belonging to PEMA at 1175 cm^{-1}. The upshift of the ν_a(COC) mode of PEMA implied that coordination of Li^+ ions from LiTf salt had occurred at the O atom of C–O–C group in PEMA/PVdF–HFP–LiTf electrolytes. Compared to ν(C=O), the position shift of the ν_a(COC) band is more significant.

Figure 4.7 (a) and (b) show the IR spectra of PEMA and PVdF–HFP samples before and after the incorporation of 30 wt.% LiTf salt. The IR spectrum of 70 wt.% PVdF–HFP–30 wt.% LiTf also showed that the ν_a(COC) band of PEMA shifted to

higher wavenumber from 1142 to 1150 cm^{-1}. On the other hand, the $\nu_a(CF_2)$ band of PVdF–HFP broadened and became more intense upon addition of 30 wt.% LiTf.

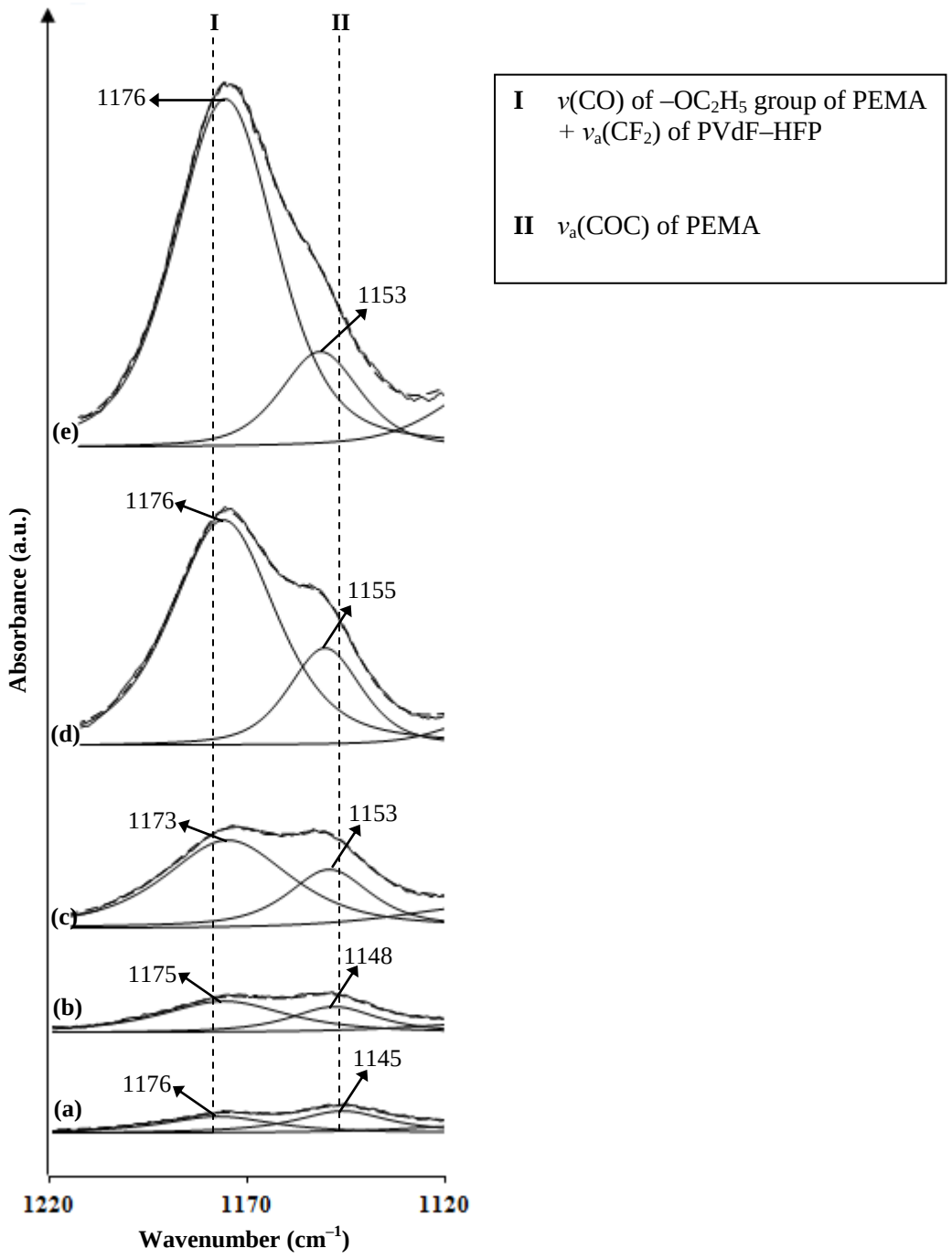

Figure 4.6 Deconvoluted FTIR spectra in the region 1220–1120 cm^{-1} for (a) S–0, (b) S–10, (c) S–20, (d) S–30 and (e) S–40

Other vibrational modes related to the C–O bond of PEMA also manifested large shifts to higher wavenumbers when incorporated up to 40 wt.% LiTf such as the

other ν_a(COC) band from 1241 to 1251 cm^{-1} and ν(CO) of –COO– group from 1272 to 1283 cm^{-1} respectively (Table 4.4). Hence, the shifting of the ν_a(COC) and ν(CO) bands due to –COO– group of PEMA indicates that the coordination of Li^+ ions occurred at the O atom of the –COC– group present in PEMA.

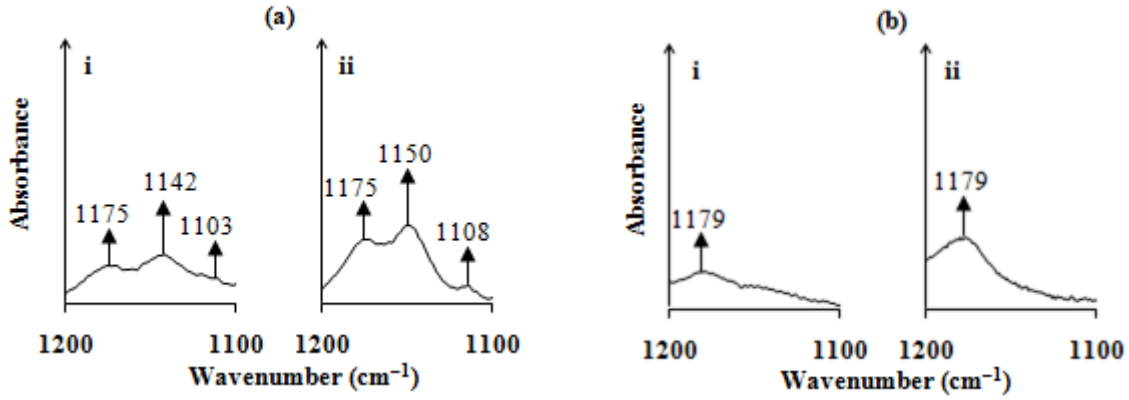

Figure 4.7 FTIR spectra in the region 1200–1100 cm^{-1} of (a) PEMA–based film, (b) PVdF–HFP based film containing i. 0 and ii. 30 wt. % of LiTf

Upon the addition of LiTf, the IR spectra of PEMA/PVdF–HFP films showed that the band due to $\nu_a(CF_2)$ of PVdF–HFP + ν(CO) of $–OC_2H_5$ group of PEMA shifted from 1176 to 1175 cm^{-1} in S–10 and to 1173 cm^{-1} in S–20 with tremendous increase in intensity, Figure 4.6 (a) to (c). This band then returned to its original position at 1176 cm^{-1} with increased intensity for S–30, Figure 4.6 (d). In S–40, this peak records the highest intensity although the wavenumber maintained at 1176 cm^{-1}. The change in shape for the $\nu_a(CF_2)$ band of 70 wt.% PVdF–HFP–30 wt.% LiTf in Figure 4.7 (b) indicates that Li^+ ions have coordinated onto the CF_2 group in S–30 and S–40 samples although no wavenumber shift was observed. The changes in the wavenumbers of the band comprised of both $\nu_a(CF_2)$ vibration of PVdF–HFP and ν(CO) vibrational band of PEMA suggested that coordination of Li^+ ions had occurred at the fluorine (F) atoms of CF_2 group belonging to PVdF–HFP.

In the region 1340–1200 cm^{-1}, several vibrational bands belonging to PEMA and LiTf superimposed on one another to form a broad band composed of few components which increased in intensity from low to high content of salt as depicted in Figure 4.8.

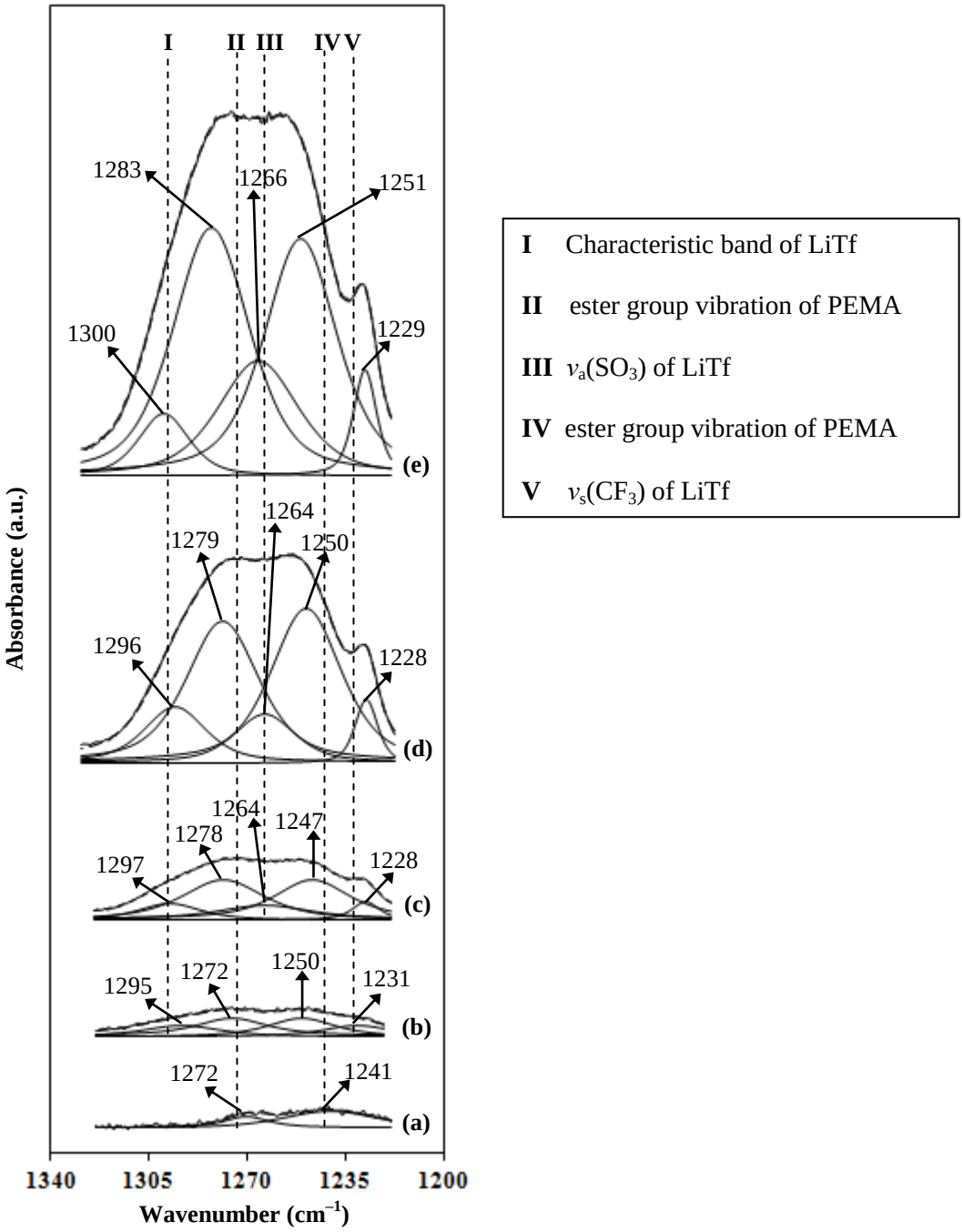

Figure 4.8 Deconvoluted FTIR spectra between 1340–1200 cm^{-1} for (a) S–0, (b) S–10, (c) S–20, (d) S–30 and (e) S–40

The band due to $\nu_s(CF_3)$ of LiTf maintained at 1229 cm^{-1} and became more intense with increasing LiTf content. Other Tf^- bands also grew in intensity with increasing salt content. Two bands at 1265 cm^{-1} and 1249 cm^{-1} in S–0 attributed to the different vibrations of the PEMA ester group ($–COOC_2H_5$) were observed to shift to higher IR positions. The shifting of the bands was caused by the interactions between Li^+ ions and the partially negative O atom of the ester group.

Figure 4.9 (a) and (b) illustrate the IR regions 1450–1350 cm^{-1} and 1100–1000 cm^{-1} where the $\omega(CH_2)$ and $\gamma(CF_3)$ bands of PVdF–HFP are situated. The $\gamma(CF_3)$ band of PVdF–HFP shifted from 1069 to 1079 cm^{-1}.

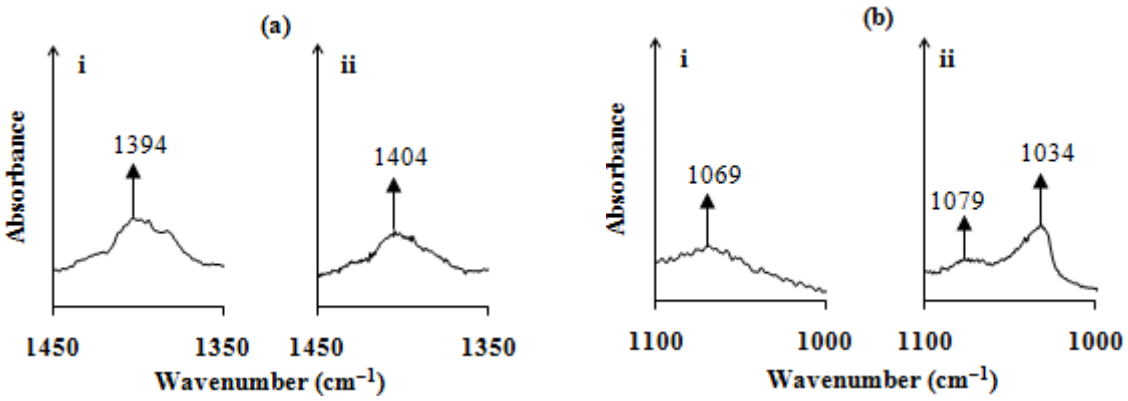

Figure 4.9 FTIR spectra in the region (a) 1450–1350 cm^{-1} and (b) 1100–1000 cm^{-1} for i. PVdF–HFP and ii. 70 wt.% PVdF–HFP–30 wt.% LiTf

At lower wavenumber region in Figure 4.1 (c), the band due to the amorphous region of PVdF–HFP shifted slightly to lower wavenumbers from 885 to 883, 882, 881 and 882 cm^{-1} in S–10, S–20, S–30 and S–40, respectively. With increasing salt content, this band was observed to become sharper with increased intensity, which indicates that more Li^+ ions interact with the amorphous region of PVdF–HFP. This implies that interaction had taken place between lithium salt with the $\gamma(CF_3)$ vibrational bands as well as the amorphous region of PVdF–HFP.

The shifting of the ν_a(COC), ν(CO) of $-OC_2H_5$ group and ν(CO) of –COO– group of PEMA and the $\nu_a(CF_2)$ band of PVdF–HFP shows that Li^+ ions have coordinated at the O atoms of C=O and C–O–C groups of PEMA, and F atoms in CF_2 group. Figure 4.10 illustrates the schematic diagram of interactions in PEMA/PVdF–HFP–LiTf system.

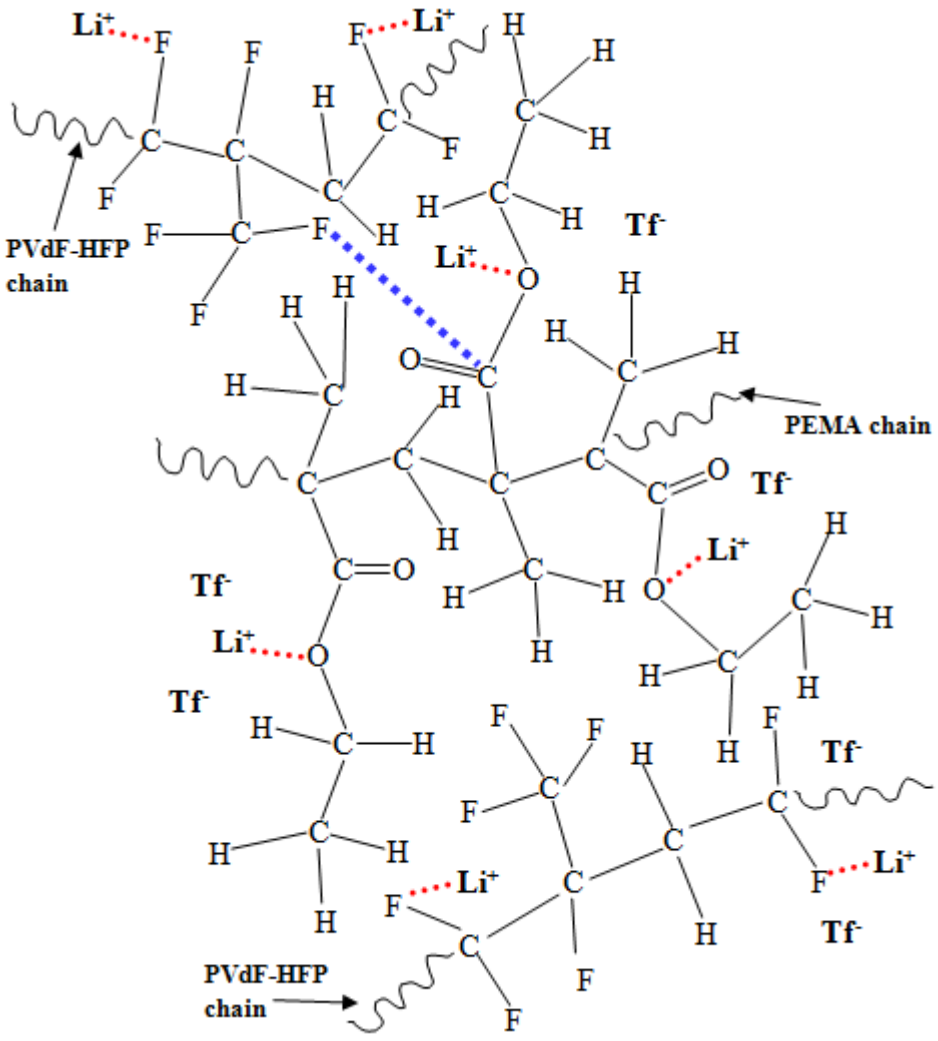

Figure 4.10 Schematic diagram of possible interactions in PEMA/PVdF–HFP–LiTf system (where ▪▪▪ represents intermolecular interactions between PEMA and PVdF–HFP and ••••represents coordinate bonds between Li^+ ions and PEMA/PVdF–HFP)

4.2.3. Interactions between Li^+ and $CF_3SO_3^-$ ions, and the expected effect on the ionic conductivity of PEMA/ PVdF–HFP–LiTf system

In Section 4.2.2, the IR results have shown that coordination of Li^+ occur at the C=O and C–O–C groups of PEMA and CF_2 group of PVdF–HFP in the polymer blend system. In order to study the ionic association between Li^+ cation and Tf^- anion, the symmetric SO_3 stretch [$\nu_s(SO_3)$] of pure LiTf was investigated in the IR region 1100–980 cm^{-1} in Figure 4.11 to determine the presence of free ions, ion pairs and highly aggregated ions in the polymer blend–salt complexes. The band located around 1019–1022 cm^{-1} belongs to the δ(C–H) band of PEMA.

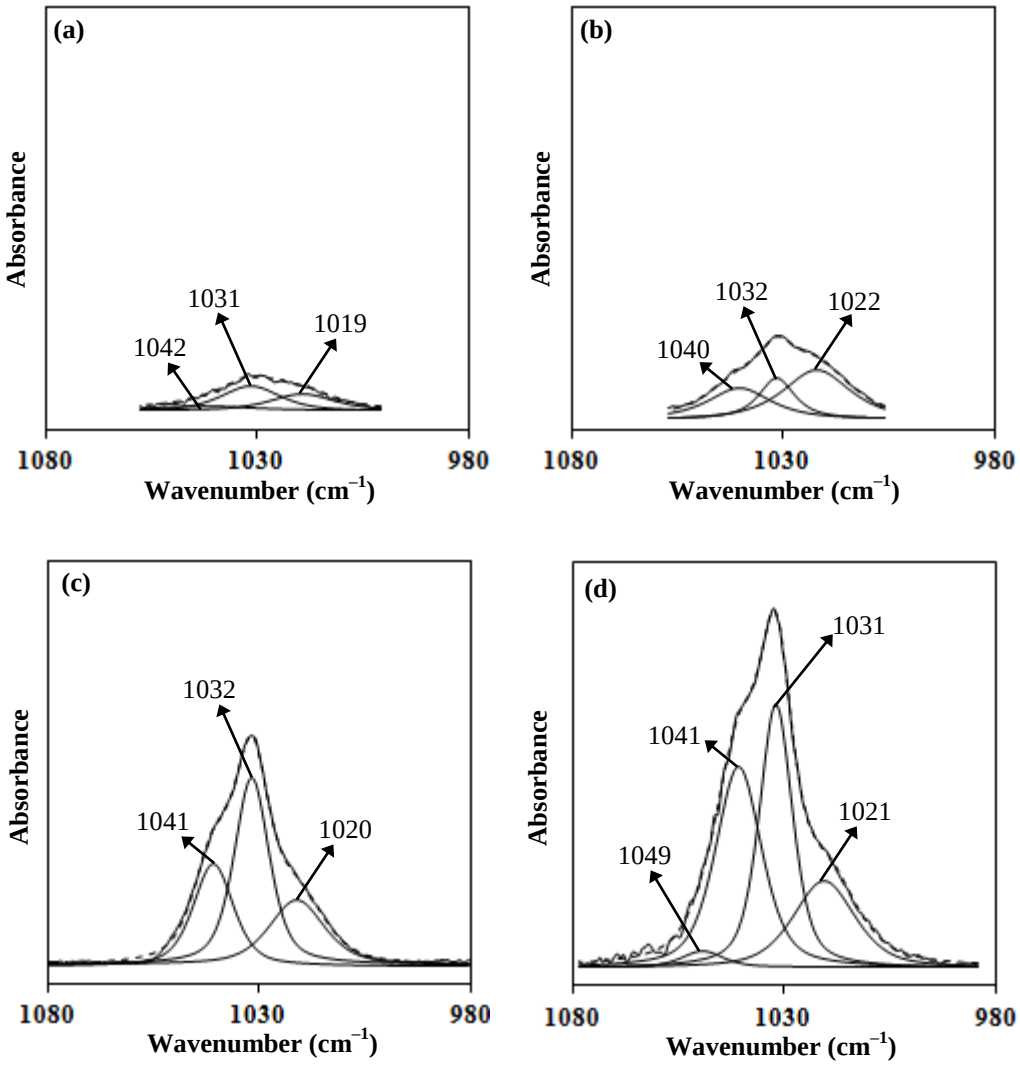

Figure 4.11 Deconvolution between 1080 and 980 cm^{-1} of (a) S–10, (b) S–20, (c) S–30 and (d) S–40

Upon the addition of LiTf salt into PEMA/PVdF–HFP blend, the $v_s(SO_3)$ band attributable to free triflate anions [Huang and Frech, 1992] was shifted from its original position at 1044 cm^{-1} to 1031–1032 cm^{-1}. In addition to free ions, another band arising from ion pairs of LiTf at 1040–1042 cm^{-1} was also observed in all samples. For S–40 sample, a new band found at 1049 cm^{-1} appeared; this IR band belongs to the ion aggregates, Figure 4.11 (d). The area of the different ionic species of the Tf^- ion with respect to the LiTf salt content is shown in Figure 4.12.

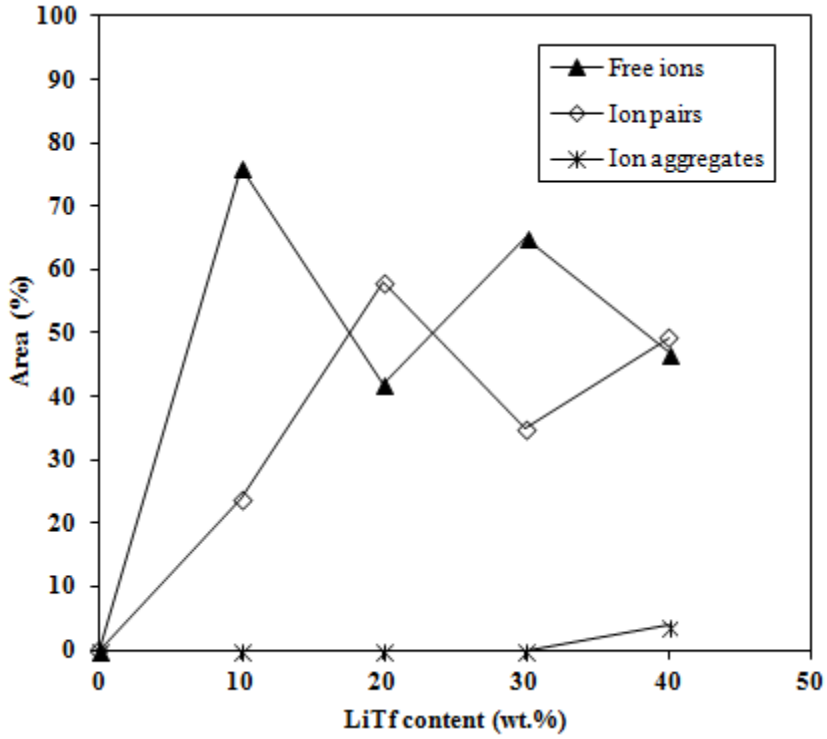

Figure 4.12 Area % of the different ionic species of the triflate anion with respect to wt. % of LiTf in PEMA/PVdF–HFP (70:30) blend

From Figure 4.12, it could be observed that area % of free ions was highest upon addition of 10 wt.% LiTf while maximum of ion pairs was present at 20 wt.% LiTf. The area % of free ions increased again at 30 wt.% LiTf before decreasing at 40 wt.% content of the salt. The $v_s(SO_3)$ band due to ion aggregates only appeared when 40 wt.% LiTf was added with area % of ~ 5 %.

Table 4.4 FTIR vibrational modes of PEMA/PVdF–HFP blend polymer electrolytes incorporated with different wt.% of LiTf

Assignment of bands	Wavenumber (cm^{-1})				
	S–0	**S–10**	**S–20**	**S–30**	**S–40**
ν(CH)	2989, 2946, 2924	2990, 2946, 2912	2992, 2944, 2911	2988, 2943, 2912	2991, 2943, 2915
ν(C=O) of PEMA	1723	1723	1722	1722	1721
$\delta(CH_2)$of PEMA	1485	1490	1482	1482	1488
$\gamma(OC_2H_5)$of PEMA	1448	1448	1449	1448	1448
$\omega(CH_2)$ of PVdF–HFP + $\tau(CH_2)$ of PEMA	1389	1387	1389	1392	1392
Characteristic band of LiTf	–	1295	1297	1296	1300
ν(CO) of –COO– group of PEMA	1272	1272	1278	1279	1283
$\nu_a(SO_3)$ of LiTf	–	–	1264	1264	1266
ν_a(COC) of PEMA	1241	1250	1247	1250	1251
$\nu_s(CF_3)$ of LiTf	–	1231	1228	1228	1229
$\nu_a(CF_2)$ of PVdF–HFP + ν(CO) of $-OC_2H_5$ group of PEMA	1176	1175	1173	1176	1176
ν_a(COC) of PEMA	1145	1148	1153	1155	1153
Characteristic band of PEMA	1106	1112	1114	1113	1110
$\nu_s(SO_3)$ ion aggregates of LiTf	–	–	–	–	1049
$\nu_s(SO_3)$ ion pairs of LiTf	–	1042	1040	1041	1041
$\nu_s(SO_3)$ free ions of LiTf	–	1031	1032	1032	1031
α–phase of PVdF–HFP	984	968	967	969	968
Amorphous region of PVdF–HFP	885	883	882	881	882
β–phase of PVdF–HFP	–	841	835	838	842
$\delta_s(CF_3)$ of LiTf	773	–	763	762	762

4.3 Plasticized PEMA/PVdF–HFP–LiTf Polymer Electrolyte Systems

4.3.1 PEMA/PVdF–HFP–LiTf–EC System

4.3.1.1 Interactions between PEMA/PVdF–HFP–LiTf and EC

The IR spectra of PEMA/PVdF–HFP–LiTf–EC films are shown in Figure 4.13. The ν(C=O) mode of EC is split into two bands located at 1791 and 1770 cm^{-1}. The splitting is due to Fermi resonance of the C=O stretching mode caused by dipole–dipole coupling of two EC molecules [Fini et al., 1973]. The electropositively charged carbon atom of the carbonyl group in one EC molecule will be electrostatically attracted to the electronegatively charged oxygen atom of another EC molecule, and vice versa. Table 4.5 displays the IR bands of EC obtained from literature.

Upon incorporation of EC into the PEMA/PVdF–HFP:LiTf system, changes in IR intensity and position were observed. The observations are tabulated in Table 4.6. Figure 4.14 depicts the IR region 1850–1600 cm^{-1} where the carbonyl stretching modes [*v*(C=O)] of PEMA and EC are present.

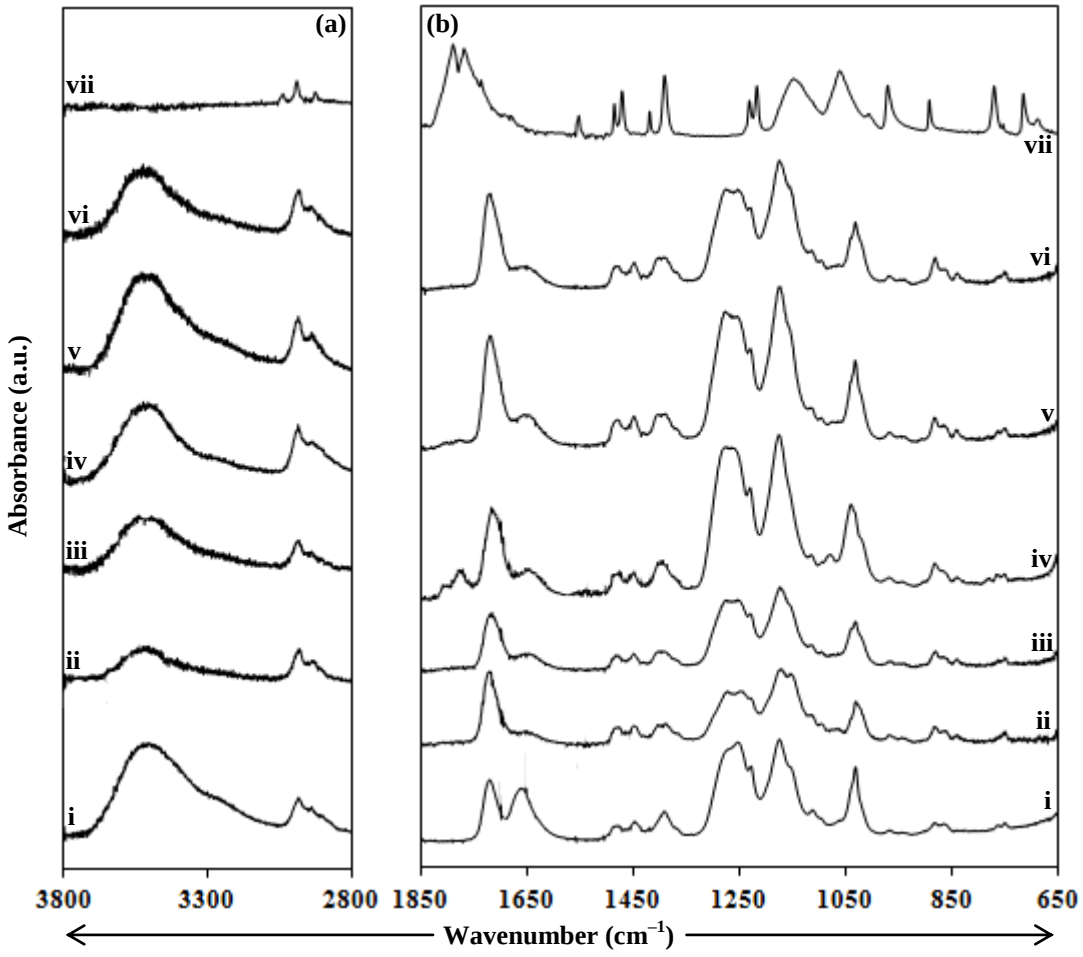

Figure 4.13 FTIR spectra in the region (a) 3800–2800 cm^{-1} and (b) 1800–800 cm^{-1} of i. EC–0, ii. EC–2, iii. EC–4, iv. EC–6, v. EC–8, vi. EC–10 and vii. EC

In all EC–added samples except EC–2, the *v*(C=O) band of PEMA shifted from 1722 cm^{-1} to lower wavenumbers, Figure 4.14 (b) to (f). Figure 4.14 (g) and (i) show that the *v*(C=O) mode of PEMA upshifted in 90 wt.% PEMA–10 wt.% EC and S–0–EC samples. This shows that the interaction between PEMA and EC tends to shift the *v*(C=O) mode of PEMA to higher wavenumber. Hence, the larger downshift of the *v*(C=O) mode of PEMA in EC–4 ($-\Delta$=5 cm^{-1}) and EC–6 ($-\Delta$=4 cm^{-1}) suggests that

more Li^+ ions instead of EC molecules have coordinated to the C=O group of PEMA. Kumutha and co–workers (2005) also reported no shifting of the *v*(C=O) mode of PMMA that was grafted onto natural rubber upon incorporation of EC and LiTf.

Table 4.5 Assignment of FTIR vibrational bands of EC

Assignment of bands	Wavenumber (cm^{-1})	Reference
v(CH)	3206, 3194, 3113–3110	Masia et al. (2004)
C=O stretch	1860	Osman et al. (2005)
	1774	Rajendran and Ramesh (2010)
	1762	Ali et al. (2006)
	1810–1871	Angell (1956)
	1776 and 1803	Fini and Mirone (1973)
	1773 and 1798	Huang et al. (1996)
	1774 and 1803	Osman and Arof (2003)
in phase CH_2 scissoring	1547	Masia et al. (2004)
out of phase CH_2 scissoring	1539	Masia et al. (2004)
CH_2 bending	1480	Angell (1956)
in phase CH_2 wagging	1421	Masia et al. (2004)
CH_2 wagging	1394 and 1420	Wang et al. (1996)
out of phase CH_2 twisting	1272	Masia et al. (2004)
in phase CH_2 twisting	1268	Masia et al. (2004)
skeletal stretching	970, 1076, 1180	Angell (1956)
out of phase CH_2 rocking	1175	Masia et al. (2004)
ring stretching	1230, 1138, 720	Masia et al. (2004)
ring breathing	1067, 890	Wang et al. (1996)
	992, 896	Masia et al. (2004)
	893	Osman and Arof (2003)
in phase CH_2 rocking	919	Masia et al. (2004)
out of plane ring C=O bending	780	Masia et al. (2004)
ring stretching	776	Idris et al. (2007)
C=O bending	715	Chintapalli and Frech (1996)

The *v*(C=O) vibrational modes of EC could only be observed clearly in EC–6 at 1811 and 1773 cm^{-1}. The large shift of the *v*(C=O) mode of EC in EC–6 from 1791 ($+\Delta$=17 cm^{-1}) and 1770 cm^{-1} ($+\Delta$=8 cm^{-1}) imply that there is large interaction between C=O group of EC and polymer blend–salt in the sample. In Figure 4.14 (k), the *v*(C=O) modes of EC were shifted in the LiTf–EC sample to 1802 and 1774 cm^{-1}. Osman and Arof (2003) also reported the upshift of the *v*(C=O) mode of EC from 1774 and 1803 cm^{-1} to 1775 and 1807 cm^{-1} in LiTf–EC sample.

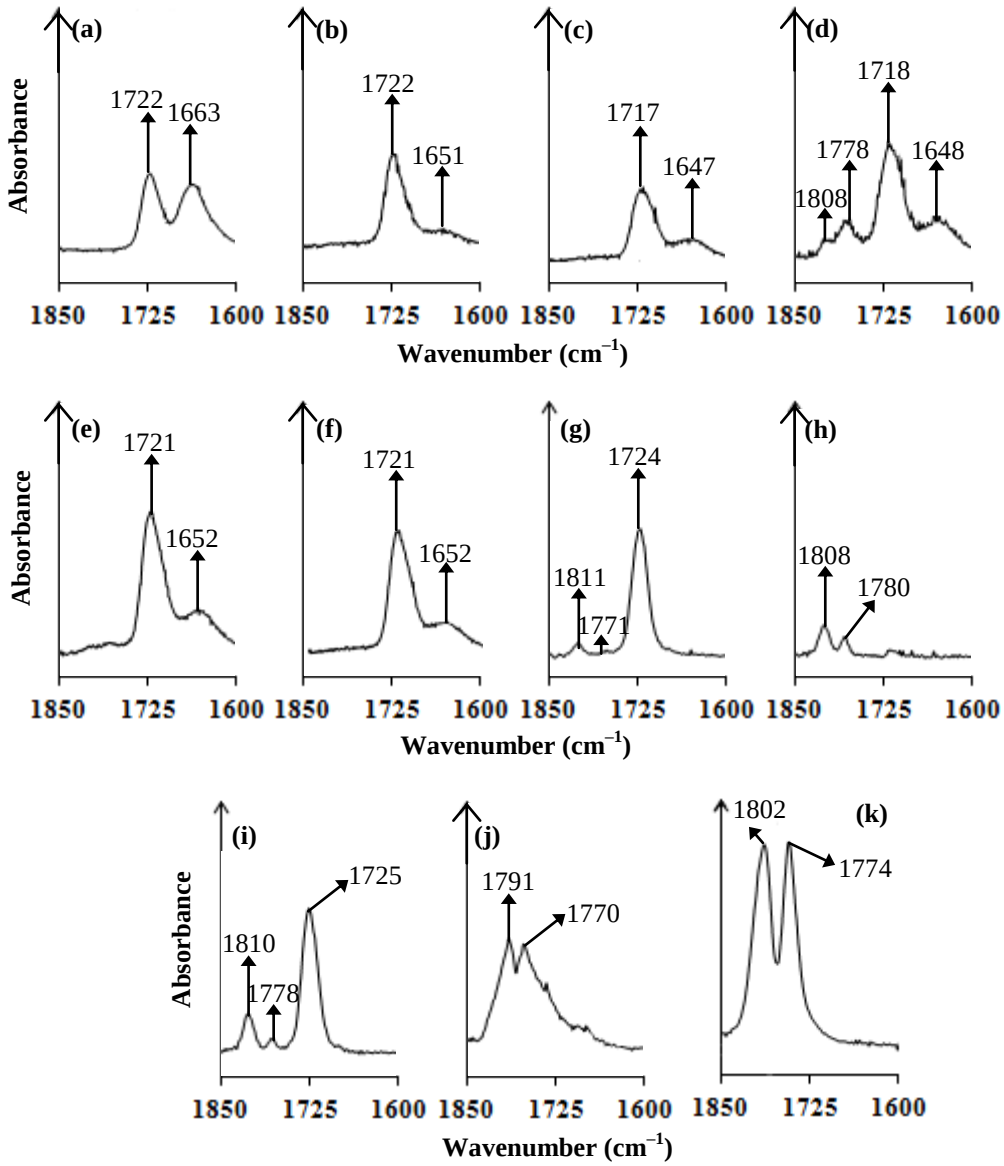

Figure 4.14 FTIR spectra in the region 1850–1600 cm^{-1} for (a) EC–0, (b) EC–2, (c) EC–4, (d) EC–6, (e) EC–8, (f) EC–10, (g) 90 wt.% PEMA–10 wt.% EC, (h) 90 wt.% PVdF–HFP–10 wt.% EC, (i) S–0–EC, (j) EC and (k) LiTf–EC

The IR shifting of the *ν*(C=O) band of EC suggests that Li^+ ions have coordinated to the O atom of the plasticizer [Osman and Arof, 2003; Chintapalli and Frech, 1996]. Thus, in the polymer blend–salt–plasticizer samples, the shifting of the *ν*(C=O) mode of EC can be due to the interaction between EC and polymer(s) or the coordination of Li^+ on EC. This is because electrostatic interactions can occur between the negatively charged O atom on the C=O group of PEMA and the positively charged C atom on C=O group of EC, and vice versa. Figure 4.15 depicts the deconvoluted IR

bands in the wavenumber region 1340–1200 cm^{-1} for PEMA/PVdF–HFP–LiTf–EC system to investigate the ν_a(COC) and ν(CO) of –COO– group of PEMA as well as $\nu_a(SO_3)$ of LiTf.

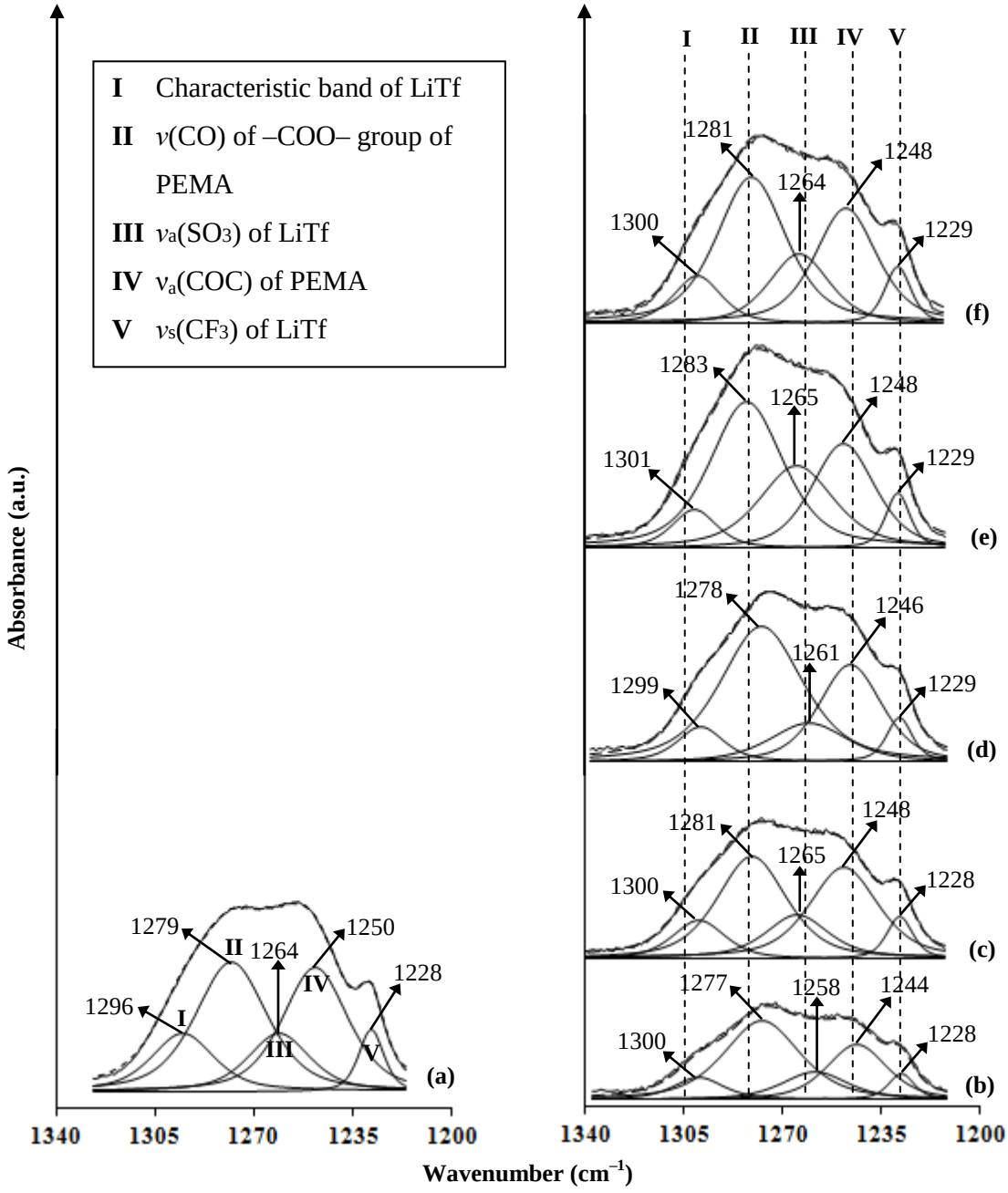

Figure 4.15 Deconvoluted FTIR spectra of (a) EC–0, (b) EC–2, (c) EC–4, (d) EC–6, (e) EC–8 and (f) EC–10 in the region 1340–1200 cm^{-1}

The $\nu_a(SO_3)$ mode of LiTf (band **III**) also manifested position shift from 1264 to 1258–1265 cm^{-1}. The $\nu_s(CF_3)$ mode (band **V**) did not show significant wavenumber

shift from its original position at 1228 cm^{-1}. On the other hand, the IR bands belonging to PEMA such as the *ν*(CO) mode of –COO– group (band **II**) originally at 1279 cm^{-1} shifted to 1277–1283 cm^{-1} while the ν_a(COC) band (band **IV**) downshifted from 1250 to 1244–1248 cm^{-1}. The shifting of the IR bands belonging to LiTf and PEMA in the IR region shown in Figure 4.15 suggests that EC has interacted with LiTf and PEMA to some extent.

Figure 4.16 shows the deconvoluted IR bands of EC, EC–0 and EC–containing PEMA/PVdF–HFP–LiTf films in the region 1220–1120 cm^{-1}. The IR spectra of EC shows the skeletal stretching (band **III**) located at 1149 cm^{-1}, Figure 4.16 (b). In all EC–added samples except EC–10, the skeletal stretching of EC appeared to downshift to 1140–1141 cm^{-1} ($-\Delta$=8 to 9 cm^{-1}). In EC–10, the skeletal stretching of EC upshifted to 1150 cm^{-1}, which is close to the original position at 1149 cm^{-1} in EC, Figure 4.16 (g). For comparison of IR spectra of PEMA, PVdF–HFP, S–0 and LiTf before and after the addition of EC, deconvolution of the EC–added samples were shown in Figure 4.17.

In PEMA–EC, PVdF–HFP–EC and polymer blend–EC samples as shown in Figure 4.17 (b–d), the skeletal stretching mode of EC shifted to lower wavenumbers upon interaction with the polymers. On the other hand, the interaction between LiTf and EC tends to upshift the IR band as shown in Figure 4.17 (a). The extent of the downshift in the IR wavenumber of the skeletal stretching mode of EC in PEMA/PVdF–HFP–LiTf–EC samples ($-\Delta$=8 to 9 cm^{-1}) incorporated with up to 8 wt.% EC is observed to be less as compared to that of S–0–EC ($-\Delta$=12 cm^{-1}). An explanation for this phenomenon is that EC has interacted with both the polymers in the polymer blend, and also with the Li^+ ions simultaneously.

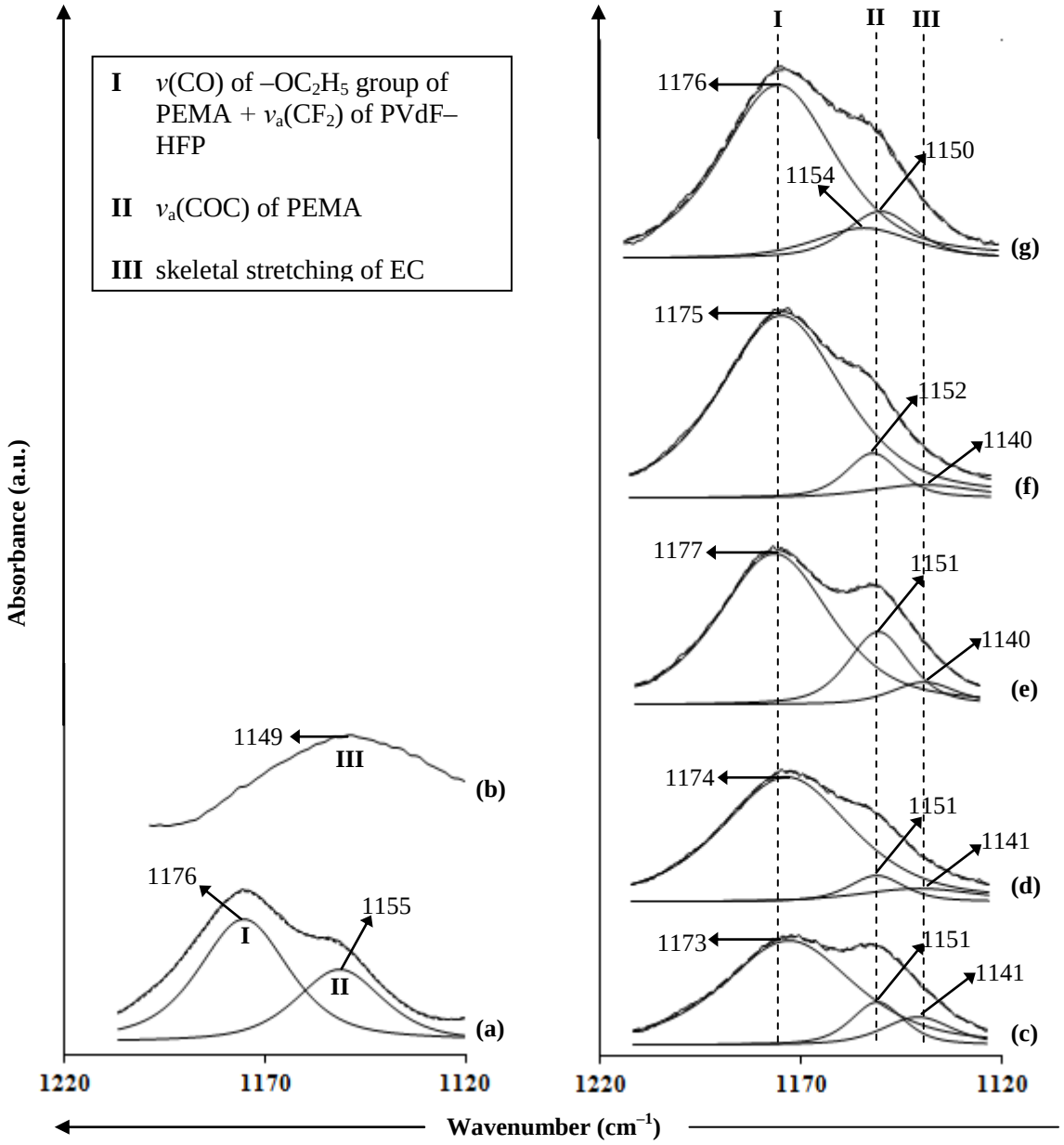

Figure 4.16 Deconvoluted FTIR spectra in the region between 1220 and 1120 cm^{-1} of (a) EC–0, (b) EC, (c) EC–2, (d) EC–4, (e) EC–6, (f) EC–8 and (g) EC–10 between 1220–1120 cm^{-1}

The larger downshift of the band in EC–2, EC–4, EC–6 and EC–8 implies that the coordination of EC onto PEMA and PVdF–HFP or/and Li^+ ions is more apparent in the samples. Hence, the upshift of the skeletal stretching band of EC to approach its original position in EC–10 could suggest decreased interactions in the sample.

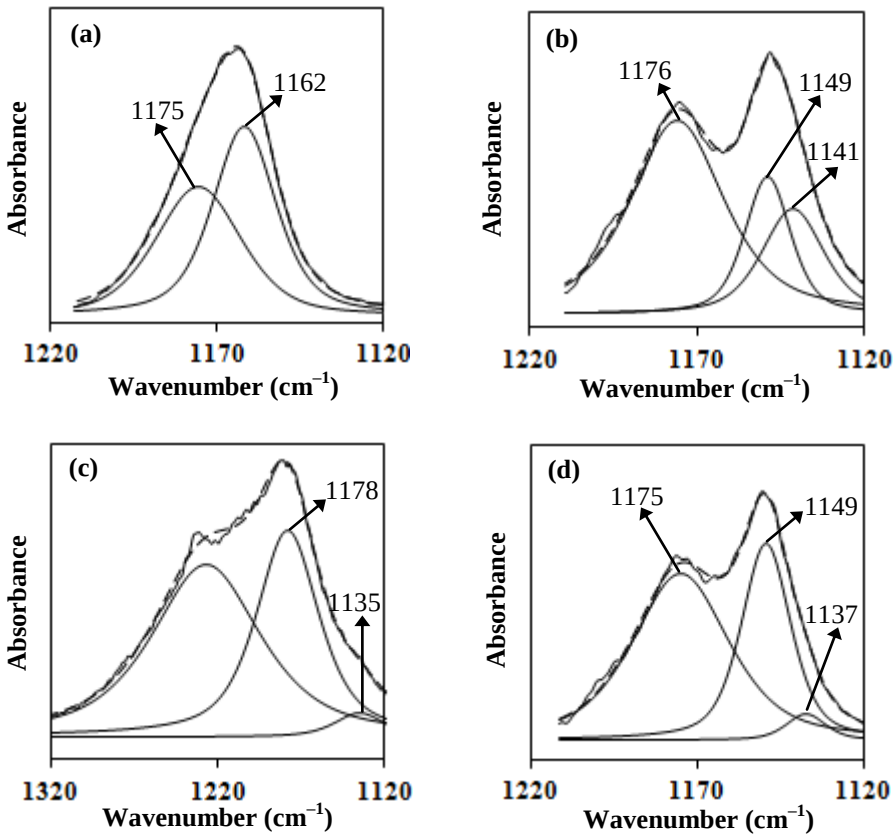

Figure 4.17 Deconvoluted FTIR spectra of (a) 6 wt.% LiTf–94 wt.% EC, (b) 90 wt.% PEMA–10 wt.% EC, (c) 90 wt.% PVdF–HFP–10 wt.% EC (in the region 1320–1120 cm^{-1}) and (d) 90 wt.% S–0–10 wt.% EC in the region 1220–1120 cm^{-1}

The $\nu_a(CF_2)$ of PVdF–HFP + ν(CO) band due to $–OC_2H_5$ group of PEMA (band **I**) located at 1176 cm^{-1} (Figure 4.16 (a)) in EC–0 film only shifted up to 3 cm^{-1} in the EC–added samples. In PEMA–EC, PVdF–HFP–EC and S–0 samples, the $–OC_2H_5$ group of PEMA and the $\nu_a(CF_2)$ mode of PVdF–HFP did not show any shift in wavenumber, indicating no interaction, Figure 4.17 (b) and (c). Hence, the increasing intensity of band **I** indicates that EC has interacted with the F atom on CF_2 groups of PVdF–HFP and the O atom in C–O–C group of PEMA.

The ν_a(COC) band of PEMA (band **II**) downshifted from 1155 cm^{-1} for EC–2, EC–4 and EC–6 samples, Figure 4.16 (c) to (e). This shifting indicates the coordination of EC onto the O atom in the C–O–C group of PEMA. Band **II** began to upshift to 1152 cm^{-1} and 1154 in EC–8 and EC–10, respectively, Figure 4.16 (f) and (g). The tendency

of the IR band to approach its original position indicates that interaction becomes less preferable in EC–8 and EC–10. The shifting of the ν_a(COC) band of PEMA in PEMA/PVdF–HFP–LiTf–EC samples indicates that EC does interact with the C–O–C group of PEMA. Thus, the shifting of the ν(C=O) and ν_a(COC) bands of PEMA and the combined $\nu_a(CF_2)$ vibration of PVdF–HFP + ν(CO) band due to $-OC_2H_5$ group of PEMA as well as the skeletal stretching and ν(C=O) band of EC infer that $Li^+\cdots$EC, $Li^+\cdots$O=C of PEMA, $Li^+\cdots$O=C of EC, C=O$\cdots$COC of PEMA and C=O$\cdots CF_2$ of PVdF–HFP interactions have occurred. The schematic diagram depicted in Figure 4.18 shows the possible interactions that take place in PEMA/PVdF–HFP–LiTf–EC polymer electrolyte system.

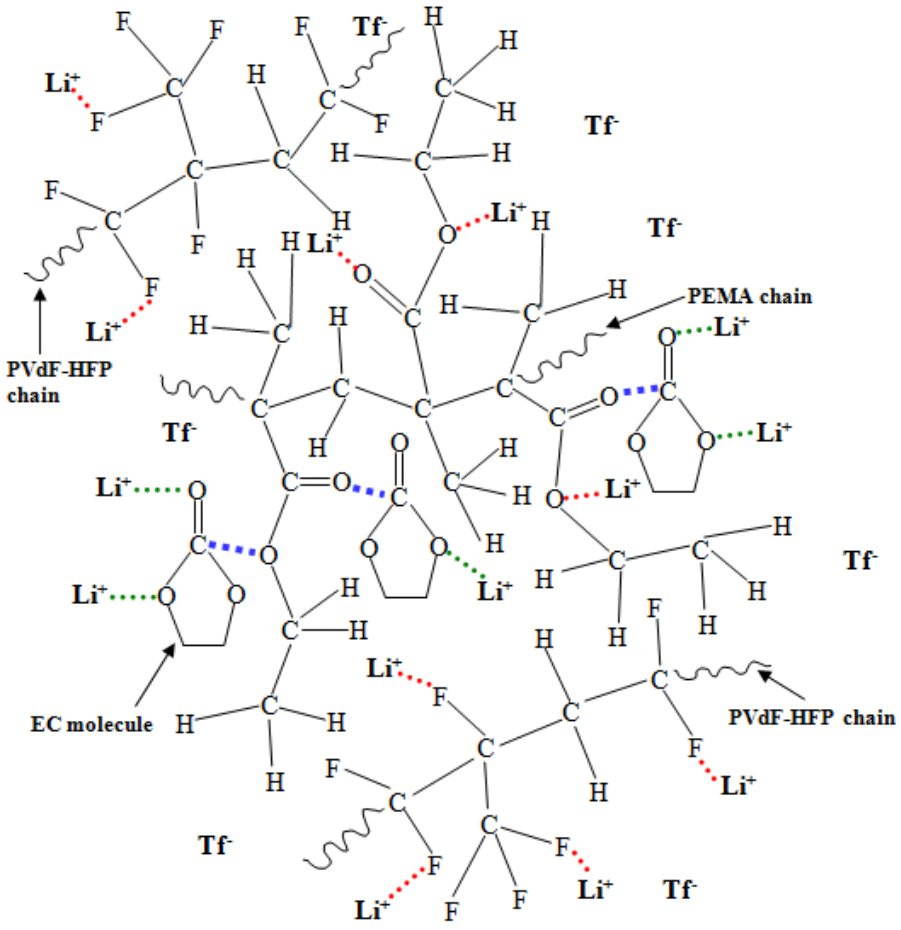

Figure 4.18 Schematic diagram of possible interactions in PEMA/PVdF–HFP–LiTf–EC system (where•••• represents the coordinate bonds with Li^+ ions,•••• represents electrostatic interactions between Li^+ and EC and▪▪▪ represents the intermolecular interactions between EC and PEMA/PVdF–HFP)

4.3.1.2 Interactions between Li^+ and $CF_3SO_3^-$ ions, and the effect expected on the ionic conductivity of PEMA/ PVdF–HFP–LiTf–EC system

In order to study the effect of EC on the ionic association of LiTf in PEMA/PVdF–HFP–LiTf–EC system, the IR region of 1080–980 cm^{-1} where the $\nu_s(SO_3)$ mode of LiTf lies is deconvoluted as shown in Figure 4.19.

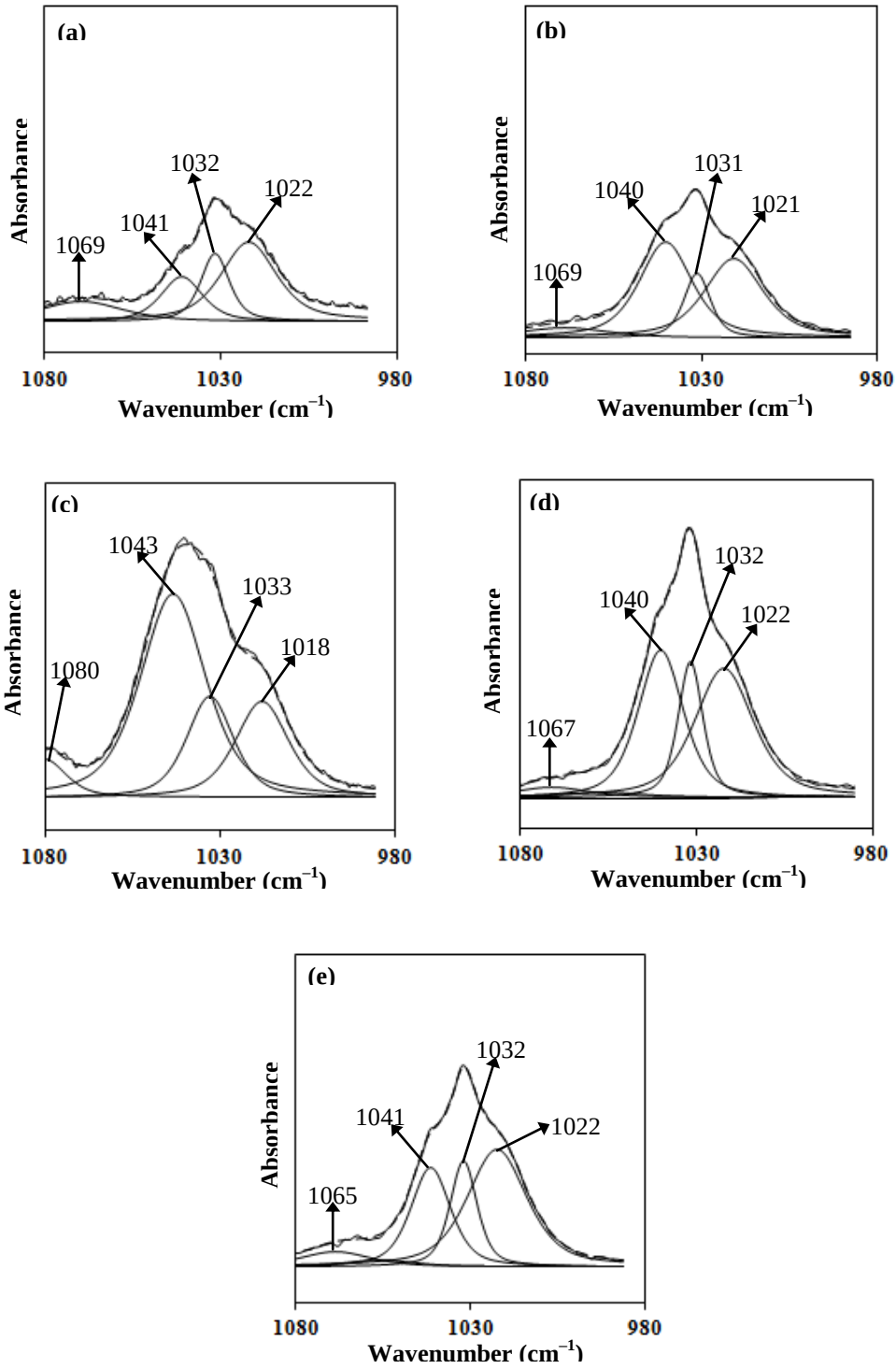

Figure 4.19 IR deconvoluted bands between 1080 and 950 cm^{-1} for samples (a) EC–2, (b) EC–4, (c) EC–6, (d) EC–8 and (e) EC–10

In all EC–containing samples, free ions and ion pairs are found at 1031–1033 cm^{-1} and 1040–1043 cm^{-1}, respectively. The band located around 1070 cm^{-1} in each spectrum (Figure 4.19 (a) to (e)) corresponds to ring breathing mode of EC originally at 1063 cm^{-1}. The δ(C–H) band of PEMA lies in the region from 1018 to 1022 cm^{-1}. The plot of area % of the different types of ionic species as a function of EC in PEMA/PVdF–HFP–LiTf–EC samples is depicted in Figure 4.20.

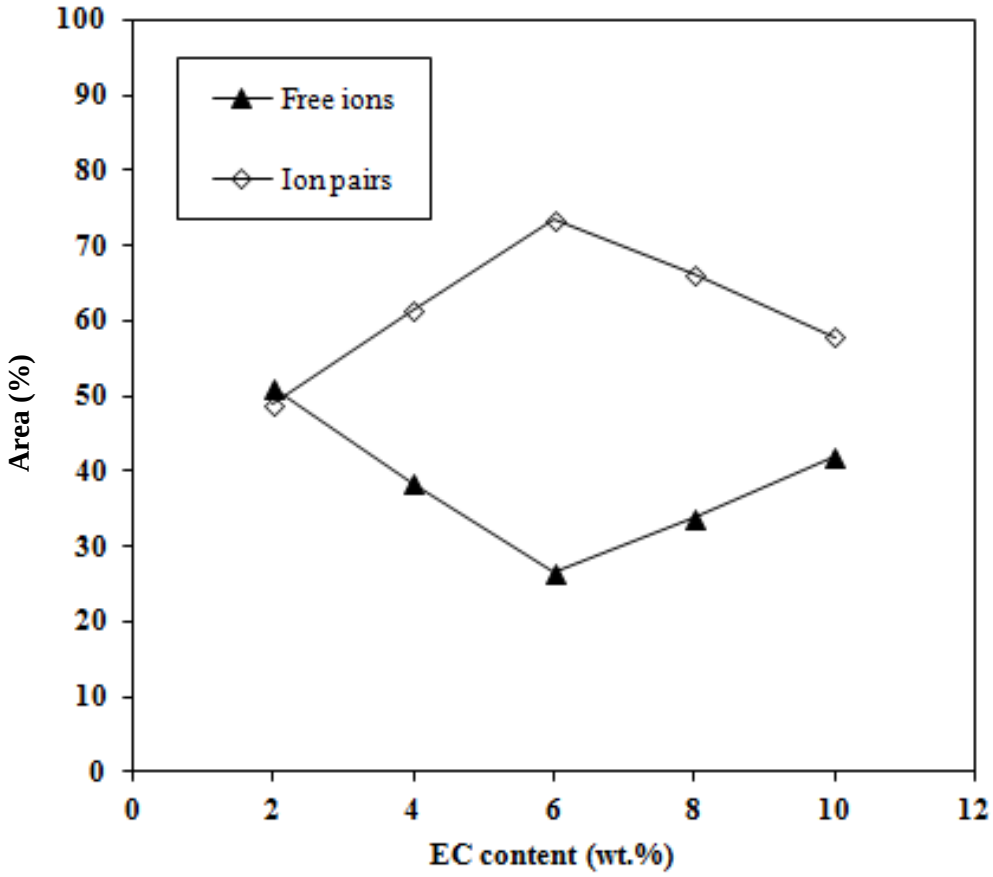

Figure 4.20 Area % of free ions and ion pairs with respect of EC content in 70 wt.% [PEMA/PVdF–HFP]–30 wt.% LiTf polymer electrolytes

The area % of ion pairs was observed to be higher than that of free ions at all EC–added samples. Ion pairs is present at its highest area % at 6 wt.% EC, while the area % of free ions was at its minimum for 6 wt.% of the plasticizer.

Table 4.6 FTIR vibrational modes of PEMA/PVdF–HFP:LiTf (70:30, w/w) blend polymer electrolytes incorporated with different wt.% of EC

Assignment of bands	Wavenumber (cm^{-1})						
	EC	**EC–0**	**EC–2**	**EC–4**	**EC–6**	**EC–8**	**EC–10**
ν(CH)	3043, 2993, 2929	2988, 2943, 2912	2985, 2943	2987, 2944	2986, 2942	2988, 2944	2987, 2944
ν(C=O) of EC	1791, 1770	–	–	–	1808, 1778	1807, 1779	–
ν(C=O) of PEMA	–	1722	1722	1717	1718	1721	1721
$\delta(H_2O)$ from LiTf	–	1663	1651	1650	1652	1653	1652
$\delta(CH_2)$of PEMA	–	1482	1479	1480	1481	1480	1484
$\gamma(OC_2H_5)$of PEMA	–	1448	1450	1450	1448	1450	1449
$\omega(CH_2)$ of PVdF–HFP + $\tau(CH_2)$ of PEMA	–	1392	1391	1390	1388	1391	1394
Characteristic band of LiTf	–	1296	1300	1300	1299	1301	1300
ν(CO) of –COO– group of PEMA	–	1279	1277	1281	1278	1283	1281
$\nu_a(SO_3)$ of LiTf	–	1264	1258	1265	1261	1265	1264
ν_a(COC) of PEMA	–	1250	1244	1248	1246	1248	1248
$\nu_s(CF_3)$ of LiTf	–	1228	1228	1228	1229	1229	1229
$\nu_a(CF_2)$ of PVdF–HFP + ν(CO) of $–OC_2H_5$ group of PEMA	–	1176	1173	1174	1177	1175	1176
ν_a(COC) of PEMA	–	1155	1151	1151	1151	1152	1154
Skeletal stretching of EC	1149	–	1141	1141	1140	1140	1150
Characteristic band of PEMA	–	1113	1114	1114	1114	1114	1114
Skeletal stretching of EC	1063	–	1069	1069	1081	1071	1069
$\nu_s(SO_3)$ ion aggregates of LiTf	–	–	–	–	–	1057	1056
$\nu_s(SO_3)$ ion pairs of LiTf	–	1041	1041	1040	1043	1040	1041
$\nu_s(SO_3)$ free ions of LiTf	–	1032	1032	1031	1033	1032	1032
α–phase of PVdF–HFP	–	969	967	969	968	969	970
Amorphous region of PVdF–HFP	–	881	882	880	881	884	882
β–phase of PVdF–HFP	–	838	841	841	840	842	841
$\delta_s(CF_3)$ of LiTf	–	762	750	750	750	750	751

4.3.2 PEMA/PVdF–HFP–LiTf–PC System

4.3.2.1 Interactions between PEMA/PVdF–HFP–LiTf and PC

The FTIR spectra of PEMA/PVdF–HFP–LiTf–PC polymer electrolyte system are shown in Figure 4.21. Table 4.7 lists the assignment of IR bands of PC from literature.

Table 4.7 Assignment of FTIR vibrational bands of PC

Assignment of band	Wavenumber (cm^{-1})	Reference
ν(CH)	2906, 2978	Rajendran and Sivakumar (2008)
ν(C=O)	1800	Deepa et al. (2002); Battisti et al. (1993); Rao (1963)
	1789	Rajendran and Prabhu (2010); Deepa et al. (2004)
	1785	Ali et al. (2006)
C–H deformation of ring	1557	Deepa et al. (2002)
$\rho_r(CH_2)$ + ring breathing		Deepa et al. (2004)
$\rho_s(CH_2)_{i.p.}$	1485	Deepa et al. (2004)
CH_3 asymmetric bending	1483	Kumar et al. (2010)
$\delta(CH_2)$ of CH_3	1450	Deepa et al. (2004)
C–H deformation of ring	1454, 1390, 1357	Deepa et al. (2002)
ν (C–O)	1300–1100	Rajendran and Sivakumar (2008)
ν(C–O) + ω(C–H)	1182	Deepa et al. (2002)
ν(C–O) + ν(C–C)	1150	Deepa et al. (2002)
ω(C–H) + δ(C–H)	1120	Deepa et al. (2002)
τ(C–H) + δ(C–H)	1051	Deepa et al. (2002)
ring breathing	948	Deepa et al. (2002); Hyodo and Okabayashi (1989); Schindler et al. (1984)
ring deformation or breathing	777	Deepa et al. (2002); Battisti et al. (1993)
symmetric ring deformation or breathing	712	Deepa et al. (2002); Battisti et al. (1993)

The symmetric stretching of CO group [ν(C–O)] of PC is found at 1226 cm^{-1} [Rajendran and Sivakumar, 2008] as shown in Figure 4.21 (b). Mixed vibrations of ν(C–O) + C–H wagging [ω(C–H)] and ν(C–O) + C–H stretching [ν(C–H)] of PC are situated at 1182 and 1148 cm^{-1} respectively [Deepa et al., 2002]. The mixed vibration of C–H twisting [τ(C–H)] + C–H deformation [δ(C–H)] of pure PC is present at 1051 cm^{-1} and shifted to 1066–1075 cm^{-1} in the PC–added samples. The ring breathing of pure PC shifted from 943 cm^{-1} to 947–949 cm^{-1} when added into the optimized polymer blend–LiTf system. The vibrational modes of PEMA/PVdF–HFP–LiTf–PC system are listed in Table 4.8.

The IR spectra of PC–added PEs in the IR region 1850–1600 cm^{-1} are shown in Figure 4.22. The ν(C=O) vibrational mode belonging to PC shifted from 1789 cm^{-1} to

lower wavenumbers at 1773 to 1786 cm^{-1} in the plasticized samples. This phenomenon was reported by Deepa et al. (2002) whereby ν(C=O) band of PC experienced a downshift by 8 cm^{-1} from 1800 to 1792 cm^{-1} when incorporated with LiTf. Shifting of this band is caused by the coordination of Li^+ ions onto the electronegative O atoms of the C=O group in PC [Wang et al., 1996]. However, since the C=O group is surrounded by two neighbouring O atoms in PC, the possible interaction between Li^+ with the ring O atoms [Wang et al., 1996], could also affect the ν(C=O) wavenumber [Battisti et al., 1993 ; Cazzanelli et al., 1997].

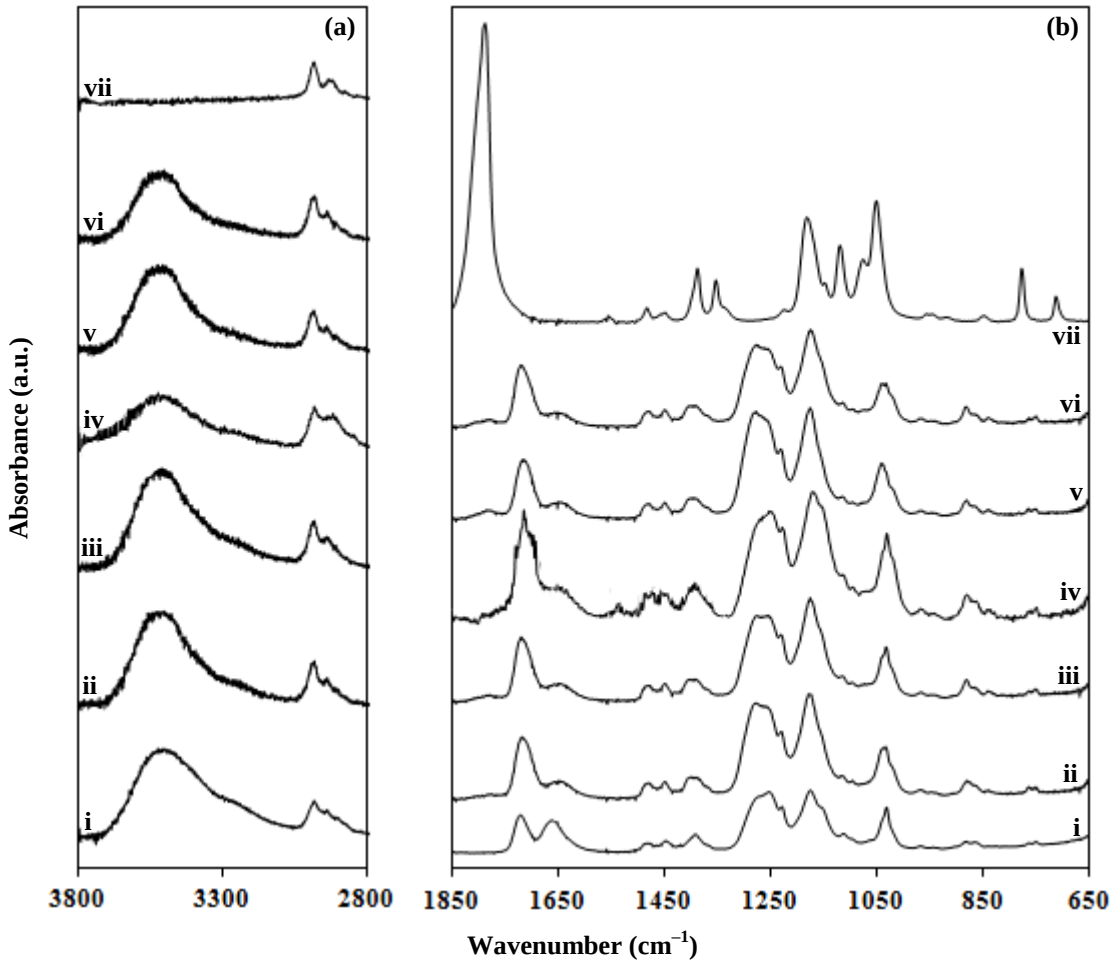

Figure 4.21 FTIR spectra between (a) 3800–2800 cm^{-1} and (b) 1850–650 cm^{-1} of i. PC–0, ii. PC–2, iii. PC–4, iv. PC–6, v. PC–8, vi. PC–10 and vii. PC

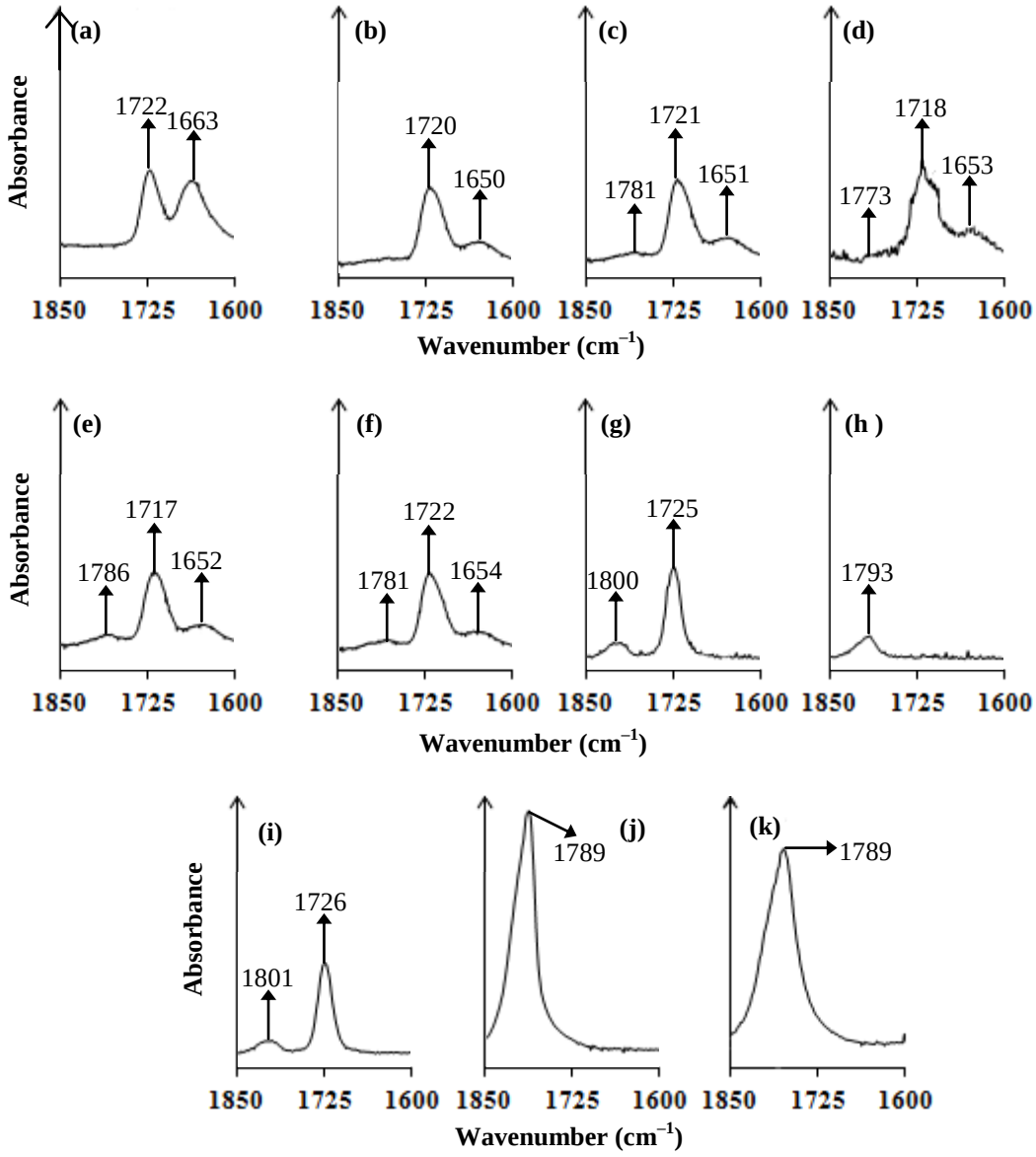

Figure 4.22 FTIR spectra in the region 1850–1600 cm^{-1} for (a) PC–0, (b) PC–2, (c) PC–4, (d) PC–6, (e) PC–8, (f) PC–10, (g) 90 wt.% PEMA–10 wt.% PC, (h) 90 wt.% PVdF–HFP–10 wt.% PC, (i) S–0–PC, (j) PC and (k) 6 wt.% LiTf–94 wt.% PC

In our work, the sample PC–6 exhibit the highest wavenumber shift of 16 cm^{-1} for the *ν*(C=O) band of PC which suggests that the solvation of Li^+ ions by O atoms in PC occurs the most in the PC–6 sample. The *ν*(C=O) mode of PEMA is observed to downshift from 1722 cm^{-1} in all samples except PC–4 and PC–10. In PC–4 and PC–10 samples, the carbonyl band did not exhibit any position change, which may indicate that PC did not interact at the C=O group of PEMA in the samples. The *ν*(C=O) mode of PEMA in PEMA–PC and S–0–PC samples shifted to higher wavenumbers, Figure 4.22 (g) and (i). This shows that the upshift of *ν*(C=O) mode of PEMA with addition of PC is

caused by the interaction between PEMA and PC. Hence, the shifting of the *ν*(C=O) mode of PEMA in PC–2, PC–6 and PC–8 is most probably due to the coordination of Li^+ ions instead of PC molecules onto the C=O group.

Although *ν*(C=O) band of PC did not manifest any wavenumber change from 1789 cm^{-1} in the LiTf–PC sample, the broadening of the full width at half–height (FWHH) of the *ν*(C=O) band as shown in Figure 4.23 indicates that PC and LiTf has interacted with one another through the formation of electrostatic interaction between negatively charged O atom in C=O group of PC and Li^+. This phenomenon was also reported by Battisti and co–workers (1993) and Starkey and Frech (1997).

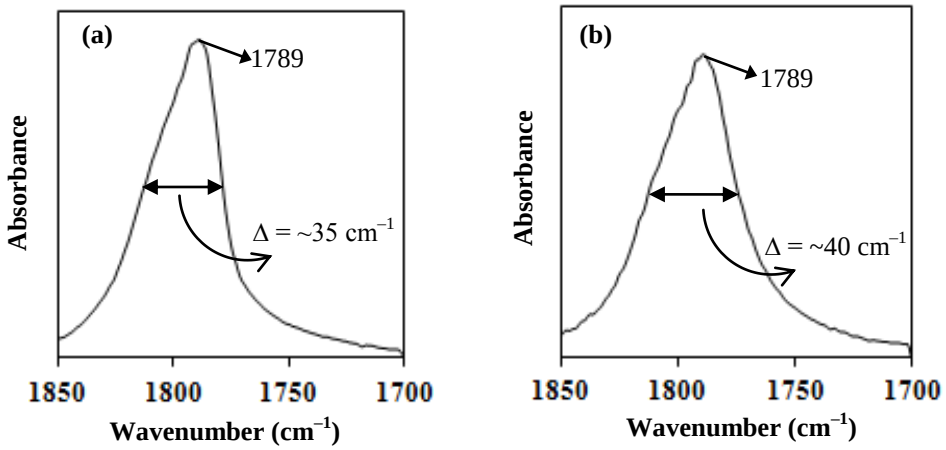

Figure 4.23 IR spectra in the wavenumber region between 1850 and 1700 cm^{-1} of (a) PC and (b) 6 wt.% LiTf–94 wt.% PC

Figure 4.24 shows the deconvoluted IR bands between 1340 and 1200 cm^{-1} of PC, PC–0 and PEMA/PVdF–HFP–LiTf–PC films to investigate the effect of PC on the ν_a(COC) and *ν*(CO) of –COO– group of PEMA, and $\nu_a(SO_3)$ and $\nu_a(SO_3)$ bands of LiTf.

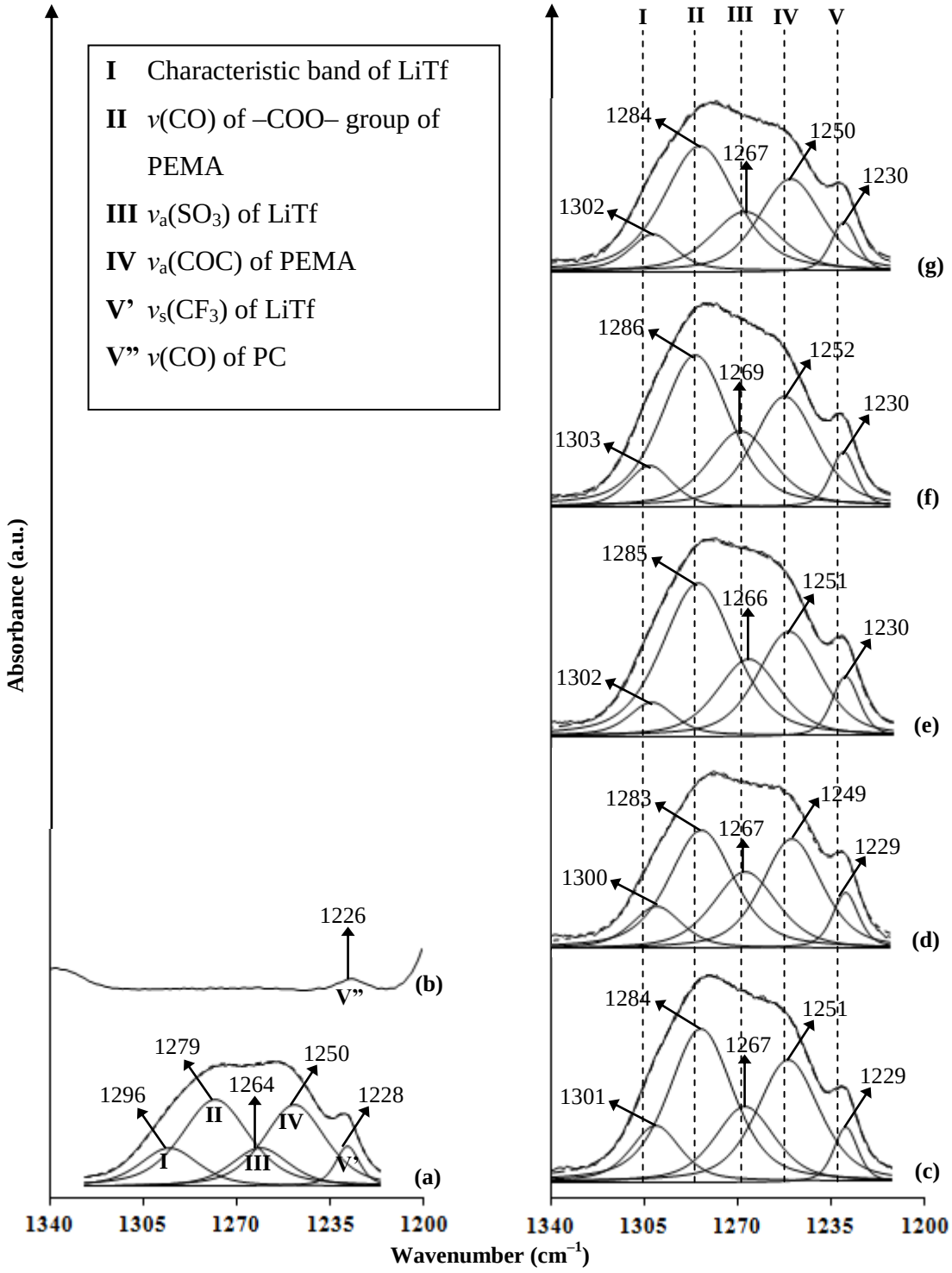

Figure 4.24 Deconvoluted FTIR spectra of (a) PC–0, (b) PC, (c) PC–2, (d) PC–4, (e) PC–6, (f) PC–8 and (g) PC–10

In the PC–plasticized samples, the $\nu_a(SO_3)$ of LiTf (band **III**) manifested upshift in position from 1264 cm^{-1} to 1266–1269 cm^{-1}. The ν(CO) of –COO– group of PEMA (band **II**) shifted from 1279 cm^{-1} to 1283–1286 cm^{-1} while the ν_a(COC) mode (band **IV**) showed changes from 1250 cm^{-1} to 1249–1252 cm^{-1}. The ν(CO) of PC (labeled **V"**)

overlapped with the $v_s(CF_3)$ of LiTf (labeled **V'**) to form a peak (labeled **V**) around 1229–1230 cm^{-1} in the PC–containing samples. The shifting of the ν(CO) of –COO– group and v_a(COC) modes of PEMA, $v_a(SO_3)$ and $v_s(CF_3)$ modes of LiTf indicate that interaction has occurred between PC and the polymer blend–salt complexes.

The deconvoluted IR bands between 1220 and 1120 cm^{-1} of PC, PC–0 and PEMA/PVdF–HFP–LiTf–PC films are depicted in Figure 4.25. Upon addition of PC into the optimized PEMA/PVdF–HFP–LiTf composition, the ν(CO) + ω(CH) mode of the plasticizer shifted from 1182 cm^{-1} to 1189–1195 cm^{-1}. The large wavenumber shift ($+\Delta$=7 to 13 cm^{-1}) of this band shows that interaction has occurred between PC and the polymer blend–salt samples. Figure 4.26 shows the deconvoluted IR spectra of PEMA, PVdF–HFP, S–0 and LiTf added with PC for comparison purposes.

Upshift in the ν(CO) + ω(CH) mode of PC was also observed in LiTf–PC, PEMA–PC, PVdF–HFP–PC and S–0–PC samples respectively, Figure 4.26 (a) to (d). Hence, the large wavenumber shifts of the ν(CO) + ω(CH) band shows the interaction between PC and the polymer blend–salt complexes.

Figure 4.25 (d) to (g) show that the ν(CO) + ν(CH) vibrational mode of PC (band **IV**) appeared only upon the addition of 4 wt.% PC. Band **IV** was observed to downshift from 1148 cm^{-1} (Figure 4.25 (b)) in PC–4 and PC–6 samples, and then upshifted in PC–8 and PC–10. The larger wavenumber shift ($+\Delta$=7 to 8 cm^{-1}) in PC–4 and PC–6 samples as compared to films containing higher PC content ($+\Delta$=2 cm^{-1}) suggests that the interaction between PC and the polymer blend–salt composition occurs at a larger extent in PC–4 and PC–6.

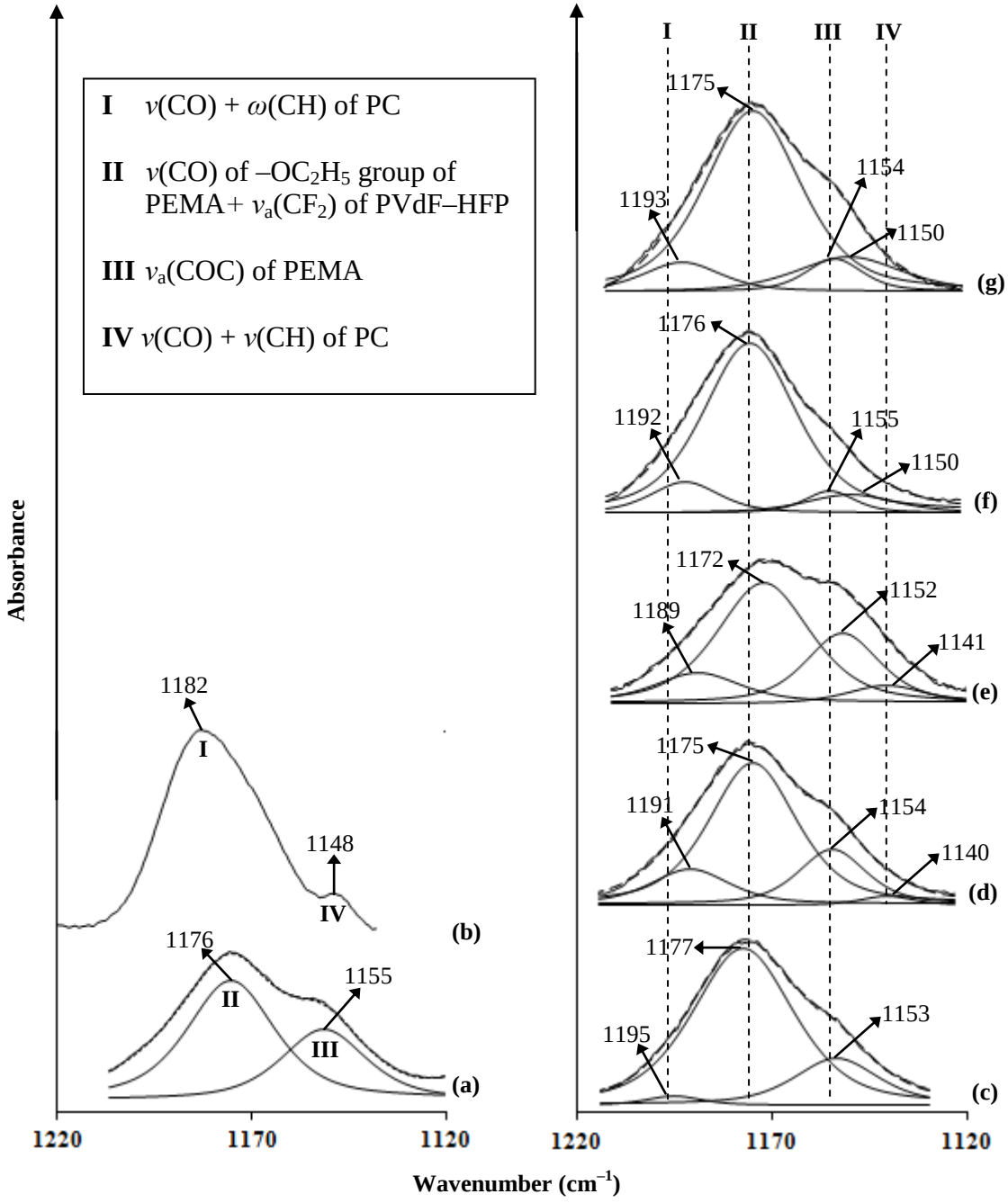

Figure 4.25 Deconvoluted FTIR spectra of (a) PC–0, (b) PC, (c) PC–2, (d) PC–4, (e) PC–6, (f) PC–8 and (g) PC–10

The IR band due to $\nu_a(CF_2)$ vibration of PVdF–HFP + ν(CO) band of $–OC_2H_5$ group of PEMA (band **II**) showed the largest wavenumber shift of 4 cm^{-1} in PC–6 (Figure 4.25 (e)) as compared to other PC–added samples ($\pm\Delta$=1 cm^{-1}). The shift of the ν_a(COC) band of PEMA (band **III**) of 3 cm^{-1} is largest in PC–6 as compared to other PC–containing films. As larger wavenumber shifts are observed in PC–6 film, it is

suggested that interaction between PC and the PEMA/PVdF–HFP–LiTf composition is most apparent in that sample.

Thus, the shiftings of the ν(C=O), ν(CO) of –COO– and ν_a(COC) of PEMA, skeletal stretching of PC and the $\nu_a(CF_2)$ vibration of PVdF–HFP + ν(CO) band of $-OC_2H_5$ group of PEMA have shown that PC has interacted with the O atom in the C=O and C–O–C groups of PEMA and F atom in the CF_2 group of PVdF–HFP in PEMA/PVdF–HFP–LiTf–PC system. Figure 4.27 shows the schematic diagram of possible interactions that occur in PEMA/PVdF–HFP–LiTf–PC system.

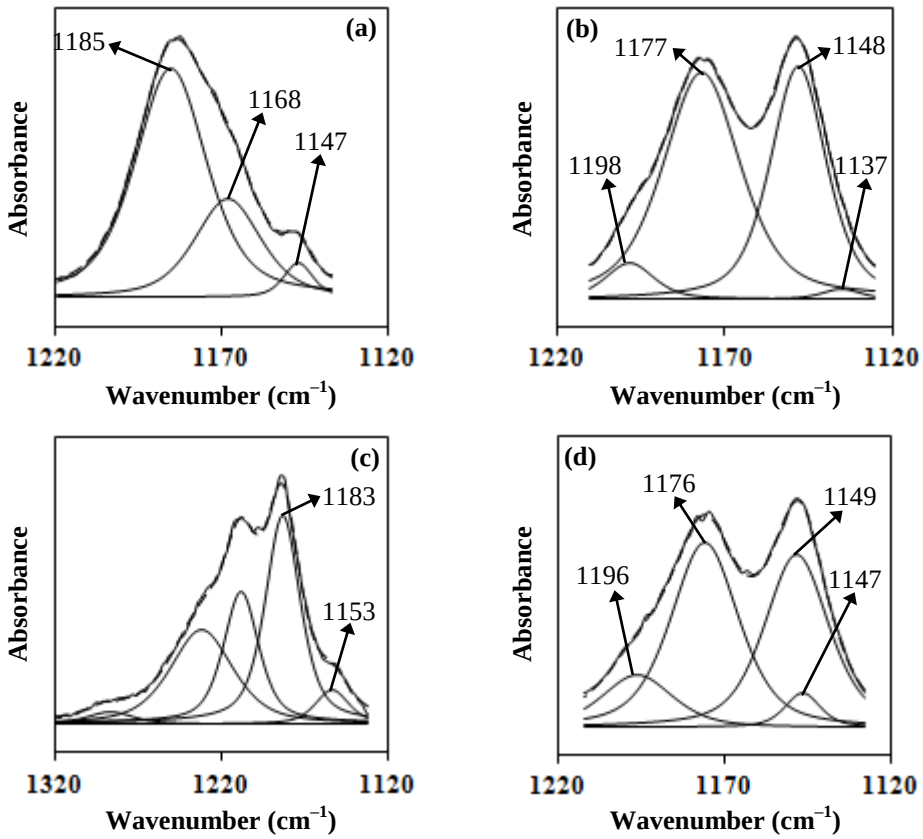

Figure 4.26 Deconvoluted FTIR spectra of (a) 6 wt.% LiTf–94 wt.% PC, (b) 90 wt.% PEMA–10 wt.% PC, (c) 90 wt.% PVdF–HFP–10 wt.% PC (between 1320 and 1120 cm^{-1}) and (d) 90 wt.% S–0–10 wt.% PC in the IR region between 1220 and 1120 cm^{-1}

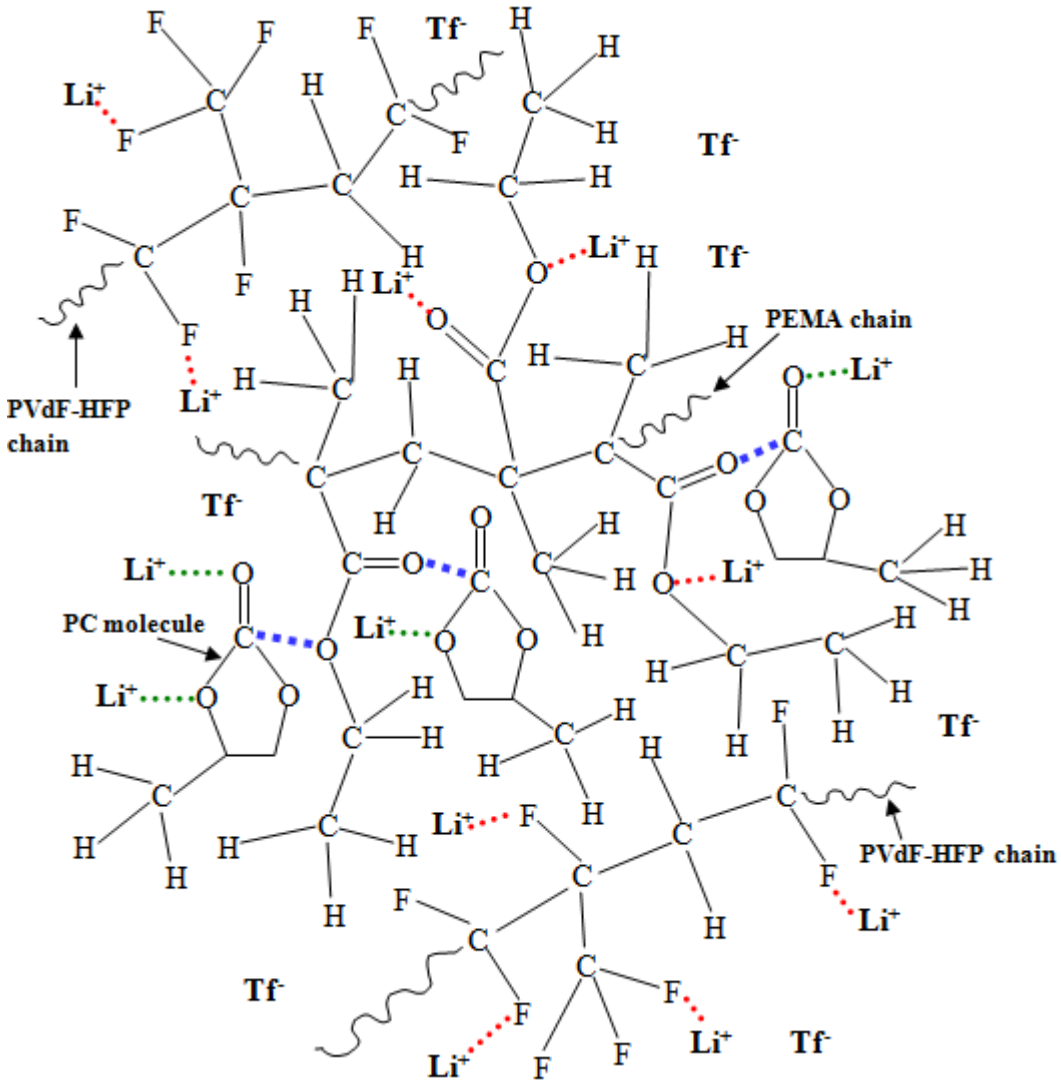

Figure 4.27 Schematic diagram of possible interactions in PEMA/PVdF–HFP–LiTf–PC system (where•••• represents the coordinate bonds with Li^+ ions,•••• represents the electrostatic interactions between Li^+ and PC and ▪▪▪ represents the intermolecular interactions between PC and PEMA/PVdF–HFP)

4.3.2.2 Interactions between Li^+ and $CF_3SO_3^-$ ions, and the expected effect on the ionic conductivity of PEMA/PVdF–HFP–LiTf–PC system

The IR region between 1100 and 950 cm^{-1} of PC–added samples are deconvoluted in Figure 4.28 to investigate the area under the $\nu_s(SO_3)$ band of LiTf to as a function of PC content.

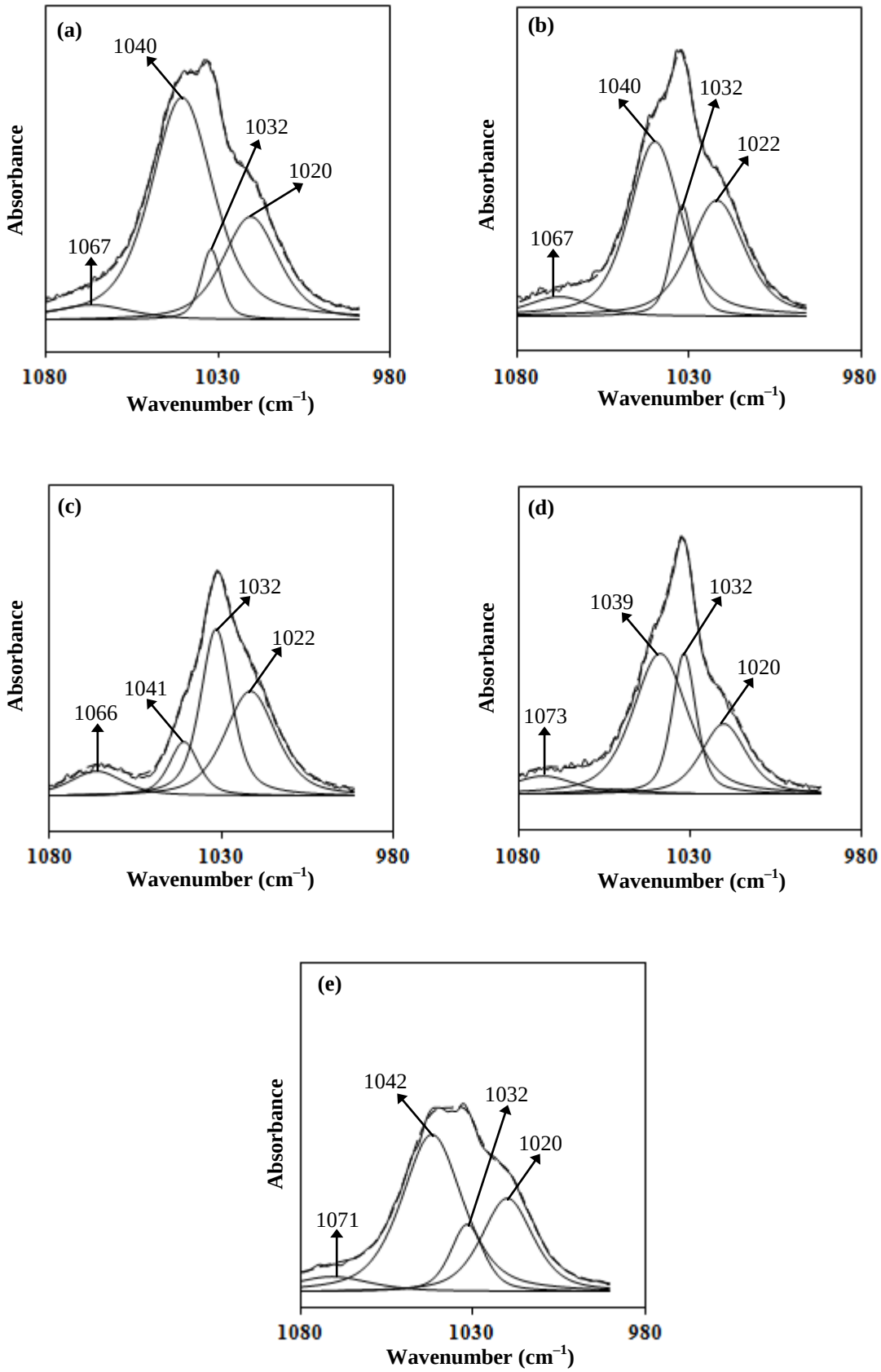

Figure 4.28 IR deconvoluted bands in the region 1080–980 cm^{-1} for (a) PC–2, (b) PC–4, (c) PC–6, (d) PC–8 and (e) PC–10

The δ(C–H) mode of PEMA lies at 1020–1022 cm^{-1}. The IR band attributed to the $\nu_s(SO_3)$ free ions is located at 1032 cm^{-1} belongs in all PC–containing samples. The plot of area % of the different ionic species of triflate anion versus PC content is illustrated in Figure 4.29.

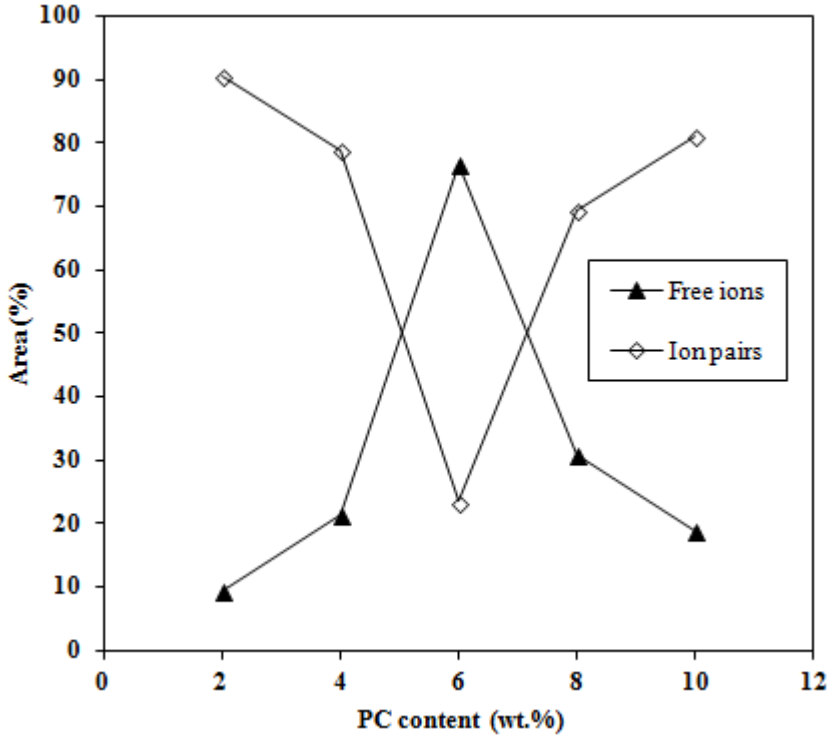

Figure 4.29 Area % of free ions and ion pairs with respect to PC content in 70 wt.% [PEMA/PVdF–HFP]–30 wt.% LiTf polymer electrolytes

From Figure 4.29, the area % of free Tf– ions was observed to increase when the amount of PC increased from 2 wt. % up to 6 wt. % which indicates increase in the number of charge carriers. On the other hand, the area % of ion pairs is at its minimum at 6 wt.% of PC. Conductivity variation at room temperature is expected to vary accordingly.

Table 4.8 FTIR vibrational modes of PEMA/PVdF–HFP:LiTf (70:30, w/w) blend polymer electrolytes incorporated with different wt.% of PC

Assignment of bands	Wavenumber (cm^{-1})						
	PC	**PC–0**	**PC–2**	**PC–4**	**PC–6**	**PC–8**	**PC–10**
ν(CH)	2987, 2931	2988, 2943, 2912	2987, 2942	2987, 2944	2989, 2940	2988, 2944	2987, 2944
ν(C=O) of PC	1789	–	1777	1781	1773	1786	1781
ν(C=O) of PEMA	–	1722	1720	1721	1718	1717	1722
$\delta(H_2O)$ from LiTf	–	1663	1650	1651	1653	1652	1652
$\delta(CH_2)$of PEMA	–	1482	1480	1478	1476	1480	1480
$\gamma(OC_2H_5)$of PEMA	–	1448	1450	1450	1448	1450	1450
$\omega(CH_2)$ of PVdF–HFP + $\tau(CH_2)$ of PEMA	–	1392	1400	1399	1400	1400	1400
Characteristic band of LiTf	–	1296	1301	1300	1302	1303	1302
ν(CO) of –COO– group of PEMA	–	1279	1284	1283	1285	1286	1284
$\nu_a(SO_3)$ of LiTf	–	1264	1267	1267	1266	1269	1267
ν_a(COC) of PEMA	–	1250	1251	1249	1251	1252	1250
$\nu_s(CF_3)$ of LiTf	–	1228	1229	1229	1230	1230	1230
ν(CO) + ω(CH) of PC	1182	–	1195	1191	1189	1192	1193
$\nu_a(CF_2)$ of PVdF–HFP + ν(CO) of $-OC_2H_5$ group of PEMA	–	1176	1177	1175	1172	1176	1175
ν_a(COC) of PEMA	–	1155	1153	1154	1152	1155	1154
ν(CO) + ν(CH) of PC	1148	–	–	1140	1141	1150	1150
Characteristic band of PEMA	–	1113	1116	1116	1114	1114	1114
τ(C–H) + δ(C–H) of PC	1051	–	1067	1067	1066	1071	1075
$\nu_s(SO_3)$ ion aggregates of LiTf	–	–	–	–	–	–	–
$\nu_s(SO_3)$ ion pairs of LiTf	–	1041	1040	1040	1041	1039	1042
$\nu_s(SO_3)$ free ions of LiTf	–	1032	1032	1032	1032	1032	1032
α–phase of PVdF–HFP	–	969	970	969	968	969	970
Ring breathing of PC	943	–	947	947	947	949	947
Amorphous region of PVdF–HFP	–	881	881	882	882	881	880
β–phase of PVdF–HFP	–	838	839	839	840	840	840
$\delta_s(CF_3)$ of LiTf	–	762	751	750	750	750	750

4.4 Ionic Liquid Based PEMA/PVdF–HFP–LiTf Polymer Electrolyte Systems

4.4.1 PEMA/PVdF–HFP–LiTf–BMII System

4.4.1.1 Interactions between PEMA/PVdF–HFP–LiTf and BMII

Figure 4.30 depicts the FTIR spectra of PEMA/PVdF–HFP–LiTf–BMII polymer electrolyte films. The IR peaks found at 3138 and 3072 cm^{-1} in BMII ionic liquid (Figure 4.30 (viii)) are attributable to the =C–H vibrational stretching modes [ν(=C–H)] of the cyclic imidazolium cation (BMI^+) [Anbu et al., 2003]. The ν(=C–H) modes of

BMII refer to the hydrogen atom attached directly to the imidazolium ring, namely at the C(2), C(4) and C(5) locations as labeled in Figure 2.4 (a). The *ν*(C–H) of the butyl and methyl groups attached to the BMI^+ ring are located at 2960, 2871 and 2931 cm^{-1} [Jiang et al., 2006]. Table 4.9 lists the IR vibrational bands of BMII from literature.

Table 4.9 Assignment of FTIR vibrational bands of BMII

Assignment of band	Wavenumber (cm^{-1})	Reference
ν(=C–H) of BMI^+ ring	3141–3027, 3019	Jeon et al. (2008), Shukla et al. (2010)
ν(CH) of butyl and methyl groups of BMI^+ cation	2966–2957, 2932, 2870, 2851	Shukla et al. (2010); Jeon et al. (2008), Jiang et al. (2006)
in–plane bending of BMI^+ ring	1593	Shukla et al. (2010)
C–C and C–N bending mode of BMI^+ ring	1569	Shi and Deng (2005)
scissoring of H–C–H in butyl group	1517	Shukla et al. (2010)
ω(H–C–H) in butyl group	1424	Shukla et al. (2010)
δ(CH_2) deformation mode	1339	Jiang et al., 2006
ρ(H–C–H) in butyl group of BMI^+ ring	1327	Shukla et al. (2010)
ν(C–NCH_3) and bending in N–CH_3	1118	Shukla et al. (2010)
ρ(HC=CH) of BMI^+ ring	827	Shukla et al. (2010)
ω(HC=CH) of BMI^+ ring	710	Shukla et al. (2010)

The *ν*(=C–H) modes due to the H atoms bonded to carbon numbered 2, 4 and 5 will be investigated instead of the *ν*(C–H) mode of BMII which overlaps with that of PEMA and PVdF–HFP. Moreover, it is more likely that the *ν*(=C–H) mode will be affected due to complexation to polymer(s) [Shalu et al., 2013].

When BMII was added into the optimized PEMA/PVdF–HFP–LiTf system, the *ν*(=C–H) bands of BMII could not be observed until 17.5 wt.% of BMII was incorporated. The *ν*(=C–H) mode of BMII shifted from 3138 and 2971 cm^{-1} to 3159 and 3112 cm^{-1} in BI–17.5, and to 3160 and 3091 cm^{-1} in BI–20. The upshift of the *ν*(=C–H) mode in BI–17.5 and BI–20 samples indicate the existence of interaction between BMII and PEMA/PVdF–HFP–LiTf system. The IR changes upon the addition of BMII into PEMA/PVdF–HFP–LiTf system are listed on Table 4.10.

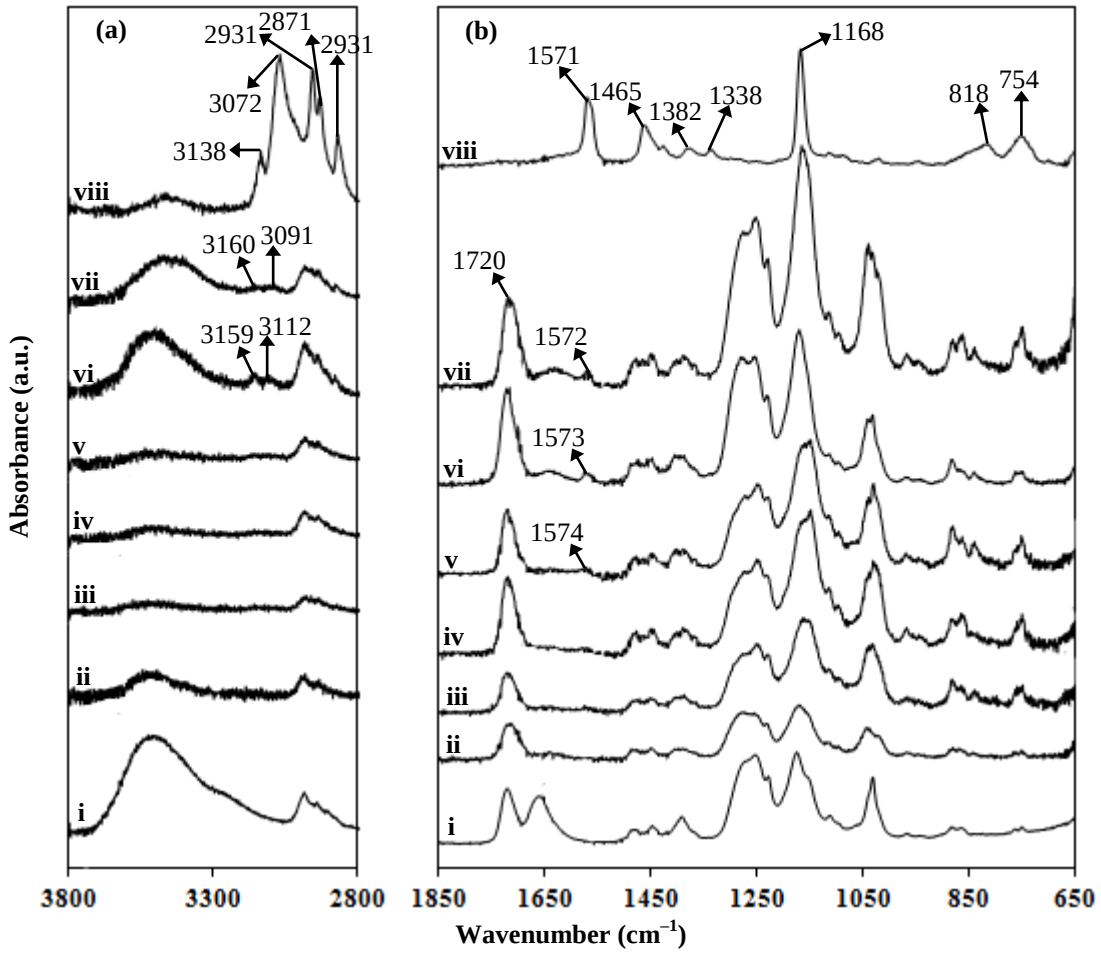

Figure 4.30 FTIR spectra between (a) 3800–2800 cm^{-1} and (b) 1850–650 cm^{-1} of i.BI–0, ii. BI–5, iii. BI–10, iv. BI–12.5, v. BI–15, vi. BI–17.5, vii. BI–20 and viii. BMII

Figure 4.31 (a) to (k) shows the IR spectra between 1850 to 1600 cm^{-1} which investigate the effect of BMII on the carbonyl band, ν(C=O) of PEMA in the PEMA/PVdF–HFP–LiTf–BMII system. It was observed that the ν(C=O) band shifted from 1722 to 1718 cm^{-1} when 5 wt.% of BI was added, Figure 4.31 (b). With further addition of BMII, the ν(C=O) band shifted back to 1721–1723 cm^{-1}, Figure 4.31 (c) to (g). Figure 4.31 (h) and (j) show that the ν(C=O) band of PEMA–BMII sample did not shift from the original position, but shifted from 1723 to 1726 cm^{-1} in PEMA/PVdF–HFP–BMII sample. This indicates that the interaction between BMII on the carbonyl group of PEMA is more apparent in the presence of PVdF–HFP. The larger shift of the ν(C=O) band observed in BI–5 sample indicates that larger interaction between BMII and the carbonyl group of PEMA has occurred, as compared to other BMII–added

samples. The deconvoluted IR bands of BMII added samples in the region between 1340 and 1200 cm^{-1} are shown in Figure 4.32.

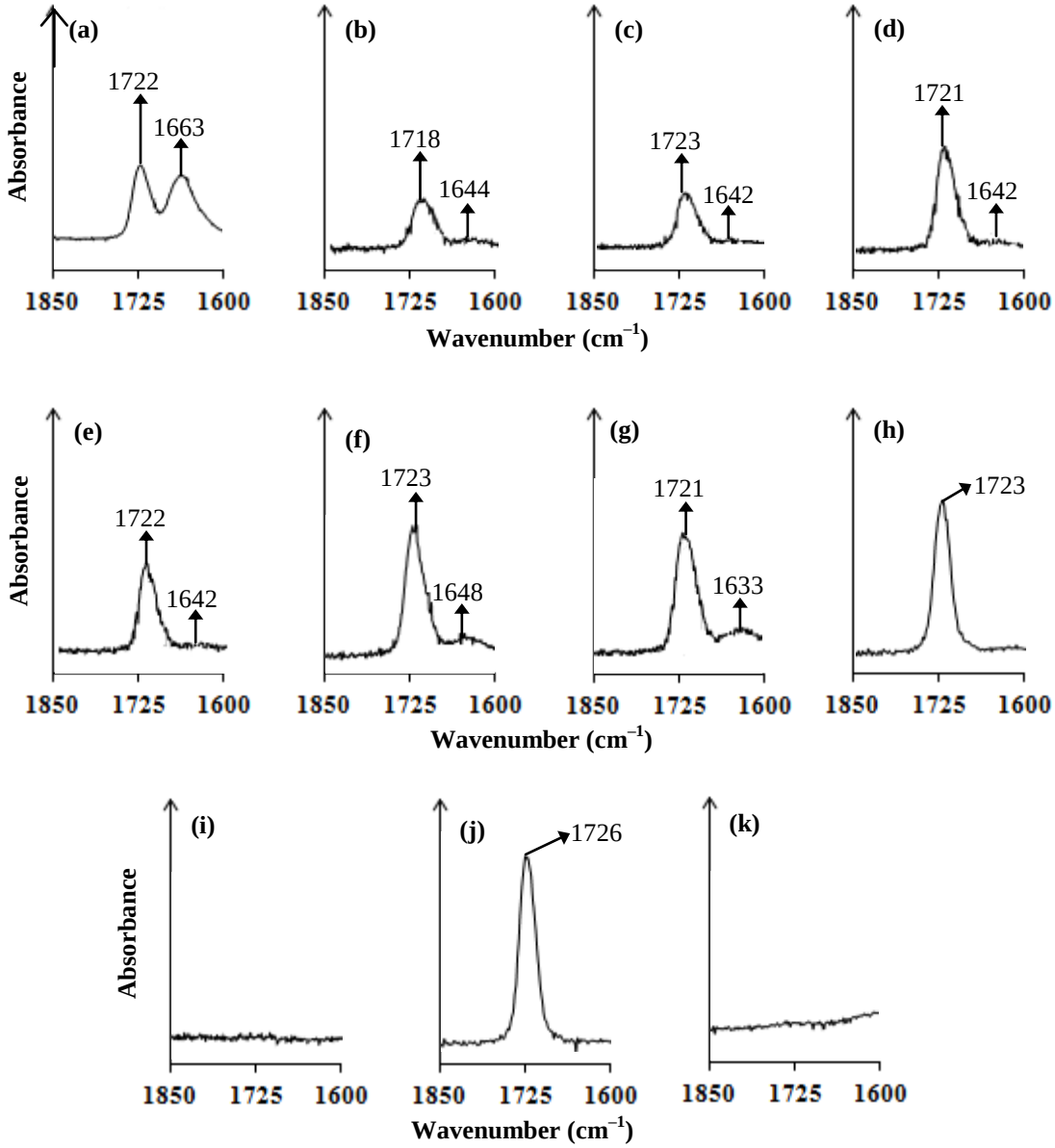

Figure 4.31 FTIR spectra in the region 1850–1600 cm^{-1} for (a) BI–0, (b) BI–5, (c) BI–10, (d) BI–12.5, (e) BI–15, (f) BI–17.5, (g) BI–20, (h) 90 wt.% PEMA–10 wt.% BMII, (i) 90 wt.% PVdF–HFP–10 wt.% BMII and (j) S–0–BMII and (k) BMII

Upon incorporation of 10 wt.% BMII, the *ν*(CO) of –COO– group and the ν_a(COC) bands shifted from 1279 to 1277 cm^{-1} in BI–15 and to 1281 cm^{-1} in BI–5, and from 1250 to 1248 cm^{-1} in BI–5 to BI–15 samples, Figure 4.32 (a). No shift was observed in the spectrum of other samples. The $\nu_a(SO_3)$ of LiTf (band **III**) and the

$v_s(CF_3)$ of LiTf (band **V**) respectively showed slight shifts from 1264 to 1262 cm^{-1} in BI–5 and 1266 cm^{-1} in BI–20, and from 1228 to 1230 cm^{-1} in BI–5. The shifting of bands mentioned above in the spectrum of the samples concerned indicates interaction with BMII.

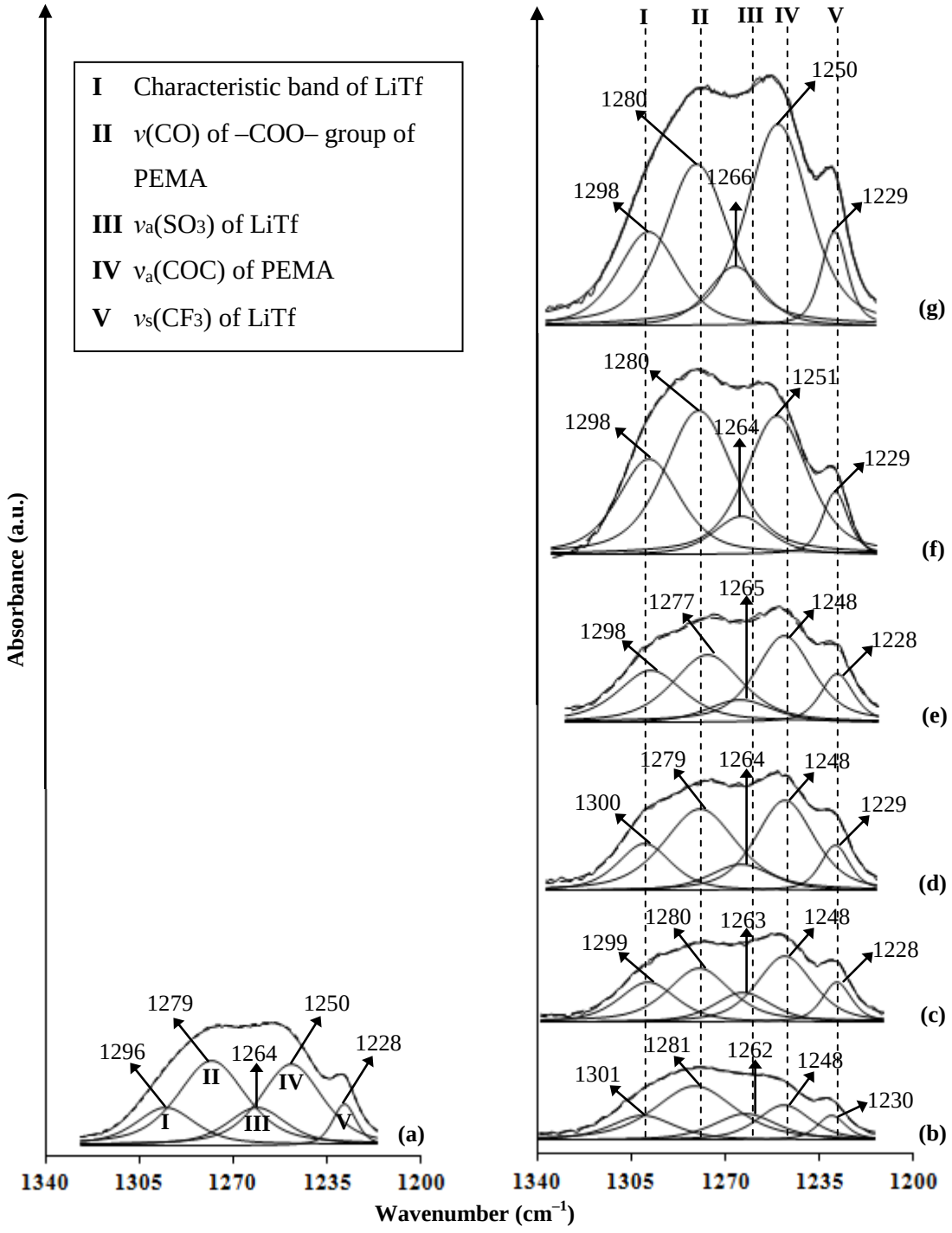

Figure 4.32 FTIR spectra in the region between 1340 and 1200 cm^{-1} of (a) BI–0, (b) BI–5, (c) BI–10, (d) BI–12.5, (e) BI–15, (f) BI–17.5 and (g) BI–20

Figure 4.33 illustrates the IR region 1220–1120 cm^{-1} to investigate the effect of varying wt.% of BMII on the PEMA/PVdF–HFP–LiTf system.

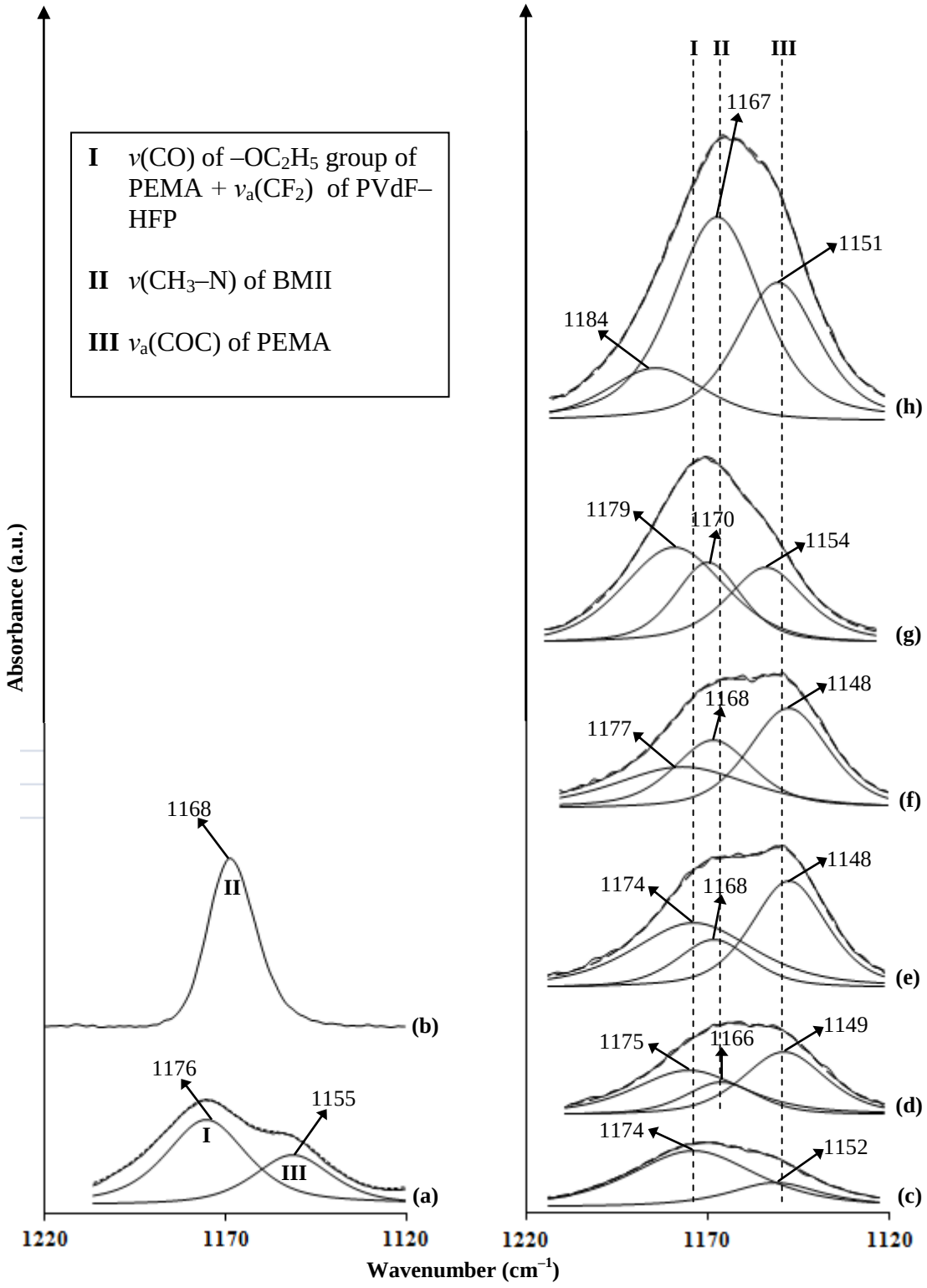

Figure 4.33 FTIR spectra in the region between 1220 and 1120 cm^{-1} of (a) BI–0, (b) BMII, (c) BI–5, (d) BI–10, (e) BI–12.5, (f) BI–15, (g) BI–17.5 and (h) BI–20

The ν(CO) of $-OC_2H_5$ group of PEMA + $\nu_a(CF_2)$ of PVdF–HFP (band **I**) was observed to show position shifts from 1176 cm^{-1} to 1174–1184 cm^{-1} when added with varied wt.% of BMII. The upshift of band **I** especially in BI–15 ($+\Delta$=1 cm^{-1}), BI–17.5 ($+\Delta$=3 cm^{-1}) and BI–20 ($+\Delta$=8 cm^{-1}) samples suggests the increased interaction between BMII with PEMA and PVdF–HFP at the $-OC_2H_5$ group and CF_2 group, respectively, Figure 4.33 (f) to (h). The shifting of the $\nu(CH_3–N)$ of BMII (band **II**) from 1168 cm^{-1} to 1166, 1170 and 1167 cm^{-1} in BI–10, BI–17.5 and BI–20 respectively suggested that BMII has interacted with the polymers in the samples. Band **II** maintained at 1168 cm^{-1} in BI–12.5 and BI–15 samples (Figure 4.33 (e) and (f)) which indicated that BMII does not interact much with the polymers present in the two samples.

Figure 4.34 shows the IR region of 1220–1120 cm^{-1} of PEMA–BMII and S–0–BMII samples. The ν_a(COC) of PEMA (band **III**) was observed to shift from 1155 cm^{-1} in BI–0 sample to 1148–1154 cm^{-1}. In 90 wt.% PEMA–10 wt.% BMII and 90 wt.% S–0–10 wt.% BMII samples as depicted in Figure 4.34 (a) and (b), the presence of 10 wt.% BMII caused the ν_a(COC) of PEMA to upshift from 1142 to 1145 cm^{-1} and from 1145 to 1149 cm^{-1}, respectively.

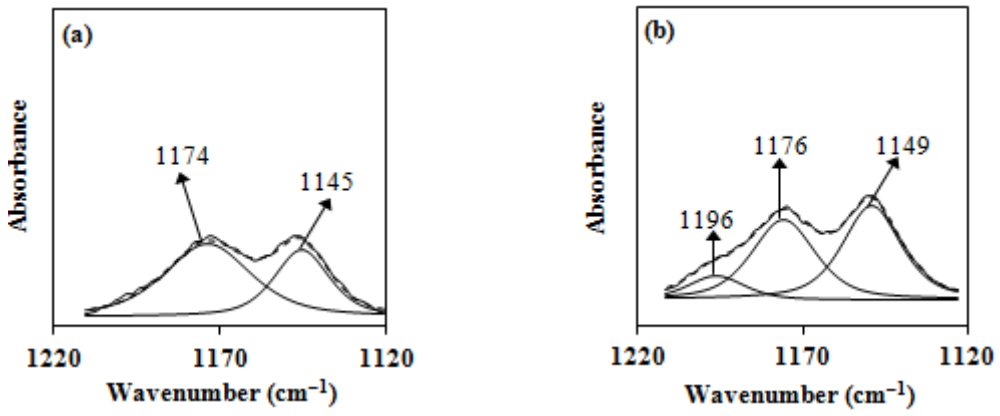

Figure 4.34 FTIR spectra in the region between 1220 and 1120 cm^{-1} of (a) 90 wt.% PEMA–10 wt.% BMII and (b) 90 wt.% S–0–10 wt.% BMII

This shows that the interaction between BMII with the –COC– group of PEMA tends to upshift the ν_a(COC) band. Since the ν_a(COC) of PEMA in BI–12.5 and BI–15 samples was located at 1148 cm^{-1} giving the lowest position in PEMA/PVdF–HFP–LiTf–BMII system, it is suggested that BMII has lower tendency to complex with PEMA at 12.5 and 15 wt.% BMII. Hence, the shifting of the ν(=C–H) and ν(CH_3–N) modes of BMII, the ν(C=O), ν(CO) of –COO–, ν_a(COC), ν(CO) of –OC_2H_5 of PEMA and the ν_a(CF_2) of PVdF–HFP shows that BMII has complexed with PEMA and PVdF–HFP via the hydrogen atoms attached directly to the imidazolium cation. Figure 4.35 depicts the schematic diagram of possible interactions that occur between BMII and PEMA/PVdF–HFP–LiTf system.

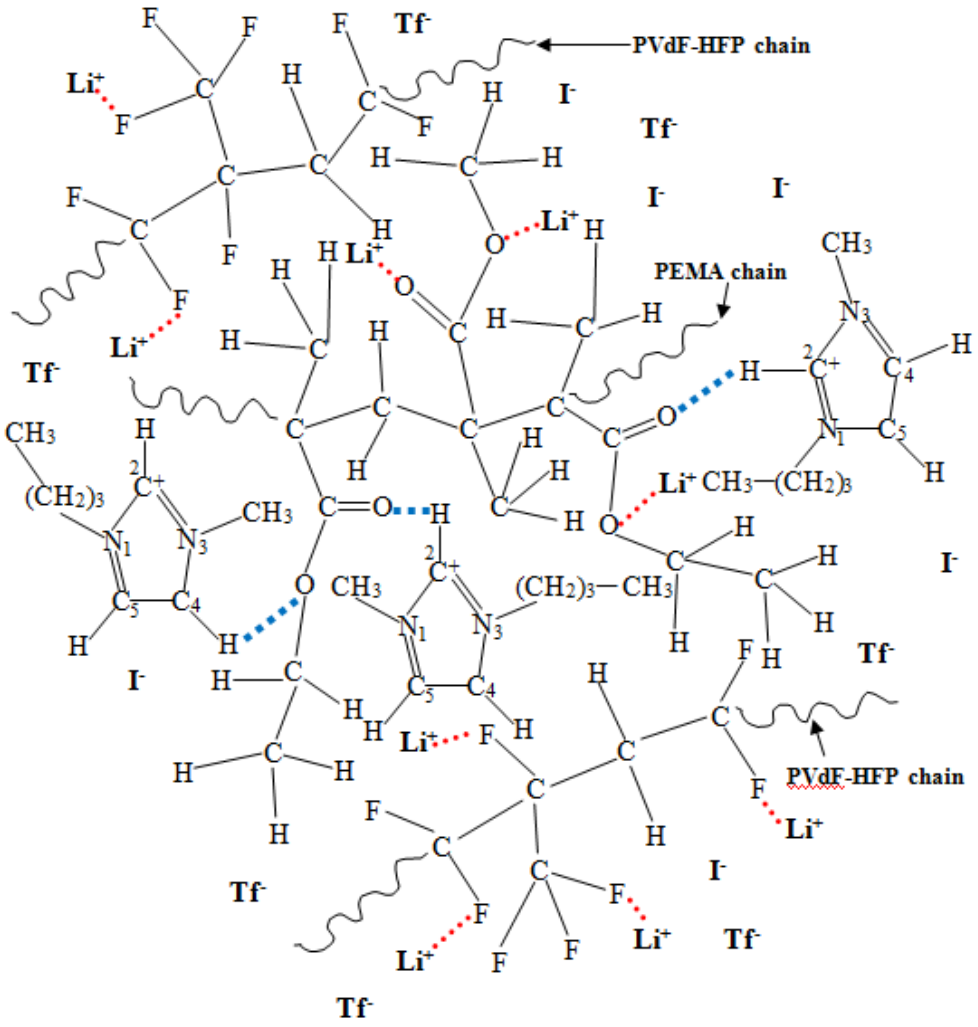

Figure 4.35 Schematic diagram of possible interactions in PEMA/PVdF–HFP–LiTf–BMII system (where•••• represents coordinate bonds with Li^+ ions and▪▪▪ represents the intermolecular interactions between BMII and PEMA/PVdF–HFP)

4.4.1.2 Interactions between Li^+ and $CF_3SO_3^-$ ions, and the expected effect on the ionic conductivity of PEMA/PVdF–HFP–LiTf–BMII system

Figure 4.36 (a) to (d) show the deconvoluted IR bands of PEMA/PVdF–HFP–LiTf containing varying wt.% of BMII in the region between 1100 and 980 cm^{-1}. In all samples, the band located at 1016–1022 cm^{-1} belongs to the δ(C–H) band of PEMA. In all samples, the bands situated at 1031–1032 cm^{-1} and 1042 to 1046 cm^{-1} are attributed to free Tf^- ions and ion pairs respectively. The area under the ion pair band was observed to increase with BMII content, except for BI–12.5 sample which has the smallest area. In BI–17.5 and BI–20, a band at higher wavenumber appeared – this band located at 1053 cm^{-1} is referred to ion aggregates.

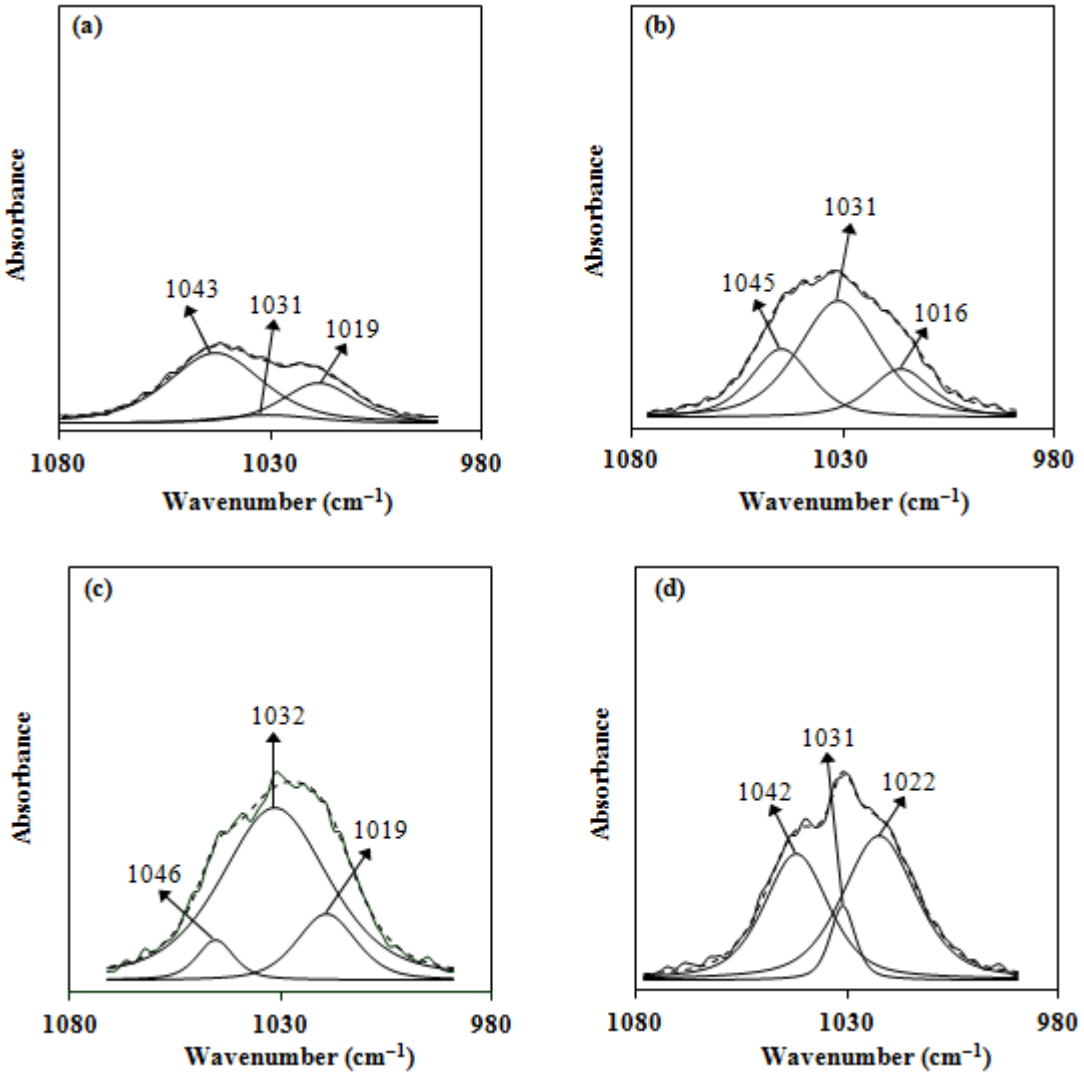

(Figure 4.36, continued)

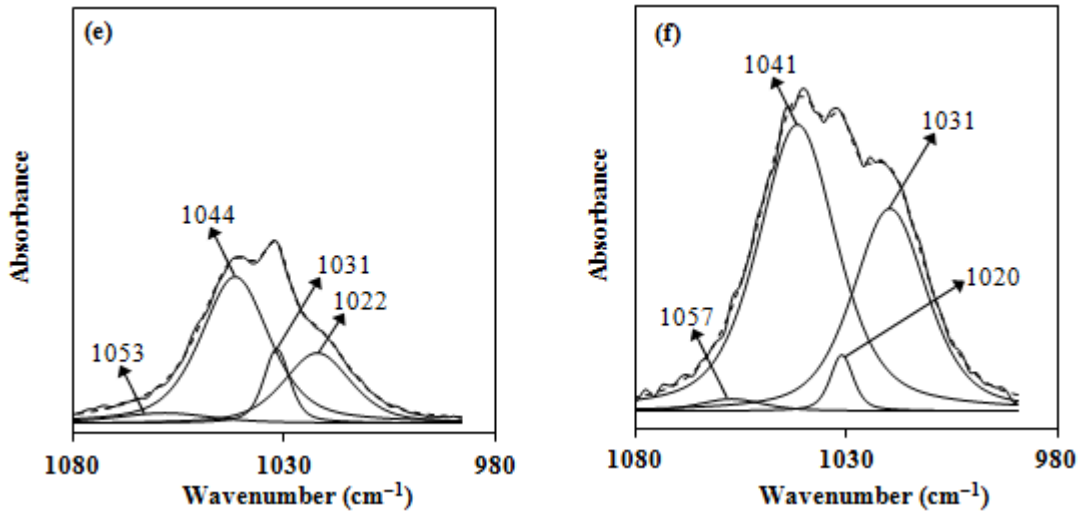

Figure 4.36 Deconvolution between 1100 and 980 cm^{-1} of (a) BI–5, (b) BI–10, (c) BI–12.5, (d) BI–15 (e) BI–17.5 and (f) BI–20

Figure 4.37 depicts the area % of free ions, ion pairs and ion aggregates as a function of BMII content. It can be seen that the area % of free ions increased up to 12.5 wt % BMII before decreasing. The area % of ion pairs is lowest at 12.5 wt.% BMII. At 17.5 and 20 wt.% BMII, ion aggregate appeared. It is expected that the sample containing 12.5 wt.% BMII is most conducting in the system due to the highest amount of free ions.

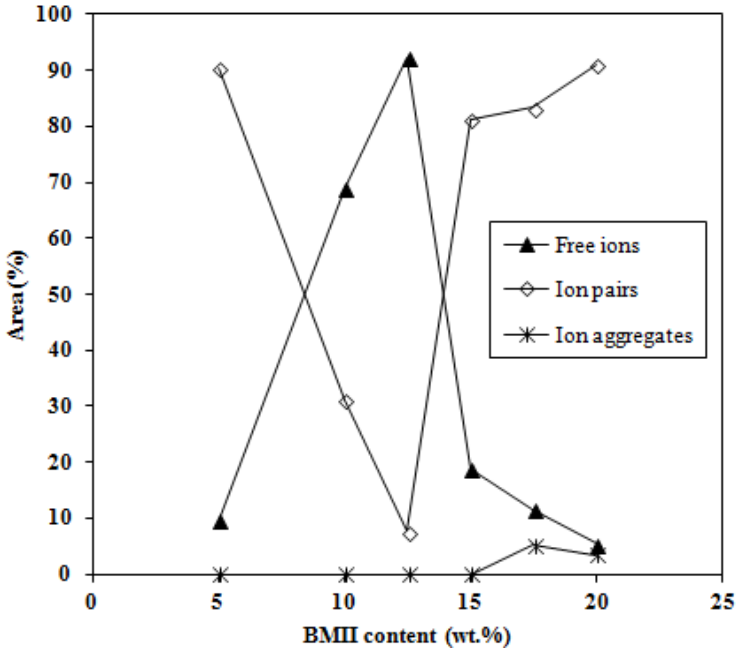

Figure 4.37 Area % of free ion, ion pair and ion aggregate as a function of BMII content

Table 4.10 FTIR vibrational modes of PEMA/PVdF–HFP:LiTf (70:30, w/w) blend polymer electrolytes incorporated with different wt.% of BMII

Assignment of bands	Wavenumber (cm^{-1})							
	BMII	**BI–0**	**BI–5**	**BI–10**	**BI–12.5**	**BI–15**	**BI–17.5**	**BI–20**
ν(=C–H) of BMI^+ ring	3138, 3072	–	–	–	–	–	3159, 3112	3160, 3091
ν(CH)	2960, 2871, 2931	2988, 2943, 2912	2984, 2962, 2934	2987, 2963, 2935	2987, 2963, 2939	2984, 2959, 2938	2986, 2966, 2940	2987, 2963, 2938
ν(C=O) of PEMA	–	1722	1718	1723	1721	1722	1718	1720
$\delta(H_2O)$ from LiTf		1663	1644	1642	1642	1642	1648	1633
C–C and C–N bending of cyclic BMI^+ ring	1571	–	–	–	–	1574	1573	1572
$\delta(CH_2)$of PEMA	–	1482	1488	1486	1482	1482	1482	1482
Characteristic band of BMII	1465	–	1478	1476	1465	1465	1465	1465
$\gamma(OC_2H_5)$of PEMA	–	1448	1449	1450	1448	1448	1448	1448
$\omega(CH_2)$ of PVdF–HFP + $\tau(CH_2)$ of PEMA	–	1392	1391	1390	1390	1390	1390	1389
Characteristic band of LiTf	–	1296	1301	1299	1300	1298	1298	1298
ν(CO) of –COO– group of PEMA	–	1279	1281	1280	1279	1277	1280	1280
$\nu_a(SO_3)$ of LiTf	–	1264	1262	1263	1264	1265	1264	1266
ν_a(COC) of PEMA	–	1250	1248	1248	1248	1248	1251	1250
$\nu_s(CF_3)$ of LiTf	–	1228	1230	1228	1229	1228	1229	1229
$\nu_a(CF_2)$ of PVdF–HFP + ν(CO) of $–OC_2H_5$ group of PEMA	–	1176	1174	1175	1174	1177	1179	1184
$\nu(CH_3–N)$ of BMII	1168	–	–	1166	1168	1168	1170	1167
ν_a(COC) of PEMA	–	1155	1152	1149	1148	1148	1154	1151
Characteristic band of PEMA	–	1113	1118	1116	1114	1116	1115	1114
$\nu_s(SO_3)$ ion aggregates of LiTf	–	–	–	–	–	–	1053	1057
$\nu_s(SO_3)$ ion pairs of LiTf	–	1041	1043	1045	1046	1042	1044	1041
$\nu_s(SO_3)$ free ions of LiTf	–	1032	1031	1031	1032	1031	1031	1031
α–phase of PVdF–HFP	–	969	968	968	968	970	971	968
Amorphous region of PVdF–HFP	–	881	881	882	882	881	882	881
β–phase of PVdF–HFP	–	838	842	840	845	840	841	840
$\delta_s(CF_3)$ of LiTf	–	762	762	760	760	760	762	762

4.4.2 PEMA/PVdF–HFP–LiTf–BMITf System

4.4.2.1 Interactions between PEMA/PVdF–HFP–LiTf and BMITf

Figure 4.38 (a) and (b) depict the IR spectra of PEMA/PVdF–HFP–LiTf–BMITf polymer electrolytes in the IR regions of 3800–2800 cm^{-1} and 1850–650 cm^{-1}. The IR vibrational bands of BMITf from literature are listed on Table 4.11. Figure 4.38 (a–viii) shows the IR spectrum of pure BMITf whereby IR bands observed at 3152 and 3116 cm^{-1} are attributable to the ν(=C–H) modes and those located at 2965, 2938 and 2879 cm^{-1} are due to the ν(C–H) modes of BMITf. The results are in close agreement with that obtained by Cione et al. (2009) who also reported the presence of five IR bands at 3156, 3118, 2970, 2942 and 2882 cm^{-1}.

Similar to BMII ionic liquid, the ν(=C–H) modes of BMITf refer to the hydrogen atom attached directly to C(2), C(4) and C(5) of the imidazolium ring while the ν(C–H) modes are due to the butyl and methyl groups attached to the imidazolium ring. The C–H vibrations of the cation are dependent on associations with the anion and are therefore distinct for different imidazolium based ionic liquids [Jeon et al., 2008; Cione et al., 2009].

Table 4.11 Assignment of FTIR vibrational bands of BMITf

Assignment of bands	Wavenumber (cm^{-1})	References
ν(=C–H) of BMI^+ ring	3156, 3118	Cione et al. (2009)
ν(C–H) of butyl and methyl groups of BMI^+ cation	2970, 2942, 2882	Cione et al. (2009)
C–C and C–N bending mode of cyclic BMI^+ ring	1569	Shi and Deng (2005)
CH_2 deformation mode of BMI^+ ring	1339	Jiang et al. (2006)
$\nu_a(SO_3)$ of Tf^- anion	1289	Cione et al. (2009)
$\nu_s(CF_3)$ of Tf^- anion	1229	Cione et al. (2009)
$\nu_s(SO_3)$ of Tf^- anion	1036	Cione et al. (2009)

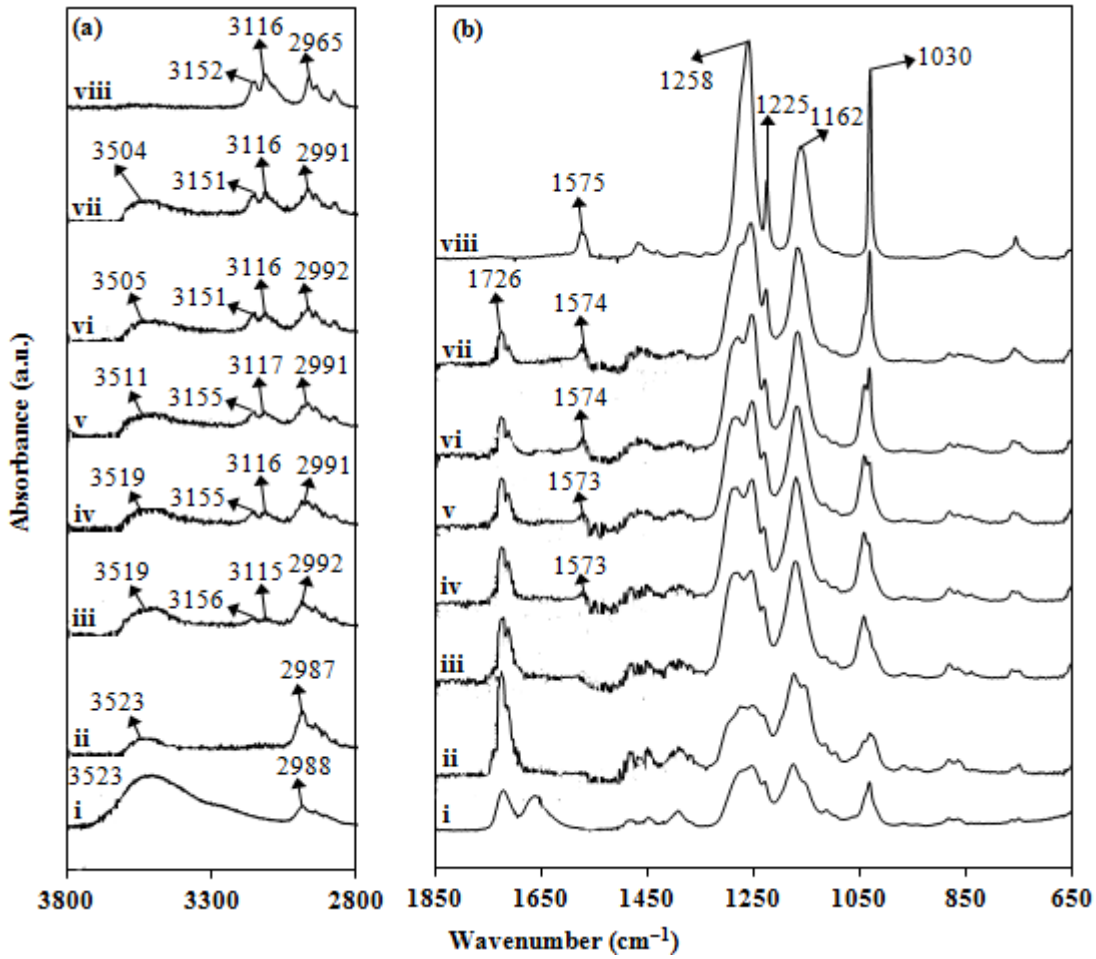

Figure 4.38 FTIR spectra wavenumber region (a) 3800–2800 cm^{-1} and (b) 1850–650 cm^{-1} of i. BT–0, ii. BT–10, iii. BT–20, iv. BT–30, v. BT–40, vi. BT–50, vii. BT–60 and viii. BMITf

The *ν*(=C–H) band located at 3152 cm^{-1} was observed to shift to 3156 (+Δ=4 cm^{-1}) when 20 wt.% of BMITf was added into the optimized PEMA/PVdF–HFP–LiTf system. Increasing the BMITf content caused the *ν*(=C–H) mode to shift to 3155 cm^{-1} in BT–30 and BT–40, Figure 4.38 (a–iv and v). The *ν*(=C–H) mode of BMITf was found at 3151 cm^{-1} in BT–50 and BT–60, Figure 4.38 (a–vi and vii). The initial upshift of the *ν*(=C–H) mode of BMI^{+} ring from 3152 to 3156 cm^{-1} in BT–20 indicates that the BMI^{+} has complexed with the O atoms in PEMA or F atoms in PVdF–HFP. The tendency of the *ν*(=C–H) mode to shift to lower wavenumbers upon further addition of BMITf content indicates reduced complexation between the BMI^{+} ring of BMITf and the polar atoms present in the polymer blend. The *ν*(C–H) modes of alkyl groups attached to the imidazolium ring were observed to merge with the C–H stretching modes belonging to

PEMA and PVdF–HFP in the PEMA/PVdF–HFP–LiTf–BMITf samples. The assignment of FTIR modes of PEMA/PVdF–HFP–BMITf films are listed in Table 4.12.

The IR band due to the carbonyl group, the *v*(C=O) mode of PEMA is investigated in the IR spectra of BMITf–added PEMA, PEMA/PVdF–HFP and PEMA/PVdF–HFP–LiTf samples in Figure 4.39 (a) to (k). The *v*(C=O) mode of PEMA was observed to shift from 1722 cm^{-1} in the polymer blend–salt sample before addition of BMITf to 1725–1726 cm^{-1} in the BMITf–containing films. The upshift of the *v*(C=O) mode indicates that some interaction has occurred between BMITf and C=O group of PEMA in the polymer blend. The shifting of *v*(C=O) is more pronounced in PEMA/PVdF–HFP–LiTf–BMITf samples (Δ=3–4 cm^{-1}) (Figure 4.39 (b) to (g)) as compared to that in the PEMA–BMITf, and PEMA/PVdF–HFP–BMITf samples which only shifted from 1723 to 1724 cm^{-1} (Δ=1 cm^{-1}), Figure 4.39 (h) and (j). The larger wavenumber shift of the *v*(C=O) band observed in PEMA/PVdF–HFP–LiTf–BMITf samples indicates that complexation of cations onto C=O group of PEMA occurs more easily in the presence of both LiTf salt and BMITf ionic liquid. The existence of BMITf could possibly enhance the dissociation of LiTf into Li^+ and Tf^- ions, and consequently increased the coordination of Li^+ onto C=O group of PEMA.

Figure 4.40 (a) to (h) shows the FTIR spectra in the wavenumber region 1350–1200 cm^{-1} for BMITf ionic liquid and BMITf–based polymer electrolytes. The *v*(CO) of –COO– mode of PEMA (band **II'**) and characteristic band of BMITf (band **II"**) of BMITf which were present at 1279 and 1276 cm^{-1} respectively overlapped with each other to form band **II** at 1293 cm^{-1} in BT–10, which manifested an upshift of about 14 to 17 cm^{-1}.

With increasing BMITf content, the band **II** shifted to lower wavenumbers at 1284, 1280, 1278, 1279 and 1279 cm^{-1} when added with 20, 30, 40, 50 and 60 wt.% BMITf, Figure 4.40 (c) to (h). Hence, the downshift and thus reduced position shift of band **II** to approach the original wavenumber before the addition of BMITf is an indication that interaction between BMI^+ cation and the polymer(s) in the polymer blend has reduced with increase in BMITf content.

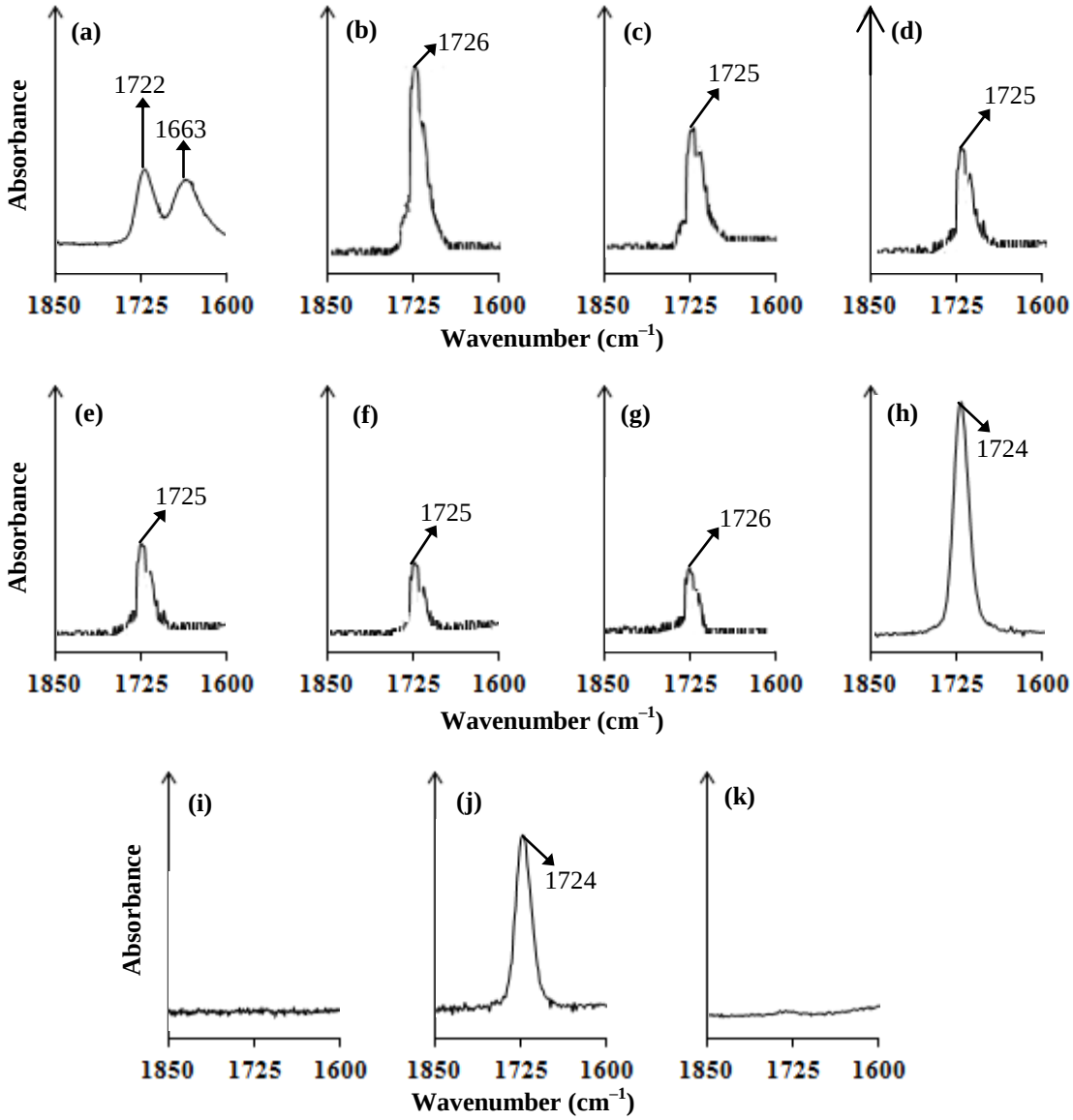

Figure 4.39 FTIR spectra in the region 1850–1600 cm^{-1} for (a) BT–0, (b) BT–10, (c) BT–20, (d) BT–30, (e) BT–40, (f) BT–50, (g) BT–60, (h) 90 wt.% PEMA–10 wt.% BMITf, (i) 90 wt.% PVdF–HFP–10 wt.% BMITf and (j) S–0–BMITf and (k) BMITf

The $\nu_a(SO_3)$ mode due to triflate anions present in both LiTf and BMITf at 1264 cm^{-1} (band **III'**) and 1258 cm^{-1} (band **III''**) respectively is manifested as one IR peak (band **III**) in PEMA/PVdF–HFP–LiTf–BMITf system; the $\nu_a(SO_3)$ mode shifted to 1274 cm^{-1} in the presence of 10 wt.% BMITf.

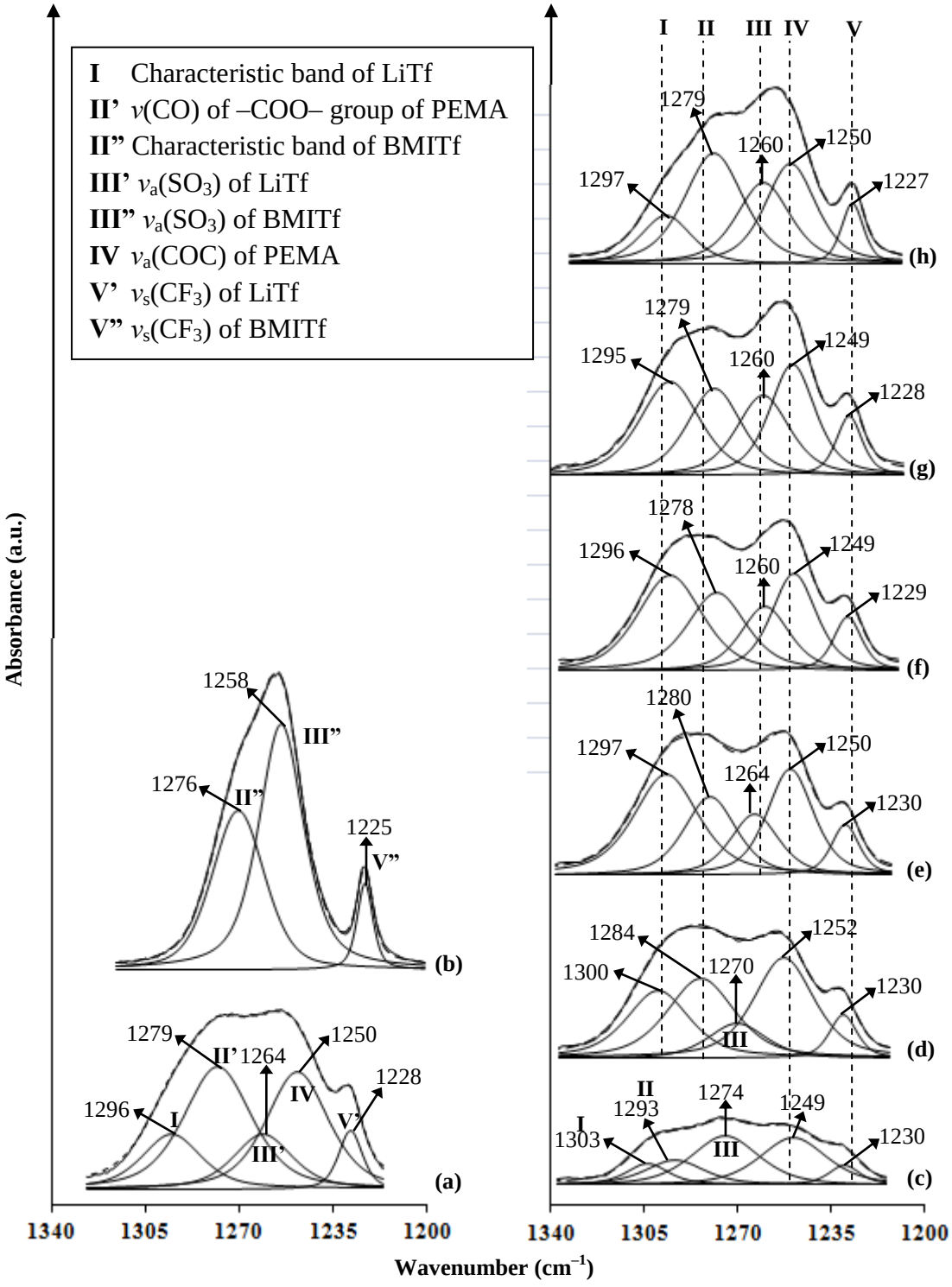

Figure 4.40 FTIR spectra in the region between 1350 and 1200 cm^{-1} of (a) BT–0, (b) BMITf, (c) BT–10, (d) BT–20, (e) BT–30, (f) BT–40, (g) BT–50 and (h) BT–60

When BMITf content was further increased to 60 wt.%, the $v_a(SO_3)$ mode was observed to shift to lower wavenumber at 1270 and 1264 cm^{-1} in BT–20 and BT–30 respectively, and then to 1260 cm^{-1} in samples containing 40 wt.% and above of BMITf. The tendency of the $v_a(SO_3)$ mode of triflate anions to shift to lower wavenumbers with increasing BMITf content suggests the increased production of free ions which is believed to result from enhanced dissociation of LiTf. The $v_s(CF_3)$ mode due to Tf^- anions located at 1228 and 1225 cm^{-1} due to LiTf and BMITf respectively is also present as one IR band (band **V)** in PEMA/PVdF–HFP–LiTf–BMITf samples. The $v_s(CF_3)$ mode (band **V**) shifted slightly to 1230 cm^{-1} in BT–10, BT–20 and BT–30 samples before moving to lower wavenumbers at 1229, 1228 and 1227 cm^{-1} in samples added with 40, 50 and 60 wt.% BMITf. The downshift of the $v_s(CF_3)$ mode at high BMITf content indicates a change in the environment of triflate anions which could possibly result from dissociation from Li^+ ions.

Figure 4.41 (a) to (h) illustrates the IR spectrum of BMITf and the deconvoluted IR spectra of BMITf–added samples in the IR region between 1220 and 1120 cm^{-1} to investigate the effect of BMITf on the ester group of PEMA, the $v_a(CF_2)$ of PVdF–HFP and the $v(CH_3–N)$ of BMITf. Upon addition of BMITf into the optimized polymer blend–salt system, the combined v(CO) of $–OC_2H_5$ group + $v_a(CF_2)$ of PVdF–HFP (band **I**) experienced large wavenumber shift from 1176 cm^{-1} to 1184 cm^{-1} ($+\Delta$=8 cm^{-1}) in BT–10, Figure 4.41 (c). Further addition of BMITf caused band **I** to shift to lower wavenumbers at 1182 cm^{-1} in BT–20, BT–30 and BT–40, to 1179 cm^{-1} in BT–50 and to 1169 cm^{-1} in BT–60, Figure 4.41 (d) to (h). Downshift of band **I** with increasing BMITf content indicates reduced coordination of the ionic liquid with the O atom in the ester group of PEMA and the F atom in the CF_2 group of PVdF–HFP.

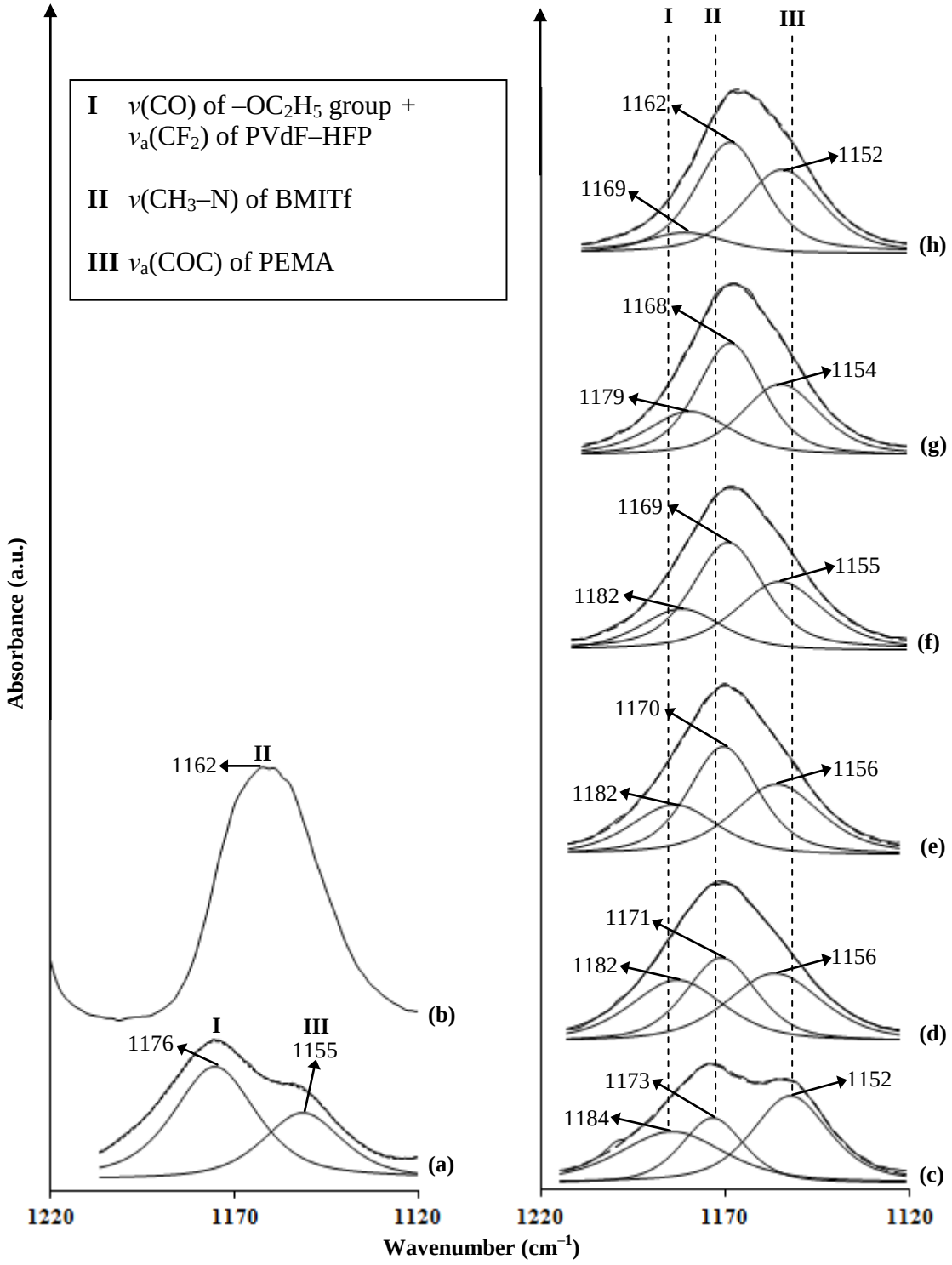

Figure 4.41 FTIR spectra in the region between 1220 and 1120 cm^{-1} of (a) BT–0, (b) BMITf, (c) BT–10, (d) BT–20, (e) BT–30, (f) BT–40, (g) BT–50 and (h) BT–60

The $\nu(CH_3–N)$ band of BMI^+ ion (band **II**) shifted from 1162 to 1173 cm^{-1} in BT–10. Further addition of BMITf gradually lowered the wavenumber of band **II** to 1162 cm^{-1} in BT–60, Figure 4.41 (d) to (h). Reduced position shift of band **II** with

increasing BMITf content indicates reduced complexation of BMI^+ cation with the polymers in the polymer blend system. This in turn, will allow more free coordination sites for Li^+ ions. Overall, the shifting of the ν(=C–H) and $\nu(CH_3–N)$ modes of BMITf, the ν(C=O), ν(CO) of –COO–, ν_a(COC), ν(CO) of $–OC_2H_5$ of PEMA and the $\nu_a(CF_2)$ of PVdF–HFP suggests that BMITf has complexed with PEMA and PVdF–HFP via the hydrogen atoms attached directly to the imidazolium cation. However, complexation of BMITf with PEMA and PVdF–HFP decreased with increasing BMITf content based on the ν(=C–H) and $\nu(CH_3–N)$ modes of BMITf; ν(CO) of –COO– and ν(CO) of $–OC_2H_5$ of PEMA; and $\nu_a(CF_2)$ of PVdF–HFP. Figure 4.42 illustrates the schematic diagram of possible interactions between BMITf and PEMA/PVdF–HFP–LiTf system.

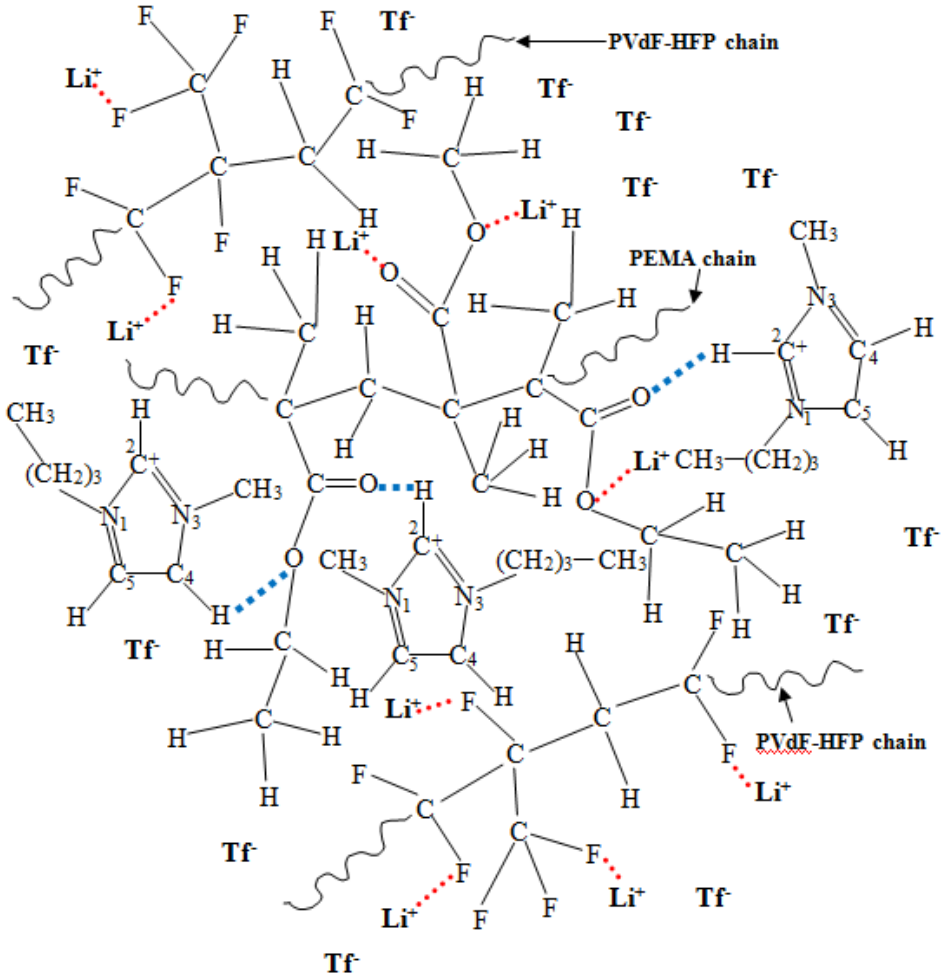

Figure 4.42 Schematic diagram of possible interactions in PEMA/PVdF–HFP–LiTf–BMITf system (where•••• represents the coordinate bonds with Li^+ ions and ▪▪▪ represents the intermolecular interactions between BMITf and PEMA/PVdF–HFP)

4.4.2.2 Interactions between Li^+ and $CF_3SO_3^-$ ions, and the expected effect on the ionic conductivity of PEMA/PVdF–HFP–LiTf–BMITf system

In order to study the ionic association between Li^+ and Tf^-, the IR envelope in the region between 1080 and 980 cm^{-1} was deconvoluted in Figure 4.43 to separate the $\nu_s(SO_3)$ vibrational mode into different ionic species, namely free ions, ion pairs and ion aggregates.

The δ(C–H) band of PEMA is found at 1021–1023 cm^{-1} in all BMITf containing samples. The $\nu_s(SO_3)$ bands due to free ions and ion pairs could be observed at 1031–1032 cm^{-1} and 1041–1043 cm^{-1} respectively, in all samples. Ion aggregates only appeared in polymer electrolytes containing 20 wt.% and above of BMITf, Figure 4.43 (b) to (f). The plot of area fraction of the free ions, ion pairs and ion aggregates of PEMA/PVdF–HFP–LiTf–BMITf system is shown in Figure 4.44.

From Figure 4.44, the area % of ion pairs started off high upon addition of 10 wt.% BMITf, but decreased continually up to 60 wt.% BMITf. On the other hand, the area % attributable to free ions was observed to increase continuously upon addition of BMITf up to 60 wt.%. The area % for ion aggregates was observed to increase with addition of 10 wt.% BMITf and then decreased above 40 wt.% BMITf. In samples containing 50 and 60 wt.% BMITf, free ions dominate over ion pairs and ion aggregates.

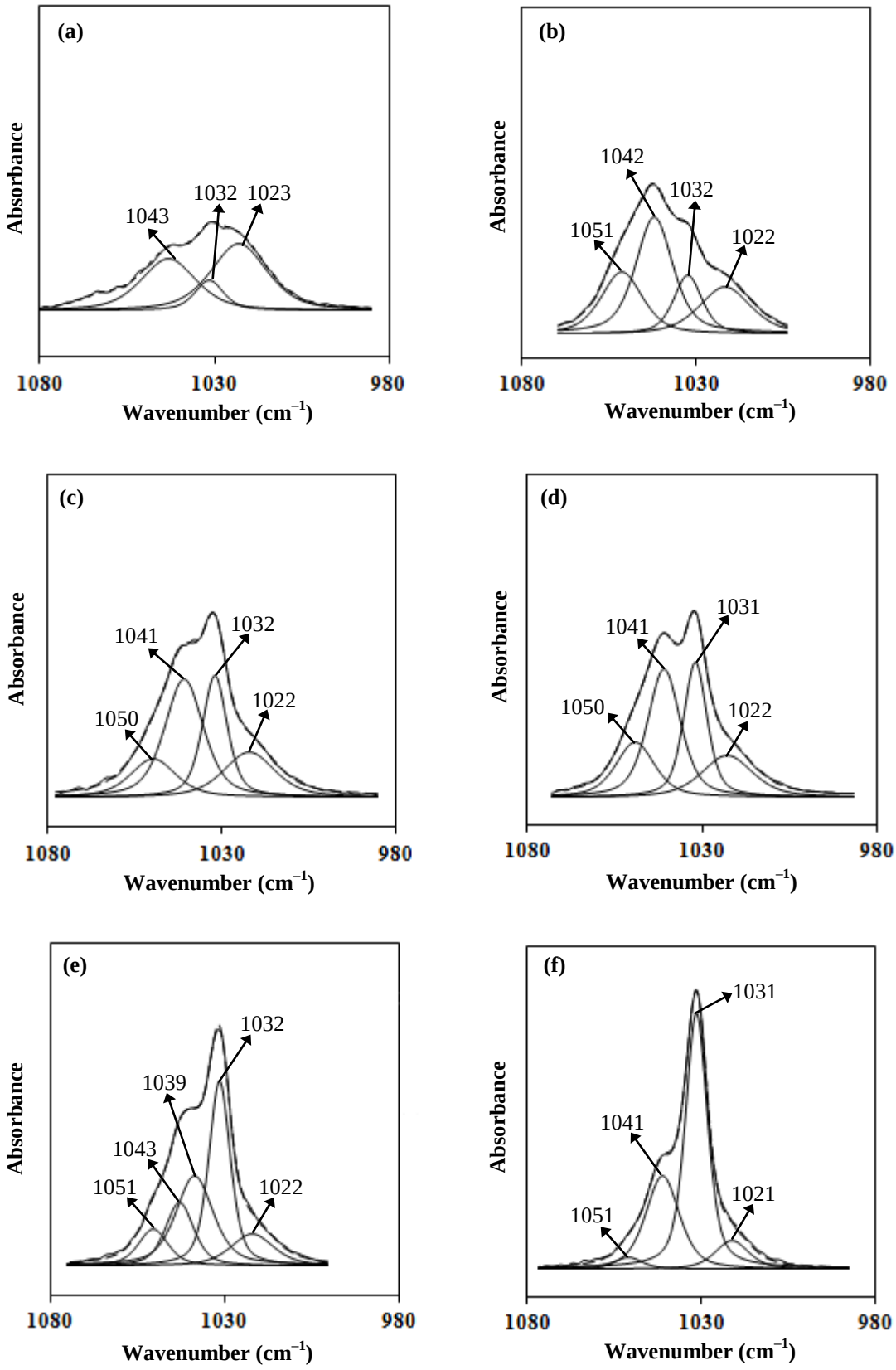

Figure 4.43 Deconvolution between 1080 and 980 cm^{-1} of (a) BT–10, (b) BT–20, (c) BT–30, (d) BT–40, (e) BT–50 and (f) BT–60

Table 4.12 FTIR vibrational modes of PEMA/PVdF–HFP:LiTf (70:30, w/w) blend polymer electrolytes incorporated with different wt.% of BMITf

Assignment of bands	Wavenumber (cm^{-1})							
	BMITf	**BT–0**	**BT–10**	**BT–20**	**BT–30**	**BT–40**	**BT–50**	**BT–60**
ν(=C–H) of BMI^+ ring	3152, 3116	–	–	3156, 3115	3155, 3116	3155, 3117	3151, 3116	3151, 3116
ν(CH)	2965, 2938, 2879	2988, 2943, 2912	2987, 2944, 2913, 2872	2992, 2943, 2912, 2872	2991, 2972, 2945, 2912, 2872	2991, 2967, 2944, 2912, 2872	2992, 2967, 2943, 2912, 2872	2991, 2972, 2943, 2913, 2872
ν(C=O) of PEMA	–	1722	1726	1725	1725	1725	1725	1726
$\delta(H_2O)$ from LiTf	–	1663	–	–	–	–	–	–
C–C and C–N bending of cyclic BMI^+ ring	1575	–	–	–	1573	1573	1574	1574
$\delta(CH_2)$of PEMA	–	1482	1485	1479	1479	1469	1469	1469
$\gamma(OC_2H_5)$of PEMA	–	1448	1450	1454	1454	1450	1454	1454
$\omega(CH_2)$ of PVdF–HFP + $\tau(CH_2)$ of PEMA	–	1392	1392	1391	1391	1391	1390	1390
Characteristic band of LiTf	–	1296	1303	1300	1297	1296	1295	1297
ν(CO) of –COO– group of PEMA	–	1279	1293	1284	1280	1278	1279	1279
Characteristic band of BMITf	1276	–						
$\nu_a(SO_3)$ of LiTf	–	1264	1274	1270	1264	1260	1260	1260
νa(SO_3) of BMITf	1258	–						
ν_a(COC) of PEMA	–	1250	1249	1252	1250	1249	1249	1250
$\nu_s(CF_3)$ of LiTf	–	1228	1230	1230	1230	1229	1228	1227
νs(CF_3) of BMITf	1225	–						
$\nu_a(CF_2)$ of PVdF–HFP + ν(CO) of –OC_2H_5 group of PEMA	–	1176	1184	1182	1182	1182	1179	1169
$\nu(CH_3–N)$ of BMITf	1162	–	1173	1171	1170	1169	1168	1162
ν_a(COC) of PEMA	–	1155	1152	1156	1156	1155	1154	1152
Characteristic band of PEMA	–	1113	1115	1117	1115	1116	1117	1117
$\nu_s(SO_3)$ ion aggregates of LiTf	–	–	–	1051	1050	1050	1051	1051
$\nu_s(SO_3)$ ion pairs of LiTf	–	1041	1043	1042	1041	1041	1039	1041
$\nu_s(SO_3)$ free ions of LiTf	–	1032	1031	1032	1031	1031	1032	1031
α–phase of PVdF–HFP	–	969	967	967	966	967	968	967
Amorphous region of PVdF–HFP	–	881	883	882	881	881	881	881
β–phase of PVdF–HFP	–	838	839	840	840	840	841	841
$\delta_s(CF_3)$ of LiTf	–	762	763	764	763	760	761	761

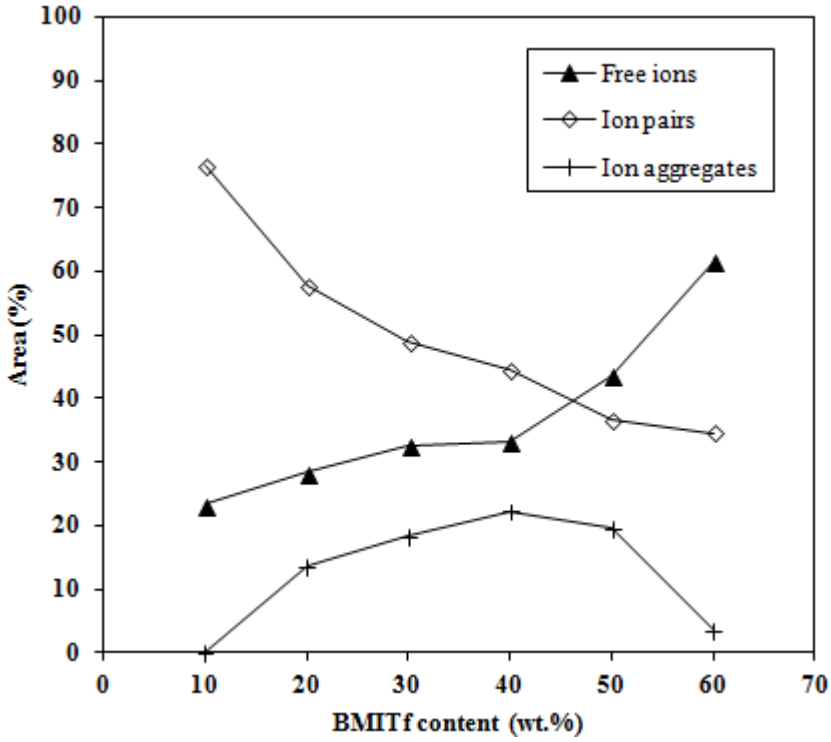

Figure 4.44 Area % of free ions, ion pairs and ion aggregates as a function of BMITf content

4.5 Summary

- Shifting of the FTIR bands: ν(CH), $\delta(CH_2)$, $\tau(CH_2)$, ν_a(COC), ν(CO) of –COO– and ν(CO) of $-OC_2H_5$ group of PEMA, and ν(CH), $\omega(CH_2)$, $\nu_a(CF_2)$, IR bands corresponding to the α–phase and amorphous region of PVdF–HFP showed that PEMA and PVdF–HFP interacted with one another to form PEMA/PVdF–HFP (70:30) blend.
- FTIR wavenumber change of $\delta_s(CF_3)$, $\nu_a(SO_3)$, $\nu_s(SO_3)$ and $\nu_a(CF_3)$ modes of LiTf, the ν(C=O), ν_a(COC), ν(CO) of $-OC_2H_5$ group and ν(CO) mode of –COO– group of PEMA as well as the $\nu_a(CF_2)$ band of PVdF–HFP indicated that Li^+ ions from LiTf have coordinated with the oxygen atoms in C=O and C–O–C groups of PEMA and with the fluorine atoms in CF_2 group of PVdf–HFP in the PEMA/PVdF–HFP blend.
- The wavenumber shift of the ν_a(COC) was significantly larger as compared to that of the ν(C=O) mode of PEMA in the PEMA/PVdF–HFP–LiTf system.

- The shifting of the skeletal stretching and ν(C=O) of EC, ν_a(COC) of PEMA and the combined $\nu_a(CF_2)$ vibration of PVdF–HFP + ν(CO) band due to $–OC_2H_5$ group of PEMA in PEMA/PVdF–HFP–LiTf–EC system shows that EC has interacted with the O atom in the C–O–C group of PEMA and F atom in the CF_2 group of PVdF–HFP in PEMA/PVdF–HFP–LiTf–EC system.
- The shifting of the skeletal stretching, ring breathing, ν(C=O), ν(CO) + ω(CH), ν(CO) + ν(CH) and τ(C–H) + δ(C–H) of PC; ν(CO) of –COO– and ν_a(COC) of PEMA; and the $\nu_a(CF_2)$ vibration of PVdF–HFP + ν(CO) band of $–OC_2H_5$ group of PEMA have shown that PC has interacted with the O atom in the C–O–C group of PEMA and F atom in the CF_2 group of PVdF–HFP in PEMA/PVdF–HFP–LiTf–PC system.
- The shifting of the ν(=C–H) and $\nu(CH_3–N)$ modes of the imidazolium cation, the ν(C=O), ν(CO) of –COO–, ν_a(COC), ν(CO) of $–OC_2H_5$ of PEMA and the $\nu_a(CF_2)$ of PVdF–HFP in the BMII– and BMITf–added PEMA/PVdF–HFP–LiTf systems showed that interaction has occurred between the imidazolium cation of each ionic liquid with the oxygen atom in C=O and C–O–C groups of PEMA, and the fluorine atom in CF_2 group in PVdF–HFP.
- Reduced wavenumber shift of the ν(=C–H) and $\nu(CH_3–N)$ modes of BMITf; ν(CO) of –COO– and ν(CO) of $–OC_2H_5$ of PEMA; and $\nu_a(CF_2)$ of PVdF–HFP with increasing BMITf content indicates decreased complexation of BMITf in the PEMA/PVdF–HFP–LiTf–BMITf system. It is expected that BMITf plays a role to enhance the dissociation of LiTf into Li^+ and $Tf^–$ which increased the coordination of Li^+ onto the polar groups of PEMA and PVdF–HFP.
- The area % of free ions was found to be highest at the following content: 40 wt.% LiTf, 6 wt.% of EC, 6 wt.% PC, 12.5 wt.% BMII and 60 wt.% BMITf.